

Development of Maximum Power Extraction Algorithms for PV system With Non-Uniform Solar Irradiances

*Dissertation submitted in partial fulfillment
of the requirements of the degree of*

Doctor of Philosophy

in

Electrical Engineering

by

Satyajit Mohanty

(Roll No: 512EE1015)

*based on research carried out
under the supervision of*

Prof. Bidyadhar Subudhi

Prof. Pravat Kumar Ray



DEPARTMENT OF ELECTRICAL ENGINEERING
NATIONAL INSTITUTE OF TECHNOLOGY ROURKELA
JANUARY 2017



CERTIFICATE OF EXAMINATION

Roll Number : 512EE1015
Name: *Satyajit Mohanty*
Title of Dissertation: *Development of Maximum Power Extraction Algorithms for PV System With Non-Uniform Irradiances*

We the below signed, after checking the dissertation mentioned above and the official record book(s) of the student, hereby state our approval of the dissertation submitted in partial fulfillment of the requirements of the degree of *Doctor of Philosophy in Electrical Engineering at National Institute of Technology Rourkela*. We are satisfied with the volume, quality, correctness, and originality of the work.

Prof. S.Karmakar
(Member, DSC)

Prof. U. C. Pati
(Member, DSC)

Prof. S.Gopalkrishna
(Member, DSC)

Prof. P.K Ray
(Co-Supervisor)

Prof. B. Subudhi
(Supervisor)

(External Examiner)

Prof. A.K Panda
(Chairman, DSC)



CERTIFICATE

This is to certify that the work presented in the dissertation entitled “**Development of Maximum Power Extraction Algorithms for PV system with Non-Uniform Solar Irradiances**” submitted by Satyajit Mohanty, Roll Number 512EE1015, is a record of original research carried out by him under the supervision and guidance in partial fulfillment of the requirements of the degree of Doctor of Philosophy in Electrical Engineering. Neither this dissertation nor any part of it has been submitted earlier for any degree or diploma to any institute or university in India or abroad.

Prof. Pravat Kumar Ray
(Co-Supervisor)

Prof. Bidyadhar Subudhi
(Supervisor)

Declaration of Originality

I, Satyajit Mohanty, Roll Number 512EE1015 hereby declare that this dissertation entitled “**Development of Maximum Power Extraction Algorithms for PV system with Non-Uniform Solar Irradiances**” presents my original work carried out as a doctoral student of NIT Rourkela and, to the best of my knowledge, contains no material previously published or written by another person, nor any material presented by me for the award of any degree or diploma of NIT Rourkela or any other institution. Any contribution made to this research by others, with whom I have worked at NIT Rourkela or elsewhere, is explicitly acknowledged in the dissertation. Works of other authors cited in this dissertation have been duly acknowledged under the sections Reference or Bibliography. I have also submitted my original research records to the scrutiny committee for evaluation of my dissertation.

I am fully aware that in case of any non-compliance detected in future, the Senate of NIT Rourkela may withdraw the degree awarded to me on the basis of the present dissertation.

Satyajit Mohanty

ACKNOWLEDGEMENT

First and foremost, I am truly indebted to my supervisors Prof. Bidyadhar Subudhi and Prof. Pravat Kumar Ray for their guidance and unwavering confidence through my study, without which this thesis would not be in its present form. I also thank them for gracious encouragement throughout the work.

I express my gratitude to the members of Doctoral Scrutiny Committee for their suggestion to improve the work. I am also very much obliged to Head of the Department of Electrical Engineering, NIT Rourkela for providing possible facilities.

Thanks to Murli, Om prakash, Subhasish, Raja, Soumya and Rajendra and all the research scholars of Electrical Department for their enjoyable and helpful company.

I also want to thank Biraja Sir, Srikant Sir and Alok Sir for their advice and encouragement at every moment. I also thank Bag Sir & Bhauja, my lovely Angel, Pradosh Bhai & Bhauja, Mrutyunjay Sir and all other SSB Hall roommates in making my stay enjoyable during this Ph.D. duration. I also thank my friends Debasis, Suchit, Sameer, Shashi, Swayam, Tapas, Tapaswini, Debashish, Alokesh, Rama, Atulya, Tanmay & Deepalok for their encouragement and support.

My wholehearted gratitude to my beloved family members, Sarat kumar Mohanty & Namita Patnaik, Bijay Mohanty & Krishna Mohanty, my grandmother Late. Renuka Mohanty, my Uncle Late. Babubichitraa Mohanty, my Uncle Sri. Saroj kumar Mohanty, my wife. Sangita Mohanty, Kishan & Bikram, Bhai, Pinku and Monu for keeping faith on me and always shower me with their unconditional love. Thank you for believing in me.

Satyajit Mohanty

Abstract

This thesis addresses the problem of extraction of maximum power from PV arrays subjected to non-uniform solar irradiances e.g partial shading. In the past, a number of maximum power point tracking algorithms (MPPTs) such as Perturb & Observe, Hill climbing, Incremental Conductance, etc. have been proposed. These are extensively used for obtaining maximum power from a PV module to maximize power yield from PV systems under uniform solar irradiance. However, these techniques have not considered partial shading conditions and the stochastic nature of solar insolation. In the event of non-uniform solar insolation, a number multiple maximum power points (MPPs) appear in the power-voltage characteristic of the PV module. In the present thesis, the stochastic nature of the solar insolation is considered to obtain the global MPP of a PV module with a focus on developing global optimization techniques for MPPT that would handle the multiple MPPs. Thus, the thesis will address the above problem by developing a number of global MPPT algorithms.

In this thesis, an extensive review on MPPT algorithms for both uniform and non-uniform insolation levels is presented. Subsequently, an analysis with respect to their merits, demerits and applications have been provided in order to design new MPPTs to achieve higher MPPT efficiency under non-uniform solar irradiances.

Firstly, PV modules are modelled with and without bypass diodes for handling Partial shading conditions (PSCs). Then, a new Ring pattern (RP) configuration has been proposed which is compared with different existing configurations such as Series-parallel (SP), Total cross tied (TCT) and Bridge linked (BL) configurations on the basis

of maximum power and fill factor.

As described earlier, under non-uniform irradiances the MPPT problem boils down to determining the global MPP. Thus, the MPPT problem can be cast as a global optimization problem. It may be noted that evolutionary computing approaches are extensively used for obtaining global optimum solutions. One of the most recent evolutionary optimization techniques called grey wolf optimization technique has gained enormous popularity as an efficient global optimization approach. In view of this, Grey wolf optimization is employed to design a global MPPT such that maximum power from PV modules can be extracted which will work under partial shading conditions. Its performance has been compared with two existing MPPTs namely P&O and IPSO based MPPT methods. From the obtained simulation and experimental results, it was found that the GWO based MPPT exhibits superior MPPT performance as compared to both P&O and IPSO MPPTs on the basis of dynamic response, faster convergence to GP and higher tracking efficiency.

Further, in order to scale down the search space of GWO which helps to speed up for achieving convergence towards the GP, a fusion of GWO-MPPT with P&O MPPT for obtaining maximum power from a PV system with different possible patterns is developed. An experimental setup of 600W solar simulator is used in the laboratory having characteristics of generating partial shading situation. Firstly, the developed algorithms were implemented for a PV system using MATLAB/SIMULINK. Subsequently, the aforesaid experimental setup is used to implement the proposed global MPPT algorithms. From the obtained simulation and experimental results it is observed that the Hybrid-MPPT converges to the GP with least time enabling highest possible maximum power from the solar PV system.

In this thesis, analytical modeling of PV modules for handling non-uniform irradiances is pursued as well as a new RP configuration of PV modules is developed to achieve maximum power and fill factor. In order to extract maximum power from PV panels subjected to non-uniform solar irradiances, two new MPPT algorithms are

developed namely Grey wolf optimization based MPPT(GWO-MPPT) and GWO assisted PO(GWO-PO).

Keywords: PV, MPPT, GWO, DC-DC Boost Converter, Partial Shading Conditions.

Contents

Abstract	i
List of Acronyms	viii
List of figures	xiii
List of tables	xiv
1 Introduction	1
1.1 Photovoltaic Power Generation	1
1.2 Photovoltaic Energy Conversion	2
1.3 Types of PV System	5
1.4 Maximum Power Extraction Algorithms	5
1.5 Partial Shading Conditions	10
1.6 Motivation of the Thesis	14
1.7 Organization of the Thesis	14
2 Literature Review on Maximum Power Extraction Algorithms and Problem Formulation	16
2.1 MPPT for Uniform Insolation	16
2.1.1 Advantages and Disadvantages of Different MPPT Techniques	23

2.2	MPPT for Non-Uniform Insolation levels	28
2.3	Review Remarks	31
2.4	Objectives of the Thesis	32
2.5	Problem Formulation	32
2.6	Chapter Summary	34
3	Development of an Experimental Setup for a PV System subjected to Non-Uniform Solar Irradiances	35
3.1	Introduction	35
3.2	Experimental Setup using Solar Panels	36
3.2.1	Solar Panel	37
3.2.2	DC-DC Boost Converter	38
3.2.3	Hall Effect Sensor	38
3.2.4	DS1104	38
3.3	Experimental Setup using Agilent Simulator	39
3.3.1	Agilent Solar Array Simulator	40
3.3.2	Solar Array Simulator(SAS) Mode:	41
3.4	Chapter Summary	43
4	Analytical Modeling and Experimental Prediction of Global Peak under Partial Shading of PV modules for a Photovoltaic System	44
4.1	Abstract	44
4.2	Introduction	45
4.3	Chapter Objectives	46
4.4	Modeling of PV System	47
4.4.1	PV Cell Modeling	47
4.4.2	PV Module Modeling	48
4.4.3	Characteristics of PV System under Partial Shading	49
4.5	Different Possible Orientations of PV Modules under PSCs	51

4.5.1	Array composed of n-multiple modules	51
4.5.2	Array composed of partially shaded module without bypass diode	53
4.6	Different possible configurations of PV cells	54
4.6.1	Series-Parallel configuration (SP configuration)	54
4.6.2	Total Cross Tied Configuration (TCT configuration)	56
4.6.3	Bridge Linked Configuration (BL-Configuration)	57
4.6.4	Proposed Ring Pattern Configuration (RP-Configuration)	59
4.7	Performance Evaluation	60
4.8	Chapter Summary	63
5	A New MPPT Design Using Grey Wolf Optimization Technique for Photovoltaic System Under Partial Shading Conditions	64
5.1	Abstract	64
5.2	Introduction	65
5.3	Chapter Objectives	67
5.4	Characteristics of a PV System under Partial Shading Conditions	68
5.4.1	Basic Characteristics of a PV cell	68
5.4.2	System Description	69
5.5	GWO and its Application in MPPT Design	69
5.5.1	Grey Wolf Optimization	69
5.5.2	Application of GWO for MPP Tracking	73
5.6	Results and Discussion	75
5.6.1	Simulation Results	75
5.6.2	Experimental Results	81
5.7	Chapter Summary	85
6	A Grey Wolf Assisted Perturb & Observe Maximum Power Point Tracking Algorithm for a PV System	86
6.1	Abstract	86

6.2	Introduction	87
6.3	Chapter Objectives	88
6.4	PV System under Partial Shading Conditions	89
6.4.1	PV System Modeling	89
6.4.2	System Description	91
6.5	Problem Formulation	92
6.6	Overview of the Proposed MPPT Method	92
6.6.1	Grey Wolf Optimization (GWO) application to MPPT Design	92
6.6.2	Perturb and Observe (P&O) MPPT	93
6.6.3	Proposed Hybrid-MPPT	94
6.7	Simulation Case Studies	95
6.7.1	Partial Shading Conditions	97
6.7.2	Rapidly Changing Insolation levels	98
6.7.3	Extreme Rapidly Changing Insolation levels	100
6.8	Experimental Results	102
6.9	Chapter Summary	105
7	Conclusion and Suggestions for Future Work	106
7.1	Overall Summary of the Thesis	106
7.1.1	Contributions of the Thesis	108
7.2	Suggestions for the future work	109
	References	110
	Publications from this thesis	121

List of Acronyms

List of Acronyms

PV	:	Photovoltaic
STC	:	Standard Test Conditions
MPP	:	Maximum Power Point
MPPT	:	Maximum Power Point Tracker
PSCs	:	Partial Shading Conditions
GP	:	Global Peak
LP	:	Local Peak
SP	:	Series Parallel
TCT	:	Total Cross Tied
BL	:	Bridge Linked
RP	:	Ring Pattern
GWO	:	Grey Wolf Optimization
4S	:	Four Series
2S2P	:	Two Series Two Parallel
3S	:	Three Series
3S2P	:	Three Series Two Parallel
PSO	:	Particle Swarm Optimization
PI	:	Proportional Integral
P&O	:	Perturb & Observe
INC	:	Incremental Conductance

FOCV	:	Fractional Open Circuit Voltage
FSCI	:	Fractional Short Circuit Current
RCC	:	Ripple Correlation Control
OCC	:	One Cycle Control
FO	:	Forced Oscillation
FLC	:	Fuzzy Logic Controller
ANN	:	Artificial Neural Network
IPSO	:	Improved Particle Swarm Optimization
GWO-PO	:	Grey Wolf Optimization-Perturb & Observe
CdTe	:	Cadmium Telluride
CIGS	:	Copper Indium Gallium Selenide
CIS	:	Copper Indium Selenide
PWM	:	Pulse Width Modulation
DSO	:	Digital Storage Oscilloscope

List of Figures

1.1	PV growth world scenario [1]	2
1.2	Conversion mechanism of solar light into electricity [2]	3
1.3	Types of Solar Cells [3]	3
1.4	Relationship between cell, module and array [3]	4
1.5	Types of PV system (a) Grid connected, (b) Stand-alone (c) Hybrid	6
1.6	(a) PV panel with directly connected load and, (b) Operating point of a PV system with direct coupled load	8
1.7	Standalone PV with MPPT	9
1.8	MPPTs under (a) Uniform Insolation, (b) Non-uniform Insolation	9
1.9	P-V characteristics curve exhibiting single MPP under uniform insolation level	10
1.10	Possible Shading Scenarios [4]	11
1.11	Effect of Bypass and Blocking diode under PSCs	13
1.12	P-V characteristics curve exhibiting multiple peaks	13
1.13	Hotspot occurrence [5]	14
2.1	Flowchart of Perturb & Observe/ Hill Climbing MPPT	17
2.2	Flowchart of Incremental Conductance MPPT	18
2.3	Flowchart of Fuzzy logic controller MPPT	20
2.4	Classification according to Control Strategies	22
2.5	A PV system with MPPT	33

3.1	(a) Block Diagram (b) Photograph of experimental setup with solar array	36
3.2	Sukam make solar panel	37
3.3	(a) DC-DC Boost Converter (b) Hall Effect Sensor	38
3.4	DS1104 Board	39
3.5	(a) Block Diagram (b) Photograph of experimental setup with simulator	40
3.6	(a)Solar Array Simulator (b) Front view (c) Rear view	42
3.7	(a) SAS Mode (b) Fixed Mode	43
4.1	Equivalent circuit of a PV cell [6]	47
4.2	PV output characteristics of a PV module under normal conditions(a) I-V characteristics, (b) P-V characteristics	49
4.3	Possible shading by cloud on a PV system	50
4.4	P-V characteristics curve with and without Bypass diode	50
4.5	Equivalent circuit of a PV array with n-modules in series	52
4.6	Equivalent circuit of a partially shaded module without bypass diode .	53
4.7	SP configuration	55
4.8	TCT configuration	56
4.9	BL configuration	58
4.10	RP configuration	59
4.11	Solar Array Simulator	61
4.12	Experimental P-V characteristics curve of a PV array(a) SP, (b) TCT, (c) BL, (d) proposed RP configuration	62
5.1	Equivalent circuit of a PV cell [6]	68
5.2	4S configuration under different shading patterns (a) Pattern 1, (b) Pattern 2, (c) P-V curves under PSCs	70
5.3	2S2P configuration under different shading patterns (a) Pattern 3, (b) Pattern 4, (c) P-V curves under PSCs	71

5.4	Hunting behavior of grey wolves:(A-C) chasing and tracking prey (D) encicling prey (E) attacking prey	72
5.5	Block diagram of the proposed MPPT method	73
5.6	Flowchart of the proposed algorithm	74
5.7	Tracking curves for 4S Configuration (a) GWO based MPPT (b) IPSO based MPPT (c) P&O based MPPT	77
5.8	Tracking curves for 2S2P Configuration (a) GWO based MPPT (b) IPSO based MPPT (c) P&O based MPPT	78
5.9	Tracking curves for pattern 1 showing response of proposed MPPT having R and R-L load under PSCs	81
5.10	Experimental results for 4S configuration (a) P-V curves, Tracking curves using (b) GWO (c) IPSO (d) P&O	82
5.11	Experimental results for 2S2P configuration (a) P-V curves, Tracking curves using (b) GWO (c) IPSO (d) P&O	83
5.12	Experimental results for pattern 5 showing response of proposed MPPT under R-L load	84
6.1	Equivalent circuit of a PV cell [7]	89
6.2	(a) 3S Configuration, (b) 3S2P Configuration	90
6.3	P-V curves exhibiting multiple peaks for (a) 3S Configuration, (b) 3S2P Configuration	91
6.4	Movement of a wolf during search process	93
6.5	Flowchart of the Hybrid-MPPT Algorithm	96
6.6	Block diagram of the proposed Hybrid-MPPT Algorithm	97
6.7	Tracking curves for 3S configuration (a) PV power of proposed Hybrid MPPT compared with other techniques like GWO,PSO+PO based MPPT, (b) zoomed view of Area A	98

6.8	Tracking curves for 3S2P configuration (a) PV power of proposed Hybrid MPPT compared with other techniques like GWO, PSO+PO based MPPT, (b) zoomed view of Area B	98
6.9	Tracking curves for 3S configuration for rapid changes in insolation	99
6.10	Tracking curves for 3S2P configuration for rapid changes in insolation	99
6.11	Tracking curves for 3S configuration for extreme rapid changes in insolation	100
6.12	Experimental Results for 3S Configuration for extreme rapidly changing insolation patterns (a) Hybrid-MPPT (b) GWO-MPPT (c) PSO-PO MPPT	103
6.13	Experimental Results for 3S2P Configuration for rapidly changing insolation patterns (a) Hybrid-MPPT (b) GWO-MPPT (c) PSO-PO MPPT	104

List of Tables

1.1	Types of PV Cell [8]	4
2.1	Comparison of different MPPT Techniques	23
4.1	Experimental comparison of peak power and fill factor	63
5.1	Parameters of KC200GT PV module at $25^{\circ}C$ and $1000W/m^2$	76
5.2	Parameters of IPSO and GWO Algorithms	76
5.3	Performance Comparison of the Proposed MPPT with P&O and IPSO MPPTs for 4S Configuration	79
5.4	Performance Comparison of the Proposed MPPT with P&O and IPSO MPPTs for 2S2P Configuration	79
5.5	Qualitative Comparison of the Proposed with P&O and IPSO MPPT Techniques	80
6.1	Performance Evaluation of the proposed MPPT method for 3S and 3S2P Configuration	101
6.2	Characteristics Comparison of the proposed Hybrid MPPT method with other MPPT Methods	102

Chapter 1

Introduction

1.1 Photovoltaic Power Generation

With increase in demand and growing prices of fossil fuels together with concern about environmental issues have generated massive interest in the exploitation of renewable energy sources such as solar, wind, hydro, geothermal, etc. for electrical power generation [9]. Among the different renewable sources, Photovoltaic (PV) Energy generation has become increasingly essential as a non-conventional source since it unveils advantages such as

- Solar insolation is freely available
- No pollution and waste products
- Low maintenance cost
- Absence of rotating parts
- Generates energy, without the need of long transmission lines

The word photovoltaic is a combination of the two words photo, which means light, and voltaic, which implies the production of electricity. PV technology is concerned with generation of electricity from solar irradiance. A solar PV cell is a device

that converts the energy in the sunlight directly into electricity using the photovoltaic effect [10] [11]. Fig.1.1 shows the statistics of world scenario of growth of PV energy.

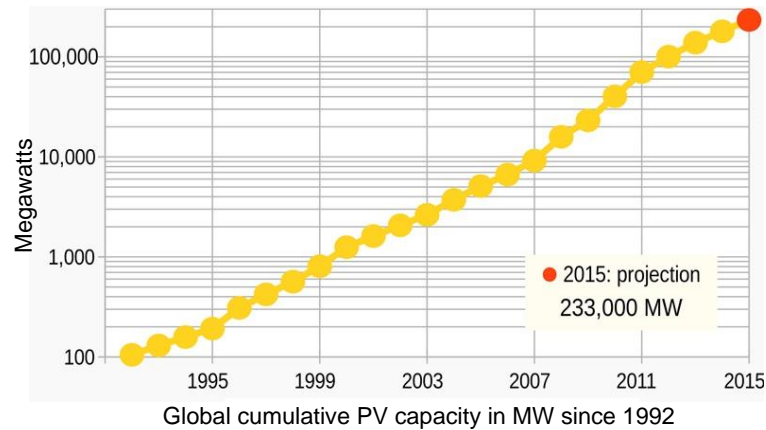


Figure 1.1: PV growth world scenario [1]

1.2 Photovoltaic Energy Conversion

When a photon of light falls on a PV cell [12], it has enough energy to knock an electron loose, allowing it to flow freely as shown in Fig.1.2. Each PV cell has two layers of silicon; namely one is positive and other is negative. When a photon of light is absorbed by one of these atoms in the N-Type silicon it will dislodge an electron, creating a free electron and a hole. The free electron and hole have sufficient energy to jump out of the depletion zone and flow through an external load. The PV cell behaves as a current source [13]. The greater the intensity of the solar insolation, the greater is the generation of current in this PV cell. Usually, a typical PV cell produces 0.5V which is very small, therefore several PV cells are connected in series and parallel according to the requirement of output power. When this PV panel is connected to a load, electrons starts moving in a particular direction, resulting in flow of current through the load.

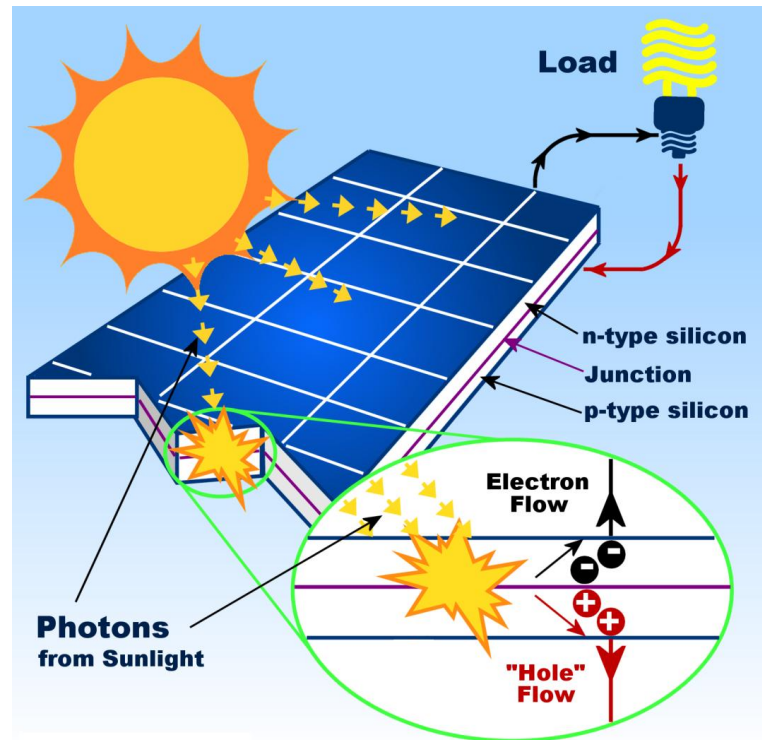
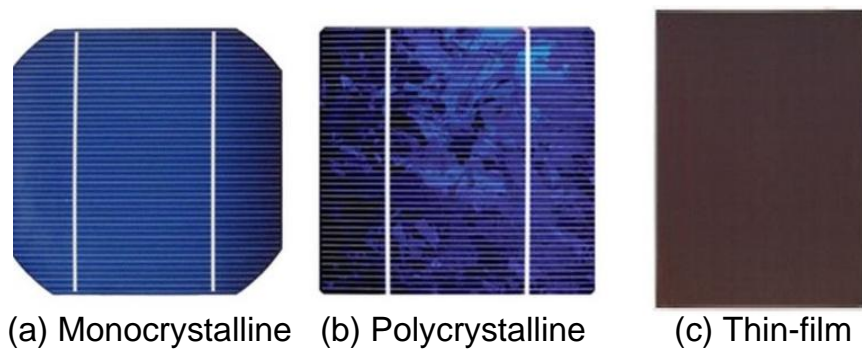


Figure 1.2: Conversion mechanism of solar light into electricity [2]



(a) Monocrystalline (b) Polycrystalline (c) Thin-film

Figure 1.3: Types of Solar Cells [3]

The PV cell can be of three types such as Mono-crystalline, Poly-crystalline and thin-film and is shown in Fig.1.3. These three different PV cells are compared in Table 1.1. PV cells are connected in series and parallel according to the requirement of voltage and current ratings of load. These PV arrays are made by connecting many

PV modules in series and parallel as shown in Fig.1.4. The power output of a PV array depends on the power output of individual PV modules [14]. By choosing appropriate sized and series-parallel combinations of PV modules, PV array of given power rating can be obtained.

Table 1.1: Types of PV Cell [8]

Sl.No	Types of PV Cell	Properties
1	Monocrystalline	Made up of single silicon material. Highly efficient in good weather conditions. Energy conversion efficiency is 12-15%.
2	Polycrystalline	Made up of small silicon crystals. Efficient in good light conditions. Energy conversion efficiency is 11-14%.
3	Thin-film	Made up of materials like CdTe,CIGS,CIS. Efficient in poor light conditions. Energy conversion efficiency is 6-12%.

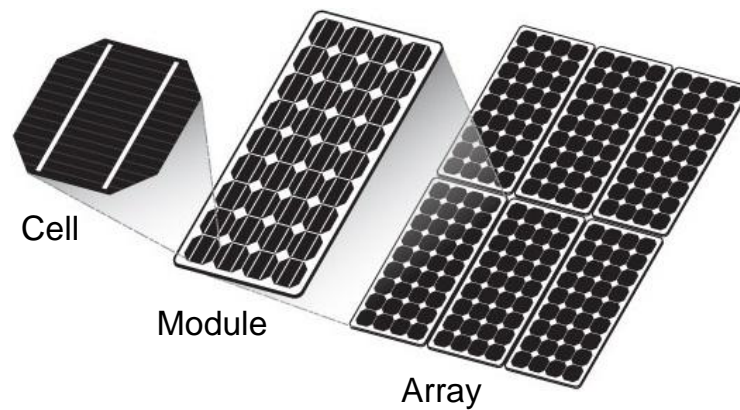


Figure 1.4: Relationship between cell, module and array [3]

1.3 Types of PV System

Fig.1.5 shows the three different connections of PV system [15].

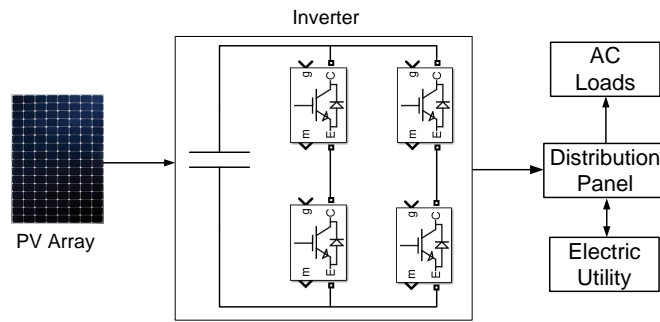
Grid Connected: It is the most popular type of PV system which is connected to the local electricity network allowing the surplus amount of the generated solar electricity to be sold to the utility. Such systems typically consist of one or more photovoltaic panels, a DC/AC power converter/inverter, racks, and electrical interconnections. Additionally, such systems could also include maximum power point trackers (MPPT), battery systems and chargers, solar trackers, software for energy management, solar concentrators etc.

Stand-alone: Stand-alone PV systems are designed to operate independent of the utility grid, and are generally designed and sized to supply certain DC and/or AC electrical loads. An inverter can be used to convert AC power from DC power generated by the PV array of the PV system, enabling the use of normal appliances without mains power.

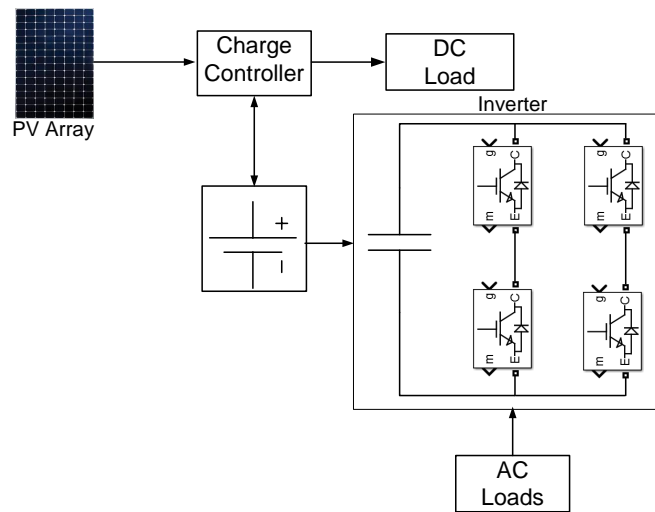
Hybrid System: The hybrid system is a combination of one or more sources like photovoltaic (PV) array, wind turbine, and battery storage via a common dc bus to ensure a consistent supply of electricity. A hybrid system can be stand-alone or grid connected PV system [16].

1.4 Maximum Power Extraction Algorithms

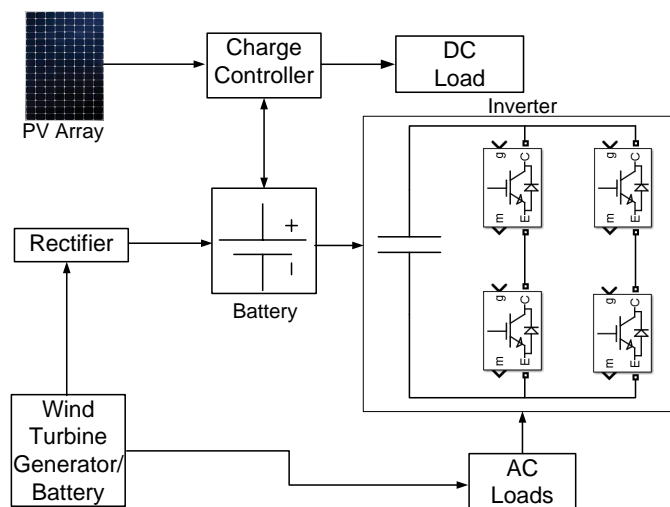
The conversion of PV energy into electrical energy is one of the rapidly growing technology across the globe, PV system has some limitations like high installation cost, low energy conversion efficiency and irregularity in power generation due to dependency on environmental changing conditions [17]. As the output characteristic of the PV panel is non-linear, fluctuation in its output power is affected by solar insolation and temperature. Therefore, some maximum power point algorithms are to be developed



(a)



(b)



(c)

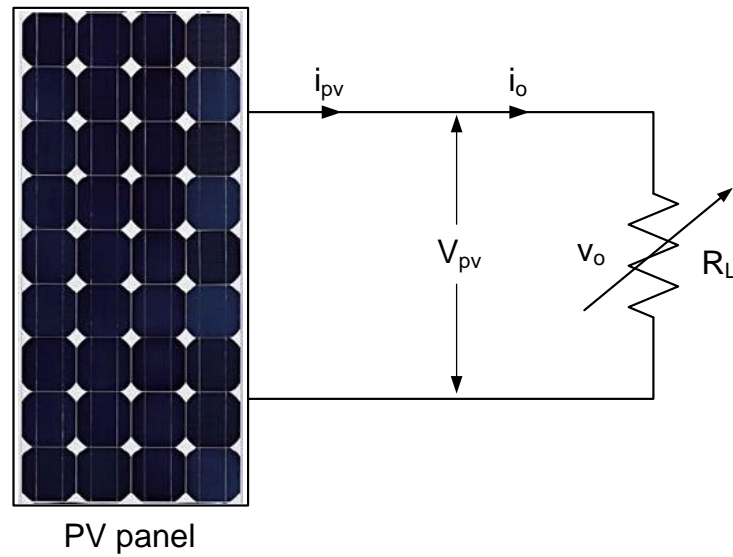
Figure 1.5: Types of PV system (a) Grid connected, (b) Stand-alone (c) Hybrid

which can extract maximum possible power from PV panels and deliver it to load. Hence, research on MPPT is of great importance for maximizing the power extraction from PV panels [18] [19] [20].

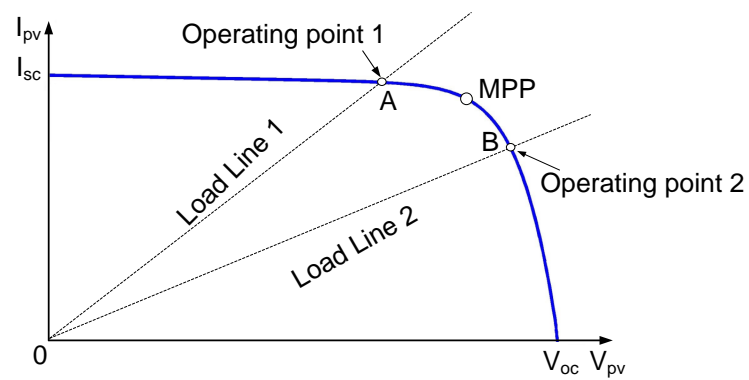
A lot of research has been carried out in the past to improve the efficiency and power quality of PV system [21]. PV systems have low energy conversion efficiency due to their nonlinear and time-varying I-V and P-V characteristics with respect to variation in solar insolation and temperature. Hence, the PV systems need to be operated at their MPPs because at the MPP, a PV panel operates most efficiently as it delivers the maximum power. To track the MPP, a maximum power point tracker (MPPT) [22] [23] is usually used in the PV system.

There exists a single point called MPP (V_{mp} , I_{mp}) at which output power of a PV panel is the maximum. When a load is directly connected to the PV panel as shown in Fig.1.6(a), then the operating point of load is defined by the intersection of its I-V characteristics with the load line as in Fig.1.6(b). There are two operating points A and B for two different values of R_L . Powers at these points A and B are definitely less than the MPP as they are not aligned with MPP. This means that the operating point of PV panel with direct coupled load is defined by the load and maximum possible power is delivered. When load varies, then the operating point of PV system also changes which is undesirable.

Therefore, a method is to be developed which will move the operating point of the load towards MPP which can be achieved by connecting an intermittent between source and the load i.e. a DC-DC converter along with the MPPT algorithm as shown in Fig.1.7. The MPPT algorithm calculates the reference operating point (V_{ref}) at which power is maximum and then the DC/DC converter forces the PV system to operate at that reference point. The PV system with MPPT is an efficient system because it changes the operating point along MPP of the PV module and gives maximum power at changing insolation conditions and is shown in Fig.1.7. The behavior of P-V characteristics curve under uniform and non-uniform insolation conditions is shown in



(a)



(b)

Figure 1.6: (a) PV panel with directly connected load and, (b) Operating point of a PV system with direct coupled load

Fig.1.8.

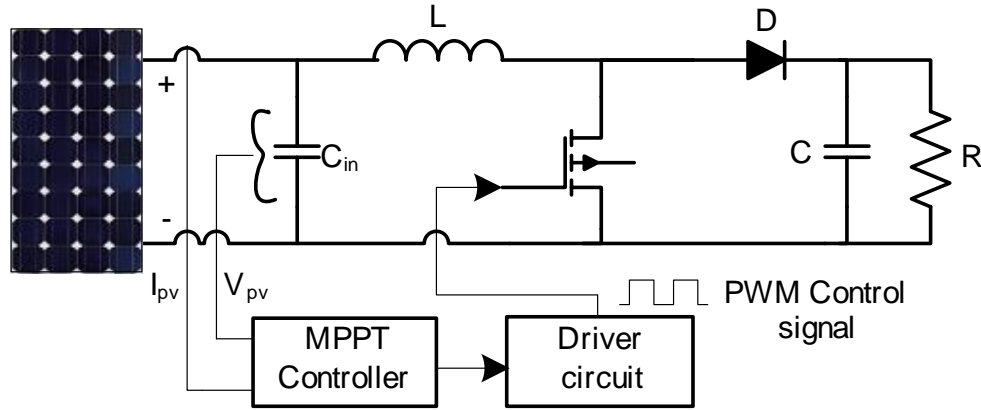


Figure 1.7: Standalone PV with MPPT

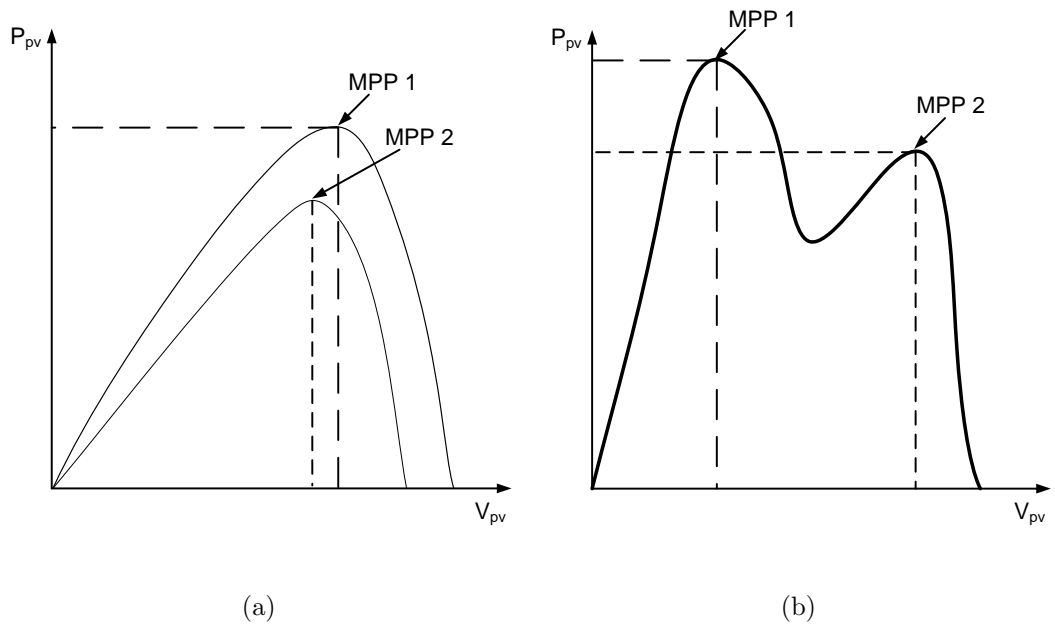


Figure 1.8: MPPTs under (a) Uniform Insolation, (b) Non-uniform Insolation

PV systems with MPPT techniques are used in many applications like water pumping, satellite power supply, grid-tied, household appliances etc. throughout the globe.

The MPPT efficiency(η) [3] can be calculated as

$$\eta = \frac{V_{pv} * I_{pv}}{IA} \quad (1.1)$$

where I , A are the irradiance levels and the area of the cell, V_{pv} , I_{pv} are the PV voltage and current. The quality of the cell is measured by a calculation called Fill Factor(FF). FF can be defined as the ratio of actual maximum power output to the ideal maximum power output. FF can be written as

$$FF = \frac{V_m I_m}{V_{oc} I_{sc}} \quad (1.2)$$

1.5 Partial Shading Conditions

Under uniform irradiance, there exists a single MPP in the Power-Voltage characteristics curve as shown in Fig.1.9.

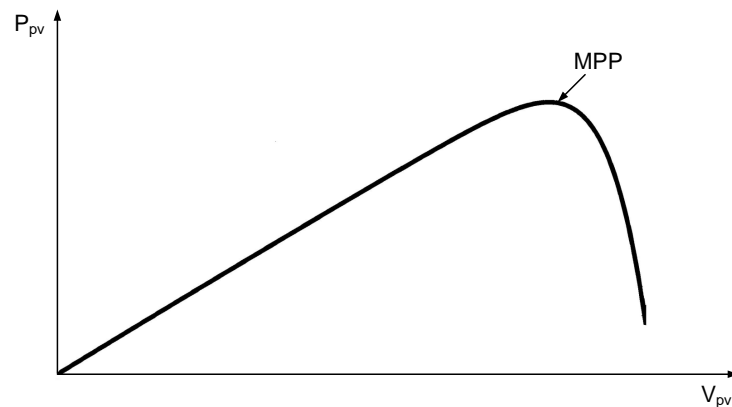


Figure 1.9: P-V characteristics curve exhibiting single MPP under uniform insolation level

But such system becomes complicated, when the PV power system receives non-uniform irradiance resulting in partial shading which is an unavoidable complication that significantly reduces the efficiency of the overall system. When one(or many) of

the module in a solar array comes under the effect of shading(which can be due to trees, neighboring buildings, clouds and many more circumstances can be as shown in Fig.1.10), its voltage drops, so, it works as a load instead of working as a generator resulting in multiple peaks with several local and one global peak (GP). Thus, this peaks leads to a great challenge for designing an appropriate MPP tracker [24] [25] for a PV system. A Bypass Diode(BD) is connected to ensure that particular shaded module does not get damaged. Voltage mismatch can occur in parallel connected modules. So, a blocking diode is connected for providing protection under such conditions.

Under Partial shading (when some part of module is under shading), BD starts conducting as shown in Fig.1.11. So, in P-V curve we do not get a single maximum power point (MPP) but receive several local peaks(LP) and one global peak(GP) as shown in Fig.1.12. BD can be uninstalled from the system to simplify the complications of multiple peaks, but as a result power is reduced which significantly increase the cost of solar power generation.



(a)

(b)

Figure 1.10: Possible Shading Scenarios [4]

Mismatch loss : Mismatch loss(ML) is a serious problem in PV modules and arrays under some conditions because the output of the entire PV module under worst case conditions is determined by the solar cell with the lowest output. For example, when one solar cell is shaded while the remaining in the module are not, the power being generated by the good solar cells can be dissipated by the

lower performance cell rather than powering the load. This in turn can lead to highly localised power dissipation and the resultant local heating may cause irreversible damage to the module. Mismatch in PV modules are mainly of two types:

Internal ML: It occurs due to the variation in PV source parameters of a module due to changes of its physical conditions.

External ML: It occurs due to change of solar irradiation i.e., partial shading.

$$ML = P_1 - P_2 \quad (1.3)$$

where P_1 and P_2 are the changes in insolation levels.

The impact and power loss due to mismatch depend on:

- the operating point of the PV module
- the circuit configuration
- the parameter which are different from the remainder of the solar cells

Hotspot situation :Hot-spot occurs in a module when its operating current exceeds the reduced short-circuit current (I_{sc}) of a shadowed or faulty cell or group of cells as shown in Fig.1.13. When such situation occurs, the affected cell or group of cells is forced into reverse bias and must dissipate power. If the power dissipation is more, the reverse biased cell can overheat resulting in melting of solder and/or silicon and deterioration of the encapsulant and backsheet.

To avoid such situation, a BD is connected in parallel, but with opposite polarity, to a solar cell. Under normal operation, each solar cell will be forward biased and therefore the BD will be reverse biased and will effectively be an open circuit. However, if a solar cell or panel becomes faulty or open-circuited, the BD provides a current path, thereby allowing the current from the good solar cells to flow in

the external circuit rather than forward biasing each good cell. Similarly, if a group of modules connected in parallel to another group or a battery, in order to avoid reverse current flow from one to another, a blocking diode is connected. The importance of bypass and blocking diode in a PV panel/array is clearly shown in Fig.1.11 and its effect on P-V characteristics curve can be seen in Fig.1.12.

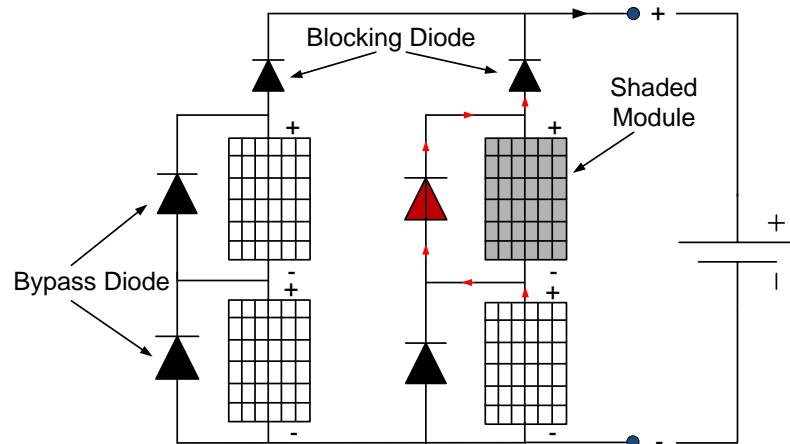


Figure 1.11: Effect of Bypass and Blocking diode under PSCs

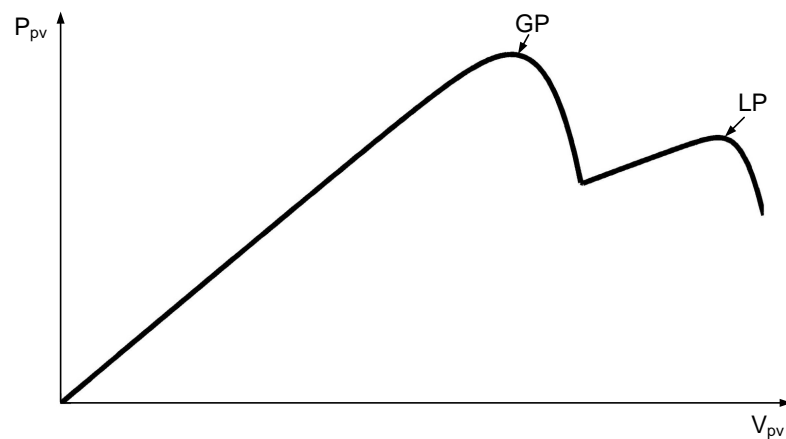


Figure 1.12: P-V characteristics curve exhibiting multiple peaks

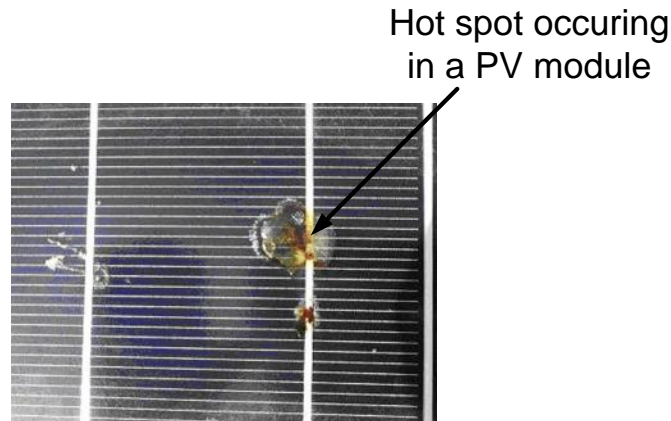


Figure 1.13: Hotspot occurrence [5]

1.6 Motivation of the Thesis

- P-V characteristics curve under PSCs exhibits multiple peaks i.e the problem is transferred from single global problem into multimodal problem i.e. no. of local minima and one GP.
- The determination of global MPPs depend on the stochastically varying shading pattern, as well as the configuration of the PV modules within a PV array. Global MPPT algorithms should be implemented considering the stochastic nature of changing solar irradiance to track the global MPP.
- Therefore, there is an opportunity to employ an efficient evolutionary computing technique to address the aforementioned optimization problem.

1.7 Organization of the Thesis

- Chapter 2 presents the literature review on maximum power extraction algorithms that have been reported in both uniform and non-uniform solar irradiation situations. Subsequently, the problem formulation is highlighted.

-
- Chapter 3 discusses about the experimental setup used in the subsequent chapters for validating the proposed MPPT controller.
 - Chapter 4 presents modeling of a PV module with and without BD and also provides detailed analysis of different configurations for finding global peak of PV arrays under PSCs.
 - Chapter 5 presents the development of a new maximum power point algorithm in view of tracking the GP under partial shading conditions. The proposed MPPT scheme overcomes the limitations of some of the existing MPPTs such as lower tracking efficiency, steady-state oscillations, and transients as encountered in conventional MPPT techniques.
 - Chapter 6 proposes a Hybrid MPPT algorithm which is able to track GP under rapidly changing insolation patterns. The proposed technique is able to scale down the search space of GWO which helps to speed up for achieving faster convergence towards the GP.
 - Chapter 7 provides the general conclusion of the thesis together with the contributions and scope of future work.

Chapter 2

Literature Review on Maximum Power Extraction Algorithms and Problem Formulation

2.1 MPPT for Uniform Insolation

Numerous MPPT techniques are presented in literature such as

- 1) Curve Fitting Technique [26]:The curve fitting defines an appropriate curve to fit the measured values and uses a curve function to analyze the relationship between the variables.
- 2) Fractional Short Circuit Current(FSCI) Technique [27]:This method uses the approximately linear relationship between the MPP current (I_{mpp}) and the short circuit current (I_{sc}), which varies with the irradiance and temperature.

$$I_{mpp} \approx K_{sc}I_{sc} \tag{2.1}$$

The value of K_{sc} varies between 0.64 and 0.85.

- 3) Fractional Open Circuit Voltage(FOCV) Technique [27]:This method uses the approximately linear relationship between the MPP voltage (V_{mpp}) and the open circuit voltage (V_{oc}), which varies with the irradiance and temperature.

$$V_{mpp} \approx K_{oc} V_{oc} \quad (2.2)$$

It is found that the value of K_{oc} varies between 0.78 and 0.92.

- 4) Perturb & Observe Technique/Hill Climbing Technique [28] [29]:

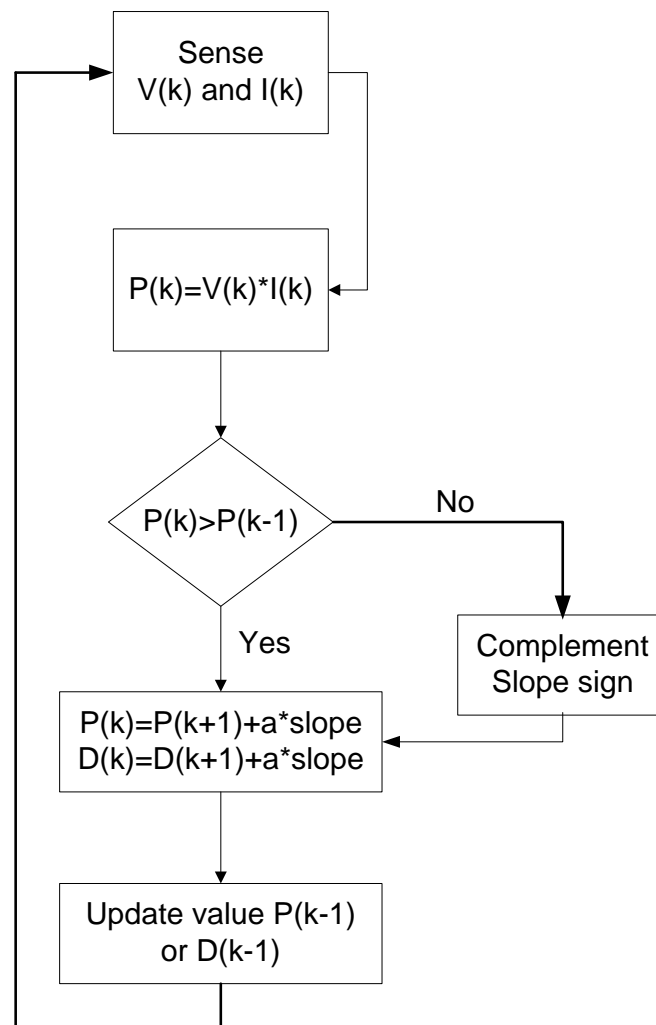


Figure 2.1: Flowchart of Perturb & Observe/ Hill Climbing MPPT

Hill-climbing involves a perturbation on the duty cycle of the power converter and P&O a perturbs the operating voltage of the DC link between the PV array and the power converter. The flowchart of P&O and duty cycle control is shown in Fig.2.1.

5) Incremental Conductance(INC) [30] [31]:

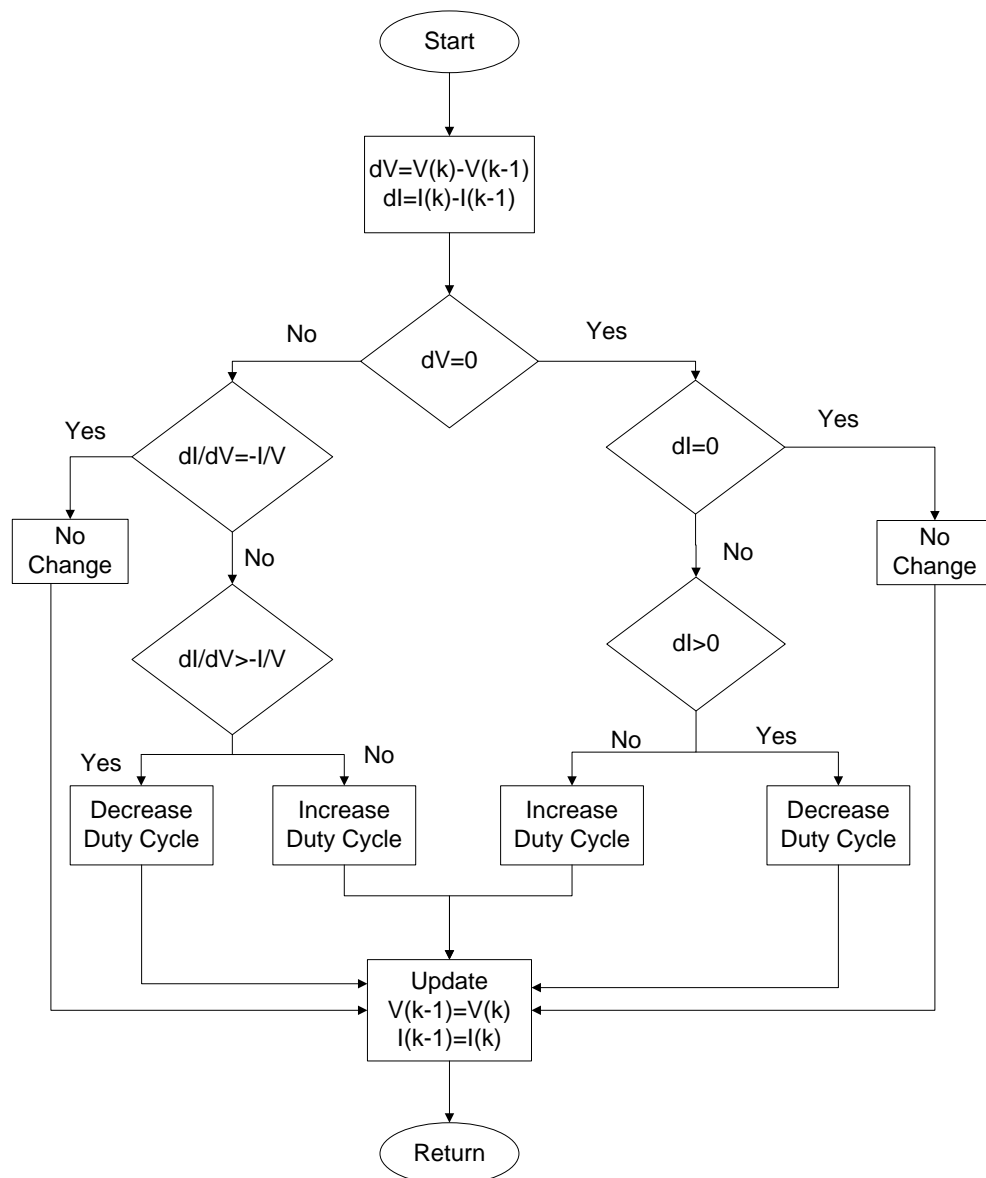


Figure 2.2: Flowchart of Incremental Conductance MPPT

The incremental conductance algorithm is based on the fact that the slope of the curve power vs. voltage (current) of the PV module is zero at the MPP, positive (negative) on the left of it and negative (positive) on the right. The flowchart of the Incremental Conductance MPPT is shown in Fig.2.3.

- 6) Ripple Correlation Control (RCC) Technique [32]: RCC uses the ripple imposed by the power converter on the PV array to track the MPP. It correlates dp/dt with di/dt or dv/dt , to drive the power gradient to zero, which happens when the MPP is reached.
- 7) Look-up Table Technique [33]: This method requires real time data or data obtained from more accurate model which mimics the behavior of the actual PV module.
- 8) Steepest Decent MPPT Technique [34]: The MPPT tracking problem considers the maximization of power (P), which can be achieved by $dP/dV=0$.

- 9) Differentiation (DF) Technique [35]: This technique determines MPP of a PV system on solving

$$\frac{dP}{dT} = \frac{d(IV)}{dT} = I \frac{dV}{dT} + V \frac{dI}{dT} = 0 \quad (2.3)$$

But, this technique is very difficult because at least eight measurements and calculations are required.

- 10) One Cycle Control (OCC) Technique [36]: OCC is a nonlinear control technique based on the integration of a switched variable (voltage or current) to force its average value to be equal to some control reference.
- 11) Forced Oscillation (FO) Technique [37]: This technique is based on injecting a small-signal sinusoidal perturbation into the switching frequency and comparing the ac component and the average value of the panel terminal voltage.
- 12) Linearization (Linr) Based MPPT Technique [38]: Both PV module and converter demonstrate nonlinear and time-variant characteristics, which make the MPPT

design difficult. Based on that relationship of voltage and current, a linear approximation of the MPP locus is derived, whose parameters are simply related to those of the electrical parameters of a PV cell.

13) Intelligent MPPT Techniques

(i) Fuzzy Logic(FLC) Based MPPT Technique [39]:

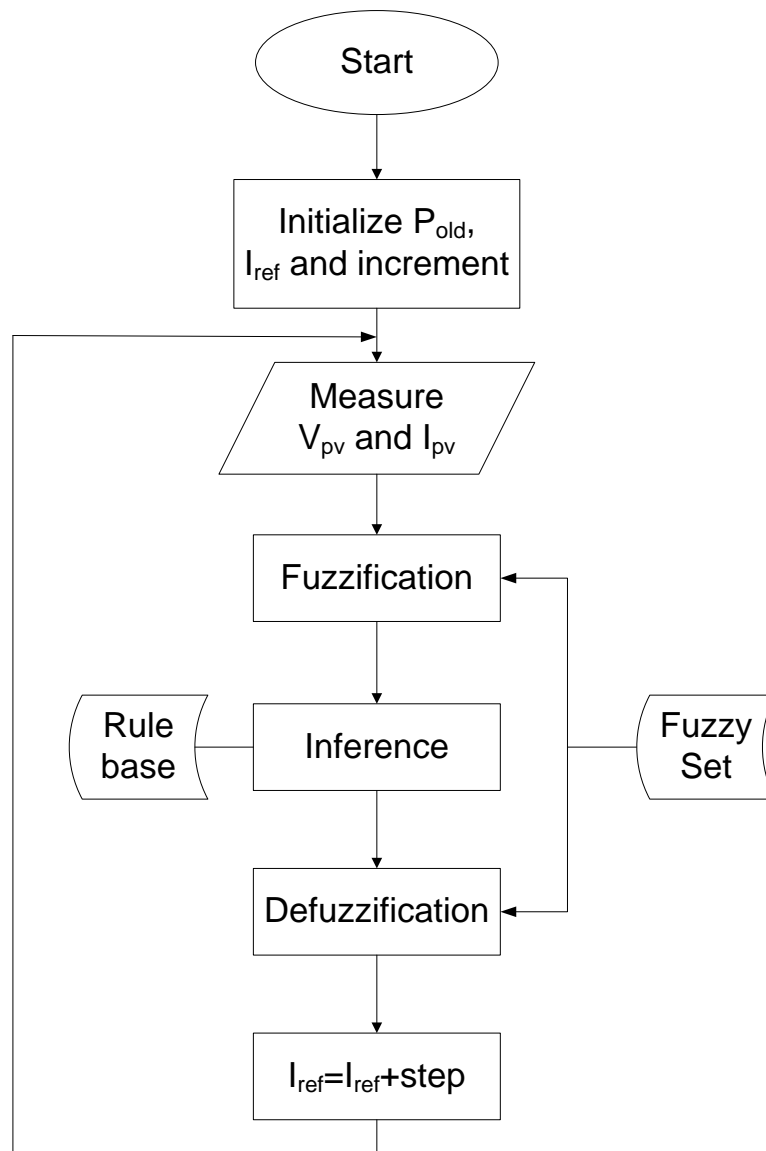


Figure 2.3: Flowchart of Fuzzy logic controller MPPT

In FLC, basic control action is determined by a set of linguistic rules which are determined by the system. Since the numerical variables are converted into linguistic variables, mathematical modeling of the system is not required in FLC. The FLC comprises three parts: fuzzification, rule base table lookup, and defuzzification.

(ii) Artificial Neural Network(ANN)Based MPPT Technique [40]:Neural networks commonly have three layers: input, hidden,and output layers. The number of nodes in each layer vary and are user-dependent. The input variables can be PV array parameters like V_{oc} and I_{sc} , atmospheric data like irradiance and temperature, or any combination of these.

15) Sliding Mode Controller(SMC) based MPPT Technique [41]:The same concept of INC is used here. The dc/dc converter is designed such that its switching control signal(u) is generated as shown as

$$u = \begin{cases} 1, & \text{if } h < 0 \\ 0, & \text{if } h \geq 0 \end{cases} \quad (2.4)$$

where $u=0$ implies the converter switch is open otherwise the switch is closed. In this way, the converter is forced to operate at MPP.

14) DC Link Capacitor Droop Control (DLCDC) Technique [42]:DC-link capacitor droop control is a MPPT technique that is specifically designed to work with a PV system that is connected in parallel with an ac system line.

It is very difficult to analyze all of these MPPT techniques by studying their structures,because each MPPT technique has its own pros and cons. Control strategies adapted are one of the ways to analyze the MPPTs which can be classified as indirect control, direct control and evolutionary computational methods.

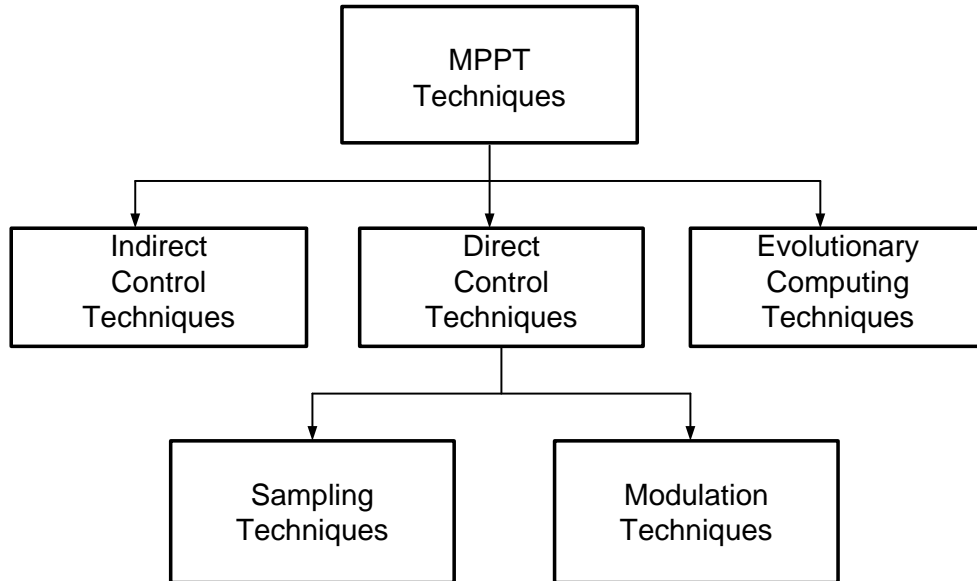


Figure 2.4: Classification according to Control Strategies

Indirect control techniques are based on use of a database that includes parameters and data such as characteristics curves of the PV panel for different irradiance and temperature or on using some mathematical empirical formula to estimate MPP. Direct control strategies can seek MPP directly by taking the variations of the PV panel operating points without any prior knowledge of the PV panel parameters. MPPT schemes can be further classified into two types based on, sampling methods and modulation methods. In sampling methods, at each sampling instant, past and previous information V_{pv} and I_{pv} are captured which are used to track the MPP location. In modulation methods, the MPP can be tracked by generating oscillations automatically by the feedback control. Fuzzy logic inference and artificial neural network methods do not necessitate exact mathematical model of a system to evaluate which still provide necessary decision outputs and can handle nonlinearities. A broad classification of MPPT control techniques is presented in Fig.2.4. Further, a comparison of different MPPT techniques according to the classification is also provided in Table 2.1.

Table 2.1: Comparison of different MPPT Techniques

MPPT Technique	Type of Control	Control Variable	Circuitry (A/D)	Parameter Tuning	Complexity
CF	Indirect	V_{pv}	Digital	Yes	Simple
FSCI	Direct	I_{pv}	Both	No	Simple
FOCV	Direct	V_{pv}	Both	No	Simple
P&O	Direct	V_{pv}, I_{pv}	Both	No	Complex
INC	Direct	V_{pv}, I_{pv}	Digital	No	Complex
RCC	Direct	V_{pv}, I_{pv}	Analog	Yes	Complex
SD	Direct	V_{pv}, I_{pv}	Digital	No	Medium
DF	Direct	V_{pv}, I_{pv}	Both	Yes	Complex
OCC	Direct	V_{pv}, I_{pv}	Both	Yes	Simple
FO	Direct	V_{pv}, I_{pv}	Analog	Yes	Complex
Linr	Direct	Irradiance	Digital	Yes	Medium
DLCDC	Direct	V_{pv}	Both	Yes	Simple
FLC	EC	V_{pv}, I_{pv}	Digital	Yes	Medium
ANN	EC	V_{pv}, I_{pv}	Digital	Yes	Medium
SMC	EC	V_{pv}, I_{pv}	Digital	No	Complex

2.1.1 Advantages and Disadvantages of Different MPPT Techniques

Curve-Fitting Technique:

Advantages:

- Cost effective and simple
- No sensors required for measurement of voltage and current during MPP tracking.

Disadvantages:

- Requires accurate information of the PV system.
- Not universal.

FOCV and FSCI Techniques:

Advantages:

- Simple and inexpensive.

Disadvantages:

- Not suitable for environmental changing conditions.

Perturb & Observe:

Advantages:

- Easy to implement and produce accurate results.
- Tracks maximum power under uniform insolation

Disadvantages:

- Accuracy is dependent on the size of perturbation.
- Output voltage and current of PV panel oscillates at steady state.

Incremental Conductance:

Advantages:

- Efficiency is same as P&O.
- Good yield under rapidly changing atmospheric conditions.

Disadvantages:

- Requires complex and costly control circuits.

- Sensors are needed to complete MPPT action.

Ripple Correlation Control(RCC) Technique:

Advantages:

- Artificial perturbation is not required as it is inherited by DC/DC converter.
- Accurate result for a wide range.

Disadvantages:

- Very complex.
- Time consuming technique.

Steepest Decent MPPT Technique:

Advantages:

- Fast MPPT performance.
- Less complex than that of Gauss-Newton because double derivative terms not present in algorithm.

Disadvantages:

- Accuracy, speed and stability are dependent on initial conditions and perturbation step-size.

Differentiation(DF) Technique:

Advantages:

- Fast MPP tracking.

Disadvantages:

- Very complex calculation.

One Cycle Control(OCC) Technique:*Advantages:*

- Constant switching frequency operating mode.
- Does not require any digital signal processors or multipliers.

Disadvantages:

- MPPT tracking performance is not good at changing weather conditions.

Forced Oscillation(FO) Technique:*Advantages:*

- Adaptive in nature.
- Easy to implement.

Disadvantages:

- Difficult to control.
- Variable operating frequency and related complex filters.

Linearization(Linr)Based MPPT Technique:*Advantages:*

- MPP estimated through a set of simple linear equations.

Disadvantages:

- Limited range of operating conditions.

DC Link Capacitor Droop Control (DLCDC) Technique:*Advantages:*

- Panel voltage is to be measured for MPP calculation.

Disadvantages:

- Needs a DC-link.
- Limited applications.

FLC Based MPPT Technique:

Advantages:

- Fast response, no overshoot and less steady state error.

Disadvantages:

- Rules based technique.

ANN Based MPPT Technique:

Advantages:

- On-line tracking is possible.
- Accurate and fast once it is tuned.
- Independent of environmental conditions.

Disadvantages:

- Tuning and MPP calculation takes large time.

Sliding-Mode Based MPPT Technique:

Advantages:

- Simple control laws and fast MPP tracking.
- Guaranteed stability.

Disadvantages:

- Applicable to limited range, tuning takes large time.
- Not suitable for changing insolation levels.

2.2 MPPT for Non-Uniform Insolation levels

When one (or many) of the module in a solar array gets shaded due to some intermittent between sun and the PV arrays like trees, neighboring buildings, clouds and many other circumstances. Such situation results in voltage drops, resulting to act as a load instead of a generator. Unfortunately, the power-voltage characteristic curve of the PV array becomes complicated resulting in multiple peaks i.e. various local peaks and one global peak. Owing to the occurrence of multiple local peaks i.e. MPPs, the conventional MPPTs are not appropriate in providing maximum power tracking. Because Partial Shading Conditions (PSCs) frequently occur due to passing clouds, trees, or buildings, it is necessary to develop different MPPT schemes that can track global peak (GP) under PSCs. The mismatch occurrence of non-uniform irradiance which leads to decrease of the output power, even generates hot-spot and causes damage to those cells. Such situations can be avoided by using bypass and blocking diodes. While some techniques have been proposed in [43] [44] such as MPPT that work well under partially shaded conditions but many of these suffer from limitations such as lower tracking efficiency and oscillations in the output power. Since the dynamics of the PV system under partial shading is time-varying, MPPT design for PV power system should possess following features: global MPP tracking ability for different conditions (shade, degradation, fault, etc.), adaptability to P-V characteristics change of PV array, smooth and steady MPPT algorithms [45] [46] [47].

As the partial shading is difficult to handle, there is a need for finding an appropriate MPPT technique which could locate the global MPP (GMPP) under any mismatching conditions [48] [49] [50]. Patel et al. [7] presented about I-V and P-V characteristics of a PV array under non-uniform insolation due to partial shading which results in multiple peaks. Some critical observations [50] such as the peaks on the PV curve occurring nearly at multiples of 80% of open-circuit voltage of the module and the minimum displacement between successive peaks being nearly 80% of V_{oc} of the module are

presented. In [51], the proposed algorithm incorporates an online current measurement and periodic interruptions to address problems related to shading conditions. In [48] and [49], global MPPT techniques based on the measurements of the PV array open-circuit voltage and short-circuit current is discussed. In [52] [53], relationship between the load line and the MPP locus is discussed for a fast converging MPPT algorithm. A control loop is introduced in [52] to ensure the PV system operates in accordance with the MPP resulting in reduction of MPP search time.

Many researchers have worked on Real MPPT (RMPPT) under PSCs [54] [55] [56] [45] [46] [47] [43] [44]. The real MPPT method [57] first detects the variations in the PV voltage and current to identify the occurrence of partial shading. Then, the operating point is changed according to a predetermined linear function and then the conventional MPPT is applied to track the real MPP. In [54], a two-stage MPPT combined with the instant on-line measurement of V_{oc} and I_{sc} was proposed. In [55] [56], authors have discussed about the relationship between changing weather conditions i.e. array configuration, irradiance and module temperature and output power of the PV array and further complications due to multiple peaks. The authors have shown experimentally about the behaviour of MPPT under the uniform and non-uniform irradiance conditions. A new method to track the GMPP of PV array under PSC is reported by controlling converter voltage by using improved P&O [58] [59]. In [60], an adaptive MPPT (AMPPT) scheme is developed which proved to track the global MPP effectively, fast and smoothly. In [61], the MPPT algorithm is developed using a Fibonacci sequence which does not provide accurate GMPP. Also, different possible ways of modeling under partial shading and different orientation of photovoltaic modules are discussed in [62] [63]. Experimental study of shading hazards in the IV characteristic of a photovoltaic module is discussed in [64]. In [65], modeling the reverse characteristics of PV cells is discussed.

A few improved IC algorithms were also proposed to improve the MPP tracking capability during fast changing irradiance level and load [66] [66]. In [66], a new

duty cycle control is proposed to track GMPP which eliminates the use of sensor circuits at the output of dc-dc converter. In [66], a method is proposed which responds accurately during increase in insolation level resulting in zero oscillation and introduces new tracking steps to detect the change in insolation level. To achieve a fast MPP tracking response, a simple trigonometric rule has been presented in [67] to establish relationship between the load line and I-V curve. The method eliminates need of an extra control loop and intermittent disconnection which provides fast convergence towards the MPP. An analytical modeling of PV system under PSC is discussed in [68] where a multidimensional PV array configuration correlating to different degrees of partial shading is presented. This model is able to emulate the behavior of different patterns of a PV system during both uniform and non-uniform insolation levels through the multidimensional PV structure. A dynamic MPPT controller for PV systems under fast varying insolation and PSCs is proposed in [69] which uses a scanning technique to determine the maximum power deliver capacity of the panel at a given operating condition.

Currently, a number of evolutionary computing techniques such as particle swarm optimization (PSO) [70] [71] [72], firefly [73], ant colony [74], cuckoo search [75] are of great interest for developing MPPT techniques to track the GP under PSCs. In [70], an improved maximum power point tracking (MPPT) method for the photovoltaic (PV) system using a modified particle swarm optimization (PSO) algorithm is discussed which reduces the steady state oscillation (to practically zero) once the maximum power point (MPP) is located. In [70] [71] [72], a new technique is proposed which replaces the PI control loop with direct duty cycle control method which makes the system more simpler. A new technique is discussed in [73] having advantages like simple computational steps, faster convergence and implementation on a inexpensive microcontroller. In [74], a new control scheme is proposed which ensures the ability to find the global MPP, but also gives a simpler control scheme and lower system cost. A cuckoo search [75] based MPPT is found to be advantageous in terms of

faster convergence, higher efficiency is proposed which outlines the concept of cuckoo search by highlighting the significance of the levy flight by influencing the algorithm's convergence.

Also, different hybrid MPPT techniques are developed which is a fusion of two techniques which guarantees to achieve faster convergence are discussed in [76] [77] [78] [79]. A highly efficient MPPT having high speed tracking by means of a fast estimate of the maximum power voltages of the PV modules and of the inverter is discussed in [76]. The combination of two basic techniques i.e. P&O and Fractional Open Circuit Voltage (FOCV) technique is discussed to overcome the inherited deficiencies found in P&O technique in [77]. In [78], a hybrid approach is discussed having the global search ability of ant-colony optimization (ACO) and local search capability of P&O method to yield faster and efficient convergence. The integration of swarm intelligence with P&O algorithm is discussed in [79] to yield faster convergence to the global peak(GP). Here, the methodology has been first simulated in two different PV configurations under varying shading patterns and experimentally verified using a microcontroller based experimental system.

2.3 Review Remarks

- Most of the MPPT algorithms reported in the literature is discussed in Section 2.1 considering uniform solar irradiances. Also, different MPPT algorithms which can handle non-uniform solar irradiances are discussed in Section 2.2.
- In order to handle conditions such as fast weather variations of PV module and partial shading where multiple peaks occur in the P-V characteristics curve, there a challenge lies to develop global MPPTs in order to extract maximum power from PV arrays under the above non-uniform solar irradiances.
- Although a few global MPPT algorithms have been suggested in the literature

but they do not consider the stochastic nature of solar irradiance and also a lot of voltage and current ripples are observed in the PV output power.

2.4 Objectives of the Thesis

- To model PV modules analytically under partial shading conditions for a Photovoltaic(PV) power system.
- To develop MPPT control algorithms in order to extract maximum power output from the PV system with changing insolation levels, temperature variations and other environmental conditions.
- To develop MPPT algorithms for a PV system under different shading conditions i.e. partial shading, complete shading, inter row shading situations.
- To develop MPPT algorithms for rapidly changing insolation levels for a PV system.
- To propose new adaptive controllers for MPPT considering the uncertainties of the PV system dynamics due to changing solar irradiance at different weather conditions.
- To simulate the proposed MPPT algorithms in MATLAB/SIMULINK and validate using an Experimental set-up.
- To evaluate the efficacy of the proposed MPPT algorithms.

2.5 Problem Formulation

Consider the power-voltage characteristics of a PV array which is subjected to different shading conditions which are more complex in the multiple local MPPs and only one global MPP. Thus, this situation is much different than the case of uniform solar

irradiances, where there is only one MPP. In view of this, there is a need of determining the global MPP. The GMPPT algorithm should be able to develop which will locate the global MPP by using different optimization techniques for maximizing the power extraction from a PV array under non-uniform solar irradiances.

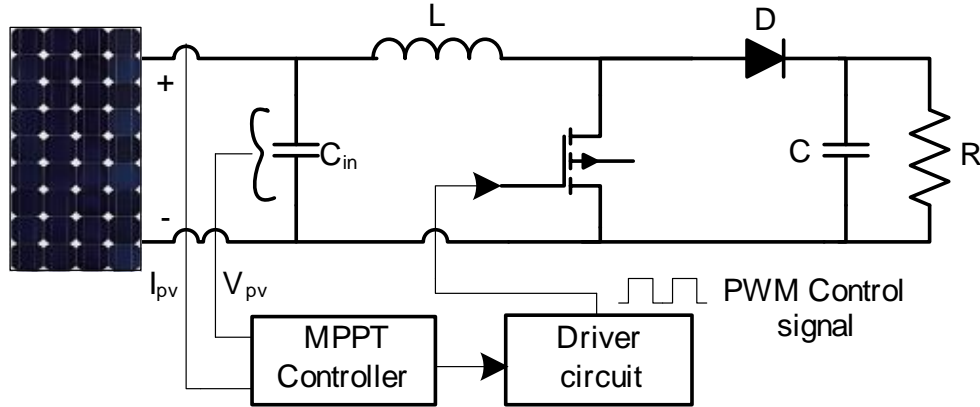


Figure 2.5: A PV system with MPPT

Fig.2.5 shows a proposed topology of MPPT scheme in which G represents irradiance level in W/m^2 , T is absolute temperature in degree Kelvin, V_{pv} and I_{pv} are voltage and current of PV arrays respectively. Thus, the MPPT control problem in case of non-uniform solar irradiance turns out as a global optimization problem resulting in a global MPPT algorithms.

The objective here is to maximize the power extraction from the PV arrays under PSCs. The optimization problem can be stated as follows. Let a solution vector of duty cycles with N_p wolves is given by:

$$x_k^i = d_g = [d_1, d_2, \dots, d_j] \quad (2.5)$$

where $j=1, \dots, N_p$, d is duty cycle, i is current grey wolves and k is iteration number.

The objective function is defined as

$$P(d_i^k) > P(d_i^{k-1}) \quad (2.6)$$

where $P = V * I$ for any instant is the operating power of PV array for the tracking problem.

2.6 Chapter Summary

This chapter provides a comprehensive review of MPPT algorithms for both uniform and non-uniform solar irradiances. Although a vast literature is available on MPPTs for uniform solar irradiances but very few algorithms are reported on MPPTs to work under non-uniform solar irradiances. The conventional MPPT algorithms such as P&O and Incremental Conductance etc. are not appropriate to provide maximum power extraction from PV arrays under PSCs due to presence of multiple peaks appearing around the Power-Voltage characteristics curve. Hence, Global optimization techniques are to be developed for MPPT that would handle the multiple MPPs for stochastically varying solar irradiance.

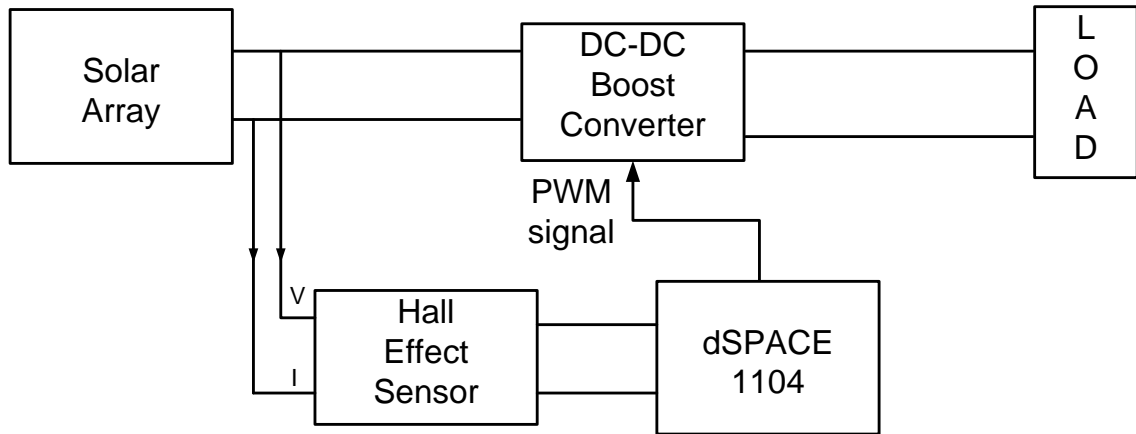
Chapter 3

Development of an Experimental Setup for a PV System subjected to Non-Uniform Solar Irradiances

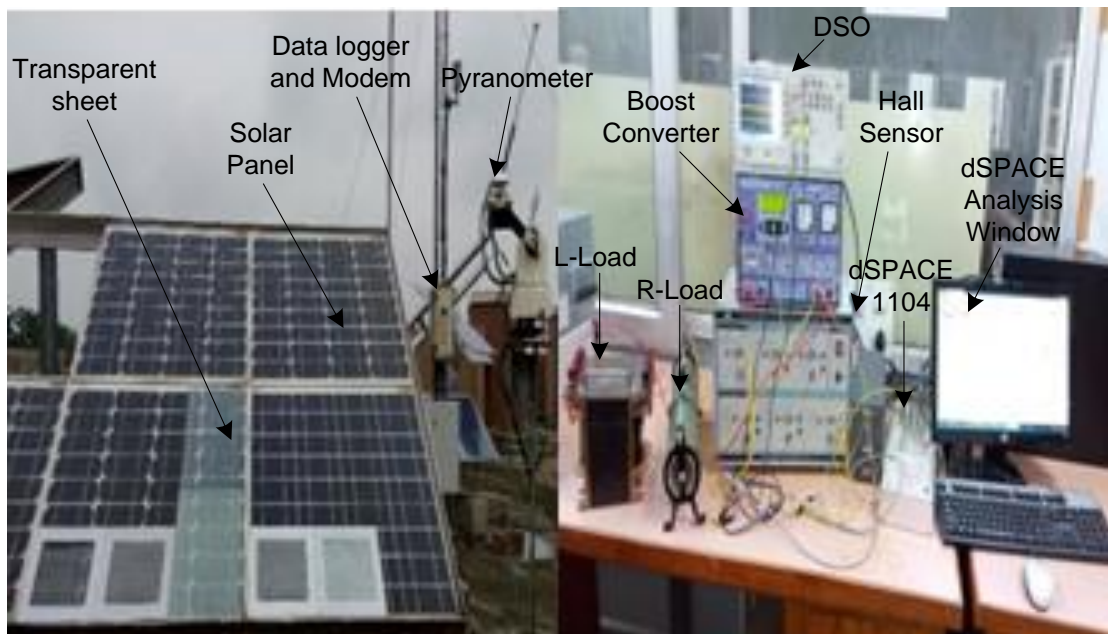
3.1 Introduction

This chapter presents the development of an experimental setup to experiment the performance of newly developed MPPTs for handling partial shading conditions. Here, two different methodologies are discussed in this chapter. One is by using solar panels which depends on insolation which comes directly from the sun and the other is by using solar simulator in order to provide a controllable indoor test facility under laboratory conditions. This chapter addresses the development of experimental setup for verifying the proposed techniques implemented in a PV system using MATLAB/SIMULINK software. The selection of the hardware configuration such as sensors, controller platform, DSO and loads used in the experimentation are discussed here. This chapter helps to implement the developed control algorithms presented in subsequent chapters.

3.2 Experimental Setup using Solar Panels



(a)



(b)

Figure 3.1: (a) Block Diagram (b) Photograph of experimental setup with solar array

To validate the effectiveness of the proposed GWO based MPPT, experiments were carried out on real PV array for both 4S and 2S2P configurations. To create partial shading, transparent sheets of different shapes were placed on PV modules. Fig.3.1 shows the block diagram and experimental setup of the proposed system.

3.2.1 Solar Panel

The solar panel used in the experimentation is of Sukam make having rating of each panel as power tolerance=5%, $V_{mp} = 17.15V$, $I_{mp} = 2.33A$, $V_{oc} = 21.2V$, $I_{sc} = 2.55A$, $K_I(V/^{\circ}C) = -2$, $K_I(mA/^{\circ}C) = 4.7$, $K_V(mV/^{\circ}C) = -2$, $K_P(\%/^{\circ}C) = -0.4$, maximum system voltage=600V and $n_s = 36$ respectively. The photograph of solar panel is shown in Fig.3.2.



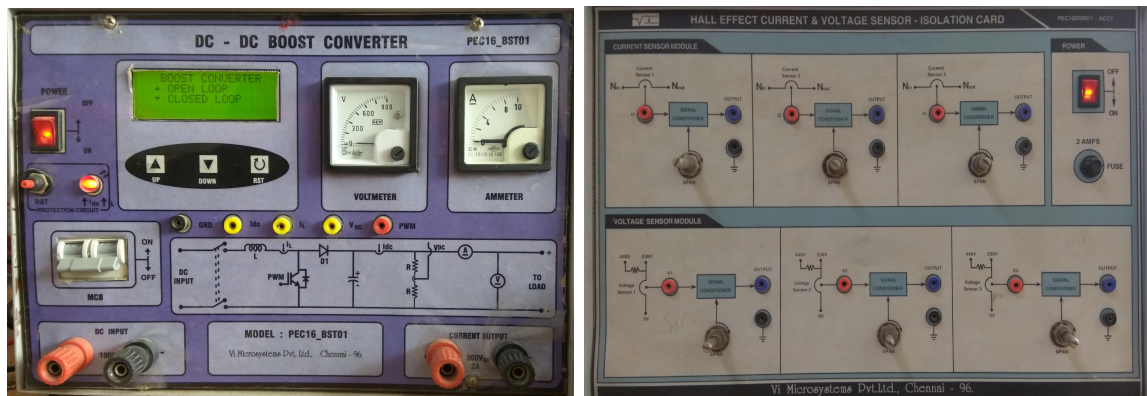
Figure 3.2: Sukam make solar panel

3.2.2 DC-DC Boost Converter

The DC-DC boost converter used in the experiment is IGBT(Model no:SKM75)driven and the components for the designed converter used in experimental set up are chosen as $f_s=25\text{kHz}$, Output voltage ripple= $\Delta V_0/V_0$, $L=10\text{mH}$, $C=33\mu\text{F}$, $V_{in}=(0-130)\text{V}$ and $V_{out}=300\text{V}$. The photograph of DC-DC Boost converter is shown in Fig.3.3(a).

3.2.3 Hall Effect Sensor

The photograph of hall effect sensor having three voltage and current sensors is shown in Fig.3.3(b). Hall effect sensor is used to sense the voltage and current of the PV array before sending it to the controller.



(a)

(b)

Figure 3.3: (a) DC-DC Boost Converter (b) Hall Effect Sensor

3.2.4 DS1104

The DS1104 R&D Controller Board upgrades a PC for rapid control prototyping. The board can be installed virtually in any PC with a PCI slot. It is fully programmable from the SIMULINK block diagram environment and all I/O can be configured graphically. Here, DS1104 is used as a controller having various 8-ADC and 8-DAC channels

to generate PWM signals which are based on 603 power PC floating point processor running at 250MHz and a slave DSP subsystem based on TMS320F240 DSP. In the experimentation, the Slave I/O ports as well as the ADC channels are used. The ADC signal senses the voltage and current from the sensors and supply the values after multiplication of scaling factor to the SIMULINK environment and then the PWM signals are generated. The photograph of the DS1104 board is shown in Fig.3.4.

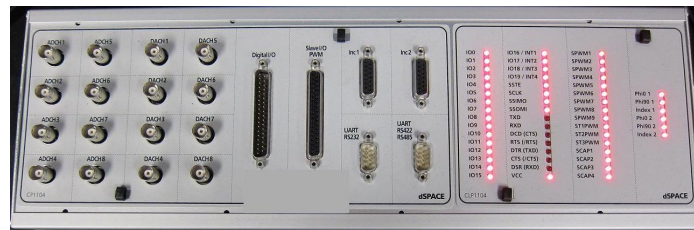
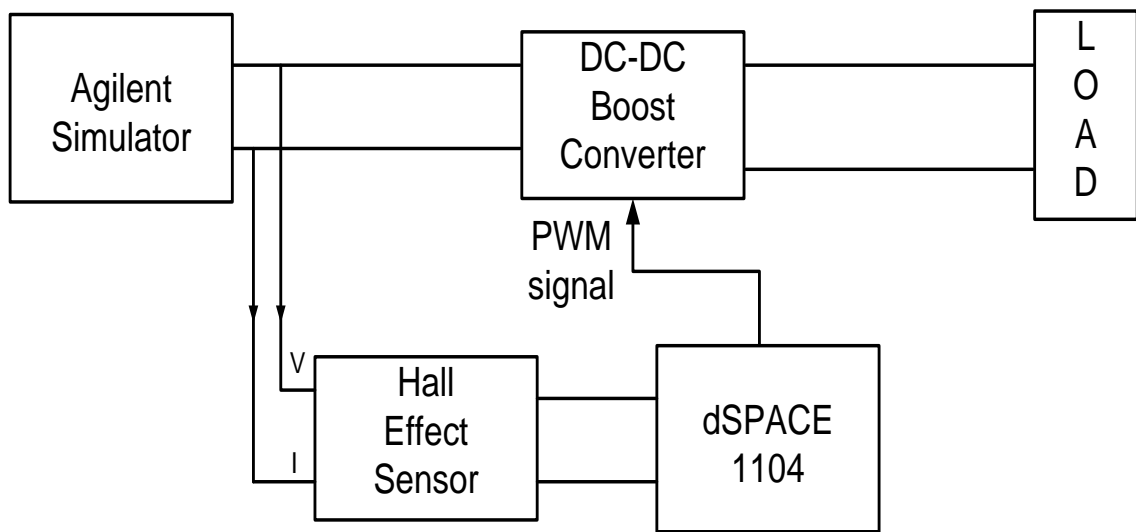


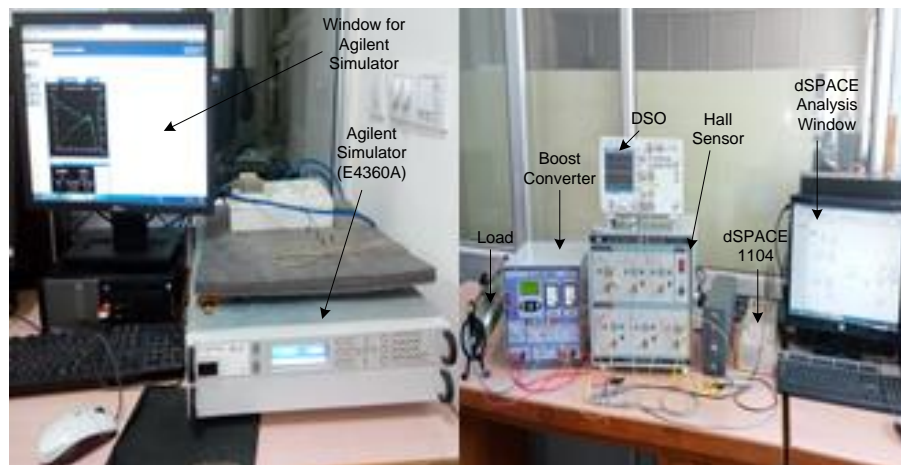
Figure 3.4: DS1104 Board

3.3 Experimental Setup using Agilent Simulator

The block diagram and experimental set up is shown in Fig.3.5. A solar array simulator (SAS), Agilent (E4360A) is used to emulate the PV source power with various situations such as rapidly changing solar insolation. It is a current source with 600W dc output source in which it is possible to generate I-V and P-V curves of PV arrays under shading conditions. The chosen I-V curve is conveniently generated using the Table mode which is fast and accurate for generating different I-V curves for partial shading conditions. dSPACE 1104 is used for implementing MPPT algorithm having 8-ADC and 8-DAC channels to produce PWM signals which is based on a 603 power PC floating point processor and a slave DSP subsystem. A Hall sensor (PEC16DSMO1) is used to sense the voltage and current of the solar simulator and a DC-DC boost converter is used as an intermittent between the source and load to extract maximum possible power.



(a)



(b)

Figure 3.5: (a) Block Diagram (b) Photograph of experimental setup with simulator

3.3.1 Agilent Solar Array Simulator

The Agilent E4360 Modular Solar Array Simulator (SAS) is a dual output programmable dc power source that simulates the output characteristics of a solar array as shown in

Fig.3.6. The E4360 SAS is primarily a current source with very low output capacitance and is capable of quickly simulating the I-V curve of different arrays under different conditions (ex. temperature, age etc.). It provides up to 2 outputs and up to 1200W in a small 2U-high mainframe. The dynamic properties of a solar array simulator are:

1. Consists of 2 outputs of 600W per output in 2U of rack space.
2. Perform remote programming via GPIB, LAN and USB interfaces with SCPI command set (drivers available).
3. Program I-V curves from the front panel without a need for a controller.

3.3.1.1 Multiple Simulation Modes

The E4360 SAS provides three operating modes, Simulator, Table and Fixed modes. To accurately simulate the I-V curve of a solar array, use simulation or table modes. When a standard power supply is needed, use fixed mode.

3.3.2 Solar Array Simulator(SAS) Mode:

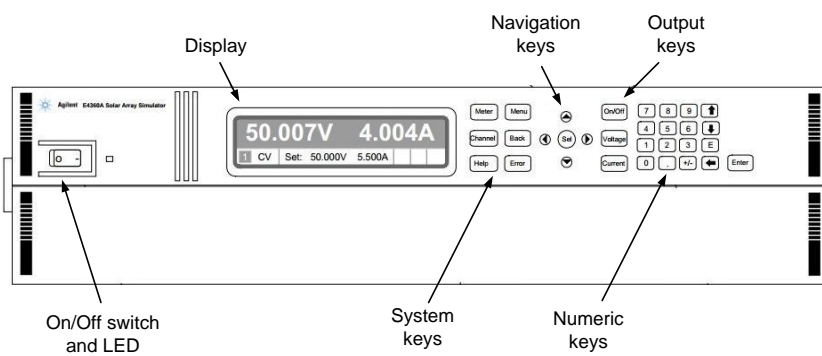
In SAS mode, the output has an I-V characteristics that follows an exponential model of a solar array as shown in Fig.3.7(a). The E4360 SAS internally generates a 4,096 I-V point table. An internal algorithm is used to approximate an I-V curve. This can be done via the I/O interfaces or from the front panel where a PC is not needed.

3.3.2.1 Table Mode:

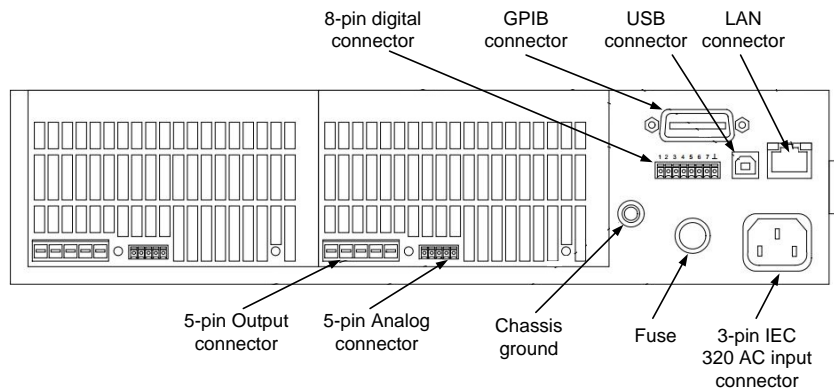
The SAS mode provides a Table mode for a fast and accurate I-V simulation of solar arrays. In this mode, a table of I-V points specifies the curve. Tables are allocated in a non-volatile memory and can be easily stored and recalled. A table can have a minimum of 3 points, up to a maximum of 4000 I-V points.



(a)



(b)



(c)

Figure 3.6: (a) Solar Array Simulator (b) Front view (c) Rear view

3.3.2.2 Fixed Mode:

This is the default mode when the unit is powered on. The unit has the rectangular I-V characteristics of a standard power supply as shown in Fig.3.7(b). It has excellent high speed constant current characteristics and low output capacitance. The main usage of fixed mode is while calibrating or verifying any instrument.

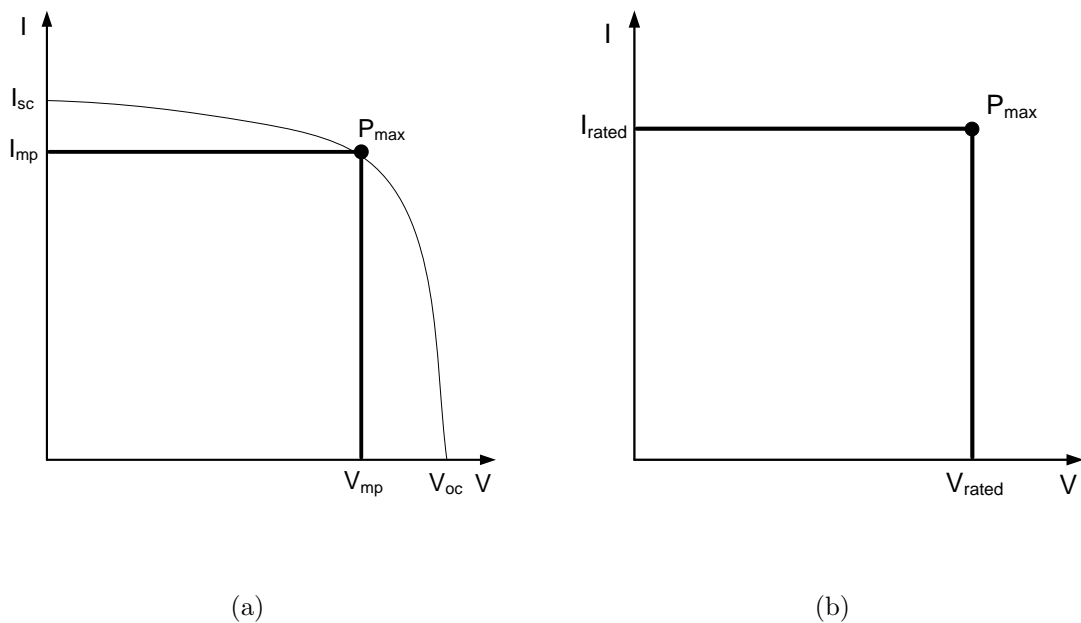


Figure 3.7: (a) SAS Mode (b) Fixed Mode

3.4 Chapter Summary

To verify the different MPPT control algorithms for maximum power extraction for a PV system subjected to partial shading conditions is necessary. So in this chapter details of development of experimental facility for the above is presented in details for verifying the algorithms in subsequent chapters.

Chapter 4

Analytical Modeling and Experimental Prediction of Global Peak under Partial Shading of PV modules for a Photovoltaic System

4.1 Abstract

Partial shading is a commonly encountered issue in a PV system. Analytical modeling of a photovoltaic (PV) system for studying the effects of partial shading with and without bypass diode as well as different orientation of PV modules is discussed here. In this work a new RP configuration is proposed and compared with Series Parallel(SP), Total cross tied(TCT), Bridge linked(BL) and examined under same shading pattern on the basis of maximum power and fill factor. Those models are studied and their performances were compared on the basis of global peak under partial shading conditions(PSCs). Each network connection was analyzed taking care of the non-linearity of the PV cell which is evaluated by using Kirchhoffs voltage and current laws. The

simulation and experimental study conclude that the proposed RP configuration exhibits superior performance over SP, TCT and BL configurations in terms of maximum power and fill factor.

4.2 Introduction

Operation of photovoltaic (PV) power generators is greatly influenced by environmental conditions such as solar insolation and temperature [80]. Under uniform irradiance conditions, the electrical characteristics such as I-V and P-V characteristics of the PV generators have only one single MPP (maximum power point) at which the maximum power can be extracted by employing a suitable MPPT algorithm. However, under non-uniform irradiance conditions, such as partial shading, the P-V characteristics curve generates multiple MPPs in the electrical characteristics of PV generators. Partial shading conditions can have a significant effect on the PV panel operation and in turn on the energy yield of the PV generators [81] [82]. Partial shading may arise due to snow, tree shadow, dirt or ageing.

Partial shading causes mismatch losses resulting in degradation of performances of the PV cells [83]. Not only the power of the shaded cells reduces, but the unshaded cells also get affected due to electrical connection exist with the shaded ones. Such situation results in reverse flow of current which yields power flow across the cells resulting in hotspots. Such adverse effect can be overcome by using bypass diodes in parallel across each module [84]. The P-V curve with and without bypass diode is shown in Fig.4.4 [42] [85] [86].

In view of extracting maximum PV power under non-uniform irradiance, the MPP extraction problem leads to finding out the global MPP rather than a single MPP in case of uniform irradiance condition. To implement a global MPP tracking strategy, the mismatch losses can be minimized by introducing alternative configurations to avoid the series connection of shaded and unshaded module within a PV array. Basically,

most investigations have focused on three configurations, namely series-parallel (SP), bridge linked (BL) and total cross tied (TCT) [62] [63]. The number of power peaks and their values may change depending upon the array configuration. Different techniques have been proposed in the literature [68] [87] to predict the I-V characteristics of PV arrays and obtain the MPP there from. Such models solve the non-linear I-V characteristics of the PV arrays for every operating point in order to determine the corresponding power peaks.

In this work, the behavior of bypass diode is discussed under two different strategies are developed under partial shading conditions. Firstly, (i) the combination of n-oriented modules with bypass diode (ii) array composed of partial shading module without bypass diode. Secondly, four different configurations such as series-parallel (SP), total cross tied (TCT), bridge linked (BL) and proposed ring pattern (RP) configuration are examined and their performances were predicted on the basis of the global peak.

This chapter discusses about the modeling of the PV system for different possible orientation of PV modules under PSCs. It presents suitable configuration needed for predicting the GP that happens under PSCs and also discusses about the performance evaluation of different configurations.

4.3 Chapter Objectives

- To investigate analytically the effects of partial shading on a PV system.
- To develop a suitable configuration of PV module installation in view of achieving maximum power under changing insolation patterns.
- To compare the performances of different PV module placement configurations under PSCs on the basis of maximum power and fill factor which is the ratio of the maximum power from the solar cell to the product of V_{oc} and I_{sc} .

4.4 Modeling of PV System

4.4.1 PV Cell Modeling

In order to analyse the effect of different PV module configurations for obtaining maximum power firstly a PV cell modeling is presented here.

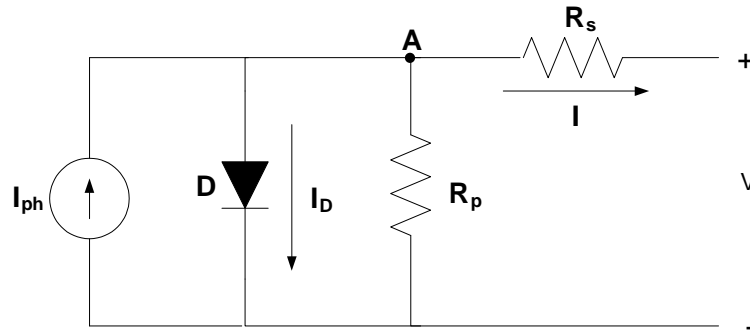


Figure 4.1: Equivalent circuit of a PV cell [6]

Fig.4.1 shows the equivalent circuit of a single diode PV cell. Applying Kirchoff's current law to node A in Fig. 4.1,

$$I = I_{ph} - I_D - \frac{V + IR_s}{R_p} \quad (4.1)$$

The output of the PV system is proportional to insolation (G) and temperature (T). The light generated current (I_{ph}) is proportional to insolation which can be written as:

$$I_{ph} = \left(\frac{G}{G_0} \right) I_{g0} + J_0(T_c - T_{ref}) \quad (4.2)$$

where G_0 denotes the reference insolation, I_{g0} is the current at G_0 , J_0 is the temperature coefficient of I_{ph} , T_c and T_{ref} are the absolute and reference cell temperatures. The

diode saturation current I_d is given by [6] and can be written as follows:

$$I_d = I_0 \left[\exp \left(\frac{qv_d}{akT} \right) - 1 \right] = I_0 \left[\exp \left(\frac{q(V + IR_s)}{akT} \right) - 1 \right] \quad (4.3)$$

where $V + IR_s$ is the voltage across diode, I_0 reverse saturation current, q is the electron charge, and V and I are the cell voltage and current respectively, R_s is series resistance, a is ideality factor and k is Boltzmann's constant.

The reverse saturation current is dependent upon temperature and can be written as

$$I_0 = I_{d0} \left(\frac{T_c}{T_{ref}} \right)^3 \exp \left[\frac{qE_g}{nk} \left(\frac{1}{T_{ref}} - \frac{1}{T_c} \right) \right] \quad (4.4)$$

4.4.2 PV Module Modeling

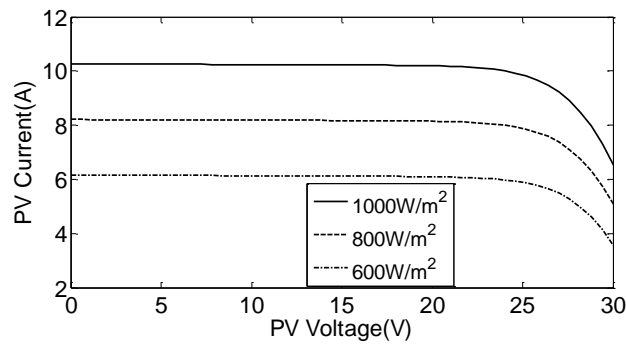
The output power of a single PV cell is typically 0.5W and hence is insufficient for any application. In order to enhance the output power, the cells are connected in series or parallel forming a PV module. The output can be calculated as

$$I = I_{ph} - I_0 \left[\exp \left(\frac{qV + qR_s I}{N_s k T a} - 1 \right) \right] - \frac{V + R_s I}{R_p} \quad (4.5)$$

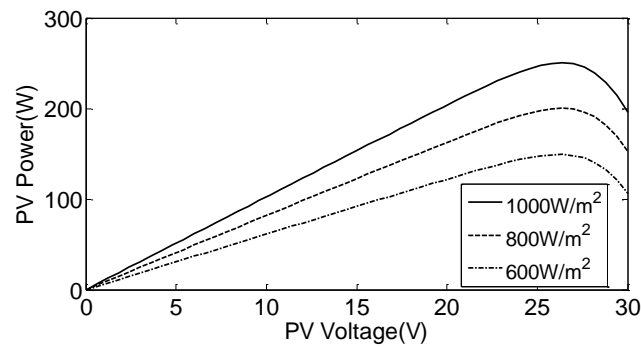
It can be seen from eq(4.5) that the output current of the PV cell (I) appear on both sides of equation which means that I cannot be expressed as a separate function from V . Thus, the output characteristics of the PV cell can be deduced by solving the following implicit form:

$$f(I, V, G) = I - \left\{ I_{ph}(G) - I_0(G) \left[\exp \left(\frac{qV + qR_s I}{N_s k T a} - 1 \right) \right] - \frac{V + IR_s}{R_p} \right\} = 0 \quad (4.6)$$

In (4.6), I_{ph}, I_0, T are the functions of insolation G . Fig 4.2 shows the output of the PV module under normal insolation levels.



(a)



(b)

Figure 4.2: PV output characteristics of a PV module under normal conditions (a) I-V characteristics, (b) P-V characteristics

4.4.3 Characteristics of PV System under Partial Shading

Under non-homogenous insolation levels, i.e due to passing of clouds, dust, trees, etc., the PV panels exhibit reverse polarity which leads to power loss and reduction in the maximum output power as shown in Fig.4.3. This absorbed power is converted into heat, resulting into a condition known as hotspot which can damage the cells. Such situation can be avoided by using bypass diode(BD) which can restrict the hotspot situation. Fig.4.3 depicts a situation in which partial shading occurs, for example

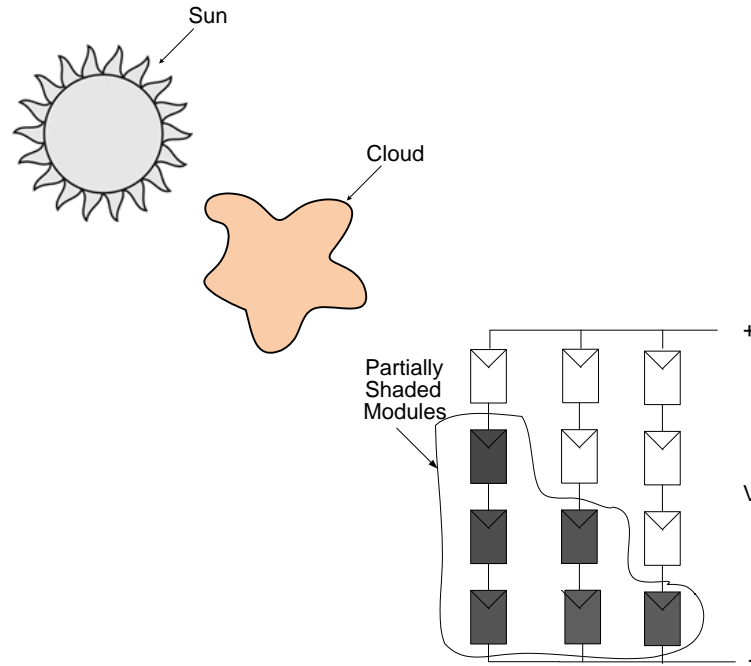


Figure 4.3: Possible shading by cloud on a PV system

when there is cloud as obstacle in between insolation and the PV arrays. Fig.4.4 gives a clear idea about the P-V characteristics curve with and without bypass diode. The BD can be uninstalled from the system to simplify the complications of multiple peaks, but as a result power is reduced. Therefore, BD is used in parallel to each module allowing the current from the healthy solar cells to flow into the external circuit.

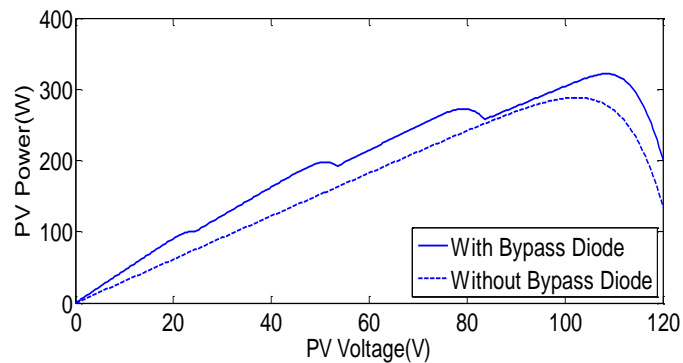


Figure 4.4: P-V characteristics curve with and without Bypass diode

4.5 Different Possible Orientations of PV Modules under PSCs

Two different cases are studied and designed:

Case I :Combination of n-oriented modules with Bypass diode

Case II :An Array composed of partial shading module without Bypass diode

4.5.1 Array composed of n-multiple modules

Fig.4.5 shows n number of PV modules connected in parallel with bypass diodes forming a PV array. When these modules receive irradiance $(G_1, G_2 \dots G_n)$, $(V_{d1}, V_{d2} \dots V_{dn})$ are the bypass diode voltages, $(I_{s1}, I_{s2} \dots I_{sn})$ are the current through series resistance and $(R_1, R_2 \dots R_n)$ are the resistance across the diode respectively, the array voltage, V must satisfy the following expressions:

$$f_m(I_{s1}, V_{d1}, G_1) = 0 \quad (4.7)$$

$$f_m(I_{s2}, V_{d2}, G_2) = 0 \quad (4.8)$$

$$f_m(I_{sn}, V_{dn}, G_n) = 0 \quad (4.9)$$

$$V_{d1} + V_{d2} + V_{dn} = V \quad (4.10)$$

$$\left(I_{s1} - \frac{V_{d1}}{R_1(-V_{d1})} \right) - \left(I_{s2} - \frac{V_{d2}}{R_2(-V_{d2})} \right) - \left(I_{sn} - \frac{V_{dn}}{R_n(-V_{dn})} \right) = 0 \quad (4.11)$$

A bypass diode is used to prevent the reverse flow of current and can be modeled in terms of resistance:

$$R_{by}(V_d) = \begin{cases} 10^6 \Omega & \text{if } V_d \leq 0 \\ 0.1 \Omega & \text{if } V_d > 0 \end{cases} \quad (4.12)$$

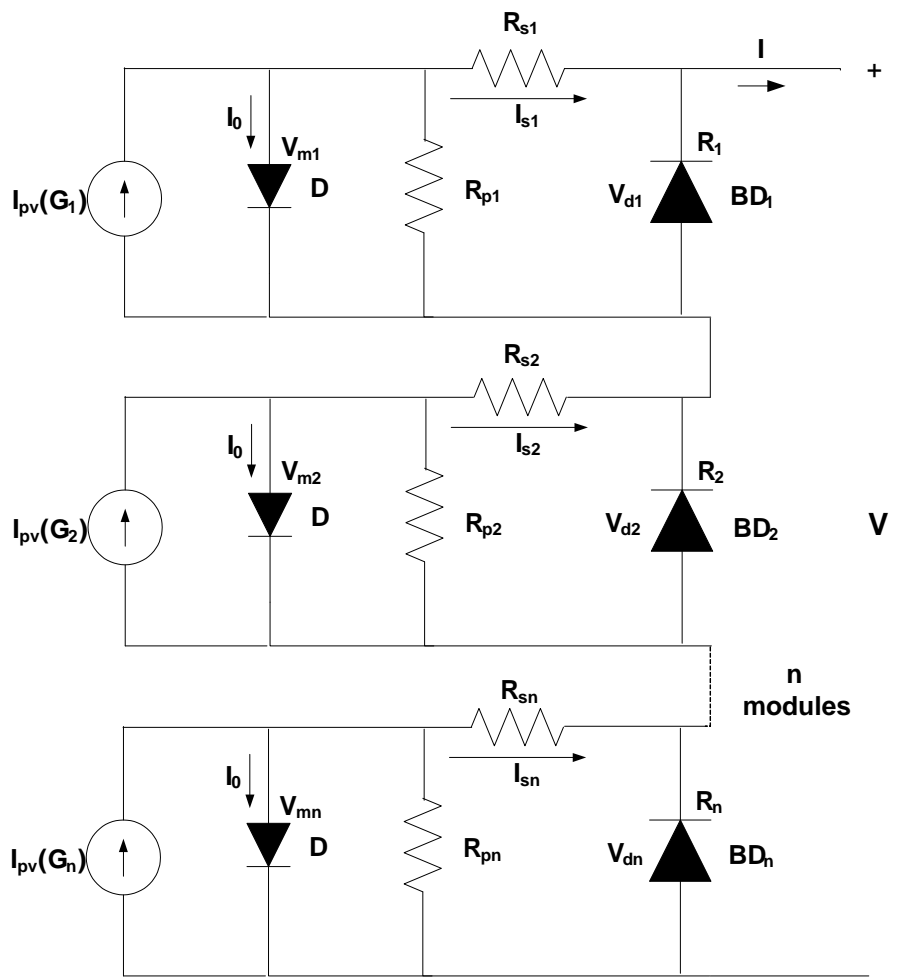


Figure 4.5: Equivalent circuit of a PV array with n-modules in series

4.5.2 Array composed of partially shaded module without bypass diode

Fig.4.6 shows the circuit model for a partially shaded PV module. Here, two groups of PV cells are connected in series receiving different irradiance levels. The module is composed of series cells where, (a-s) is the unshaded cells receiving irradiance. s is shaded cells receiving irradiance.

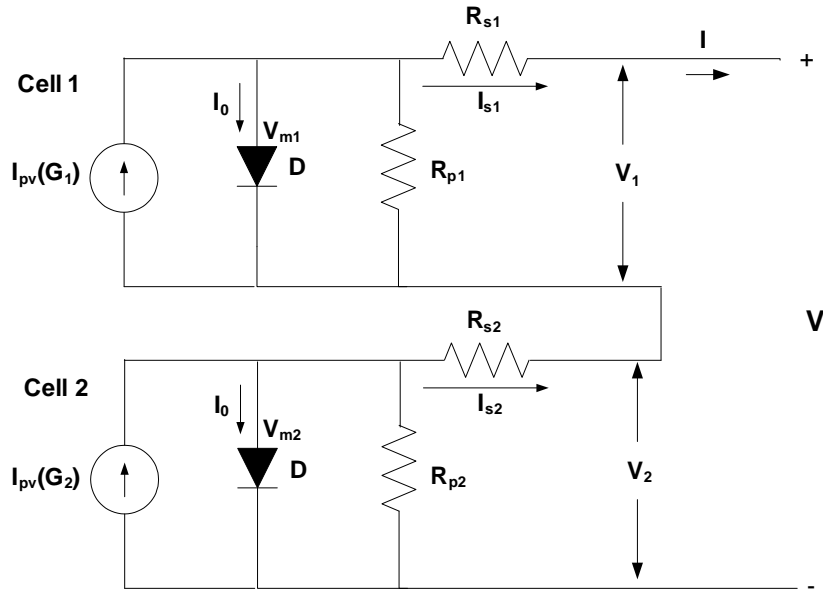


Figure 4.6: Equivalent circuit of a partially shaded module without bypass diode

I-V characteristics of the unshaded cell group (a-s) are given by

$$f_1(I_s, V_1, G_1) = I_s - \left\{ I_{pv}(G_1) - I_0(G_1) \times \left[\exp\left(\frac{q(V_1 + I_s R_{s1})}{\eta_1 k T(G_1)}\right) - 1 \right] - \frac{V_1 + I_s R_{s1}}{R_{p1}} \right\} = 0 \quad (4.13)$$

I-V characteristics of the shaded cell group (s) are given by

$$f_2(I_s, V_2, G_2) = I_s - \left\{ I_{pv}(G_2) - I_0(G_2) \times \left[\exp\left(\frac{q(V_2 + I_s R_{s2})}{\eta_2 k T(G_2)}\right) - 1 \right] \right\}$$

$$\left. -\frac{V_2 + I_s R_{s2}}{R_{p2}} \right\} = 0 \quad (4.14)$$

When the module voltage V and solar irradiance G_1 and G_2 are known, three unknowns I_s , V_1 and V_2 can be found from the following three equations:

$$f_1(I_s, V_1, G_1) = 0 \quad (4.15)$$

$$f_2(I_s, V_2, G_2) = 0 \quad (4.16)$$

$$V_1 + V_2 - V = 0 \quad (4.17)$$

$$I_s - \frac{V_1 + V_2}{R_s(-V_1 - V_2)} = 0 \quad (4.18)$$

4.6 Different possible configurations of PV cells

The evaluation of the four different configurations on the basis of maximum power and fill factor has been carried out by applying a randomly assigned irradiance of $0.02kW/m^2$ and $0.04kW/m^2$ to the 20 PV modules.

4.6.1 Series-Parallel configuration (SP configuration)

The SP configuration consists of multiple strings of modules which are connected in parallel. The total output current is the sum of the currents through all branches. The I - V relation of the SP configuration can be written as:

$$f(I_n, V_j, \lambda_j) = 0, \quad j = 1, 2, \dots, 20 \quad (4.19)$$

$$n = \begin{cases} 1 & \text{for } M_1 \dots M_5 \\ 2 & \text{for } M_6 \dots M_{10} \\ 3 & \text{for } M_{11} \dots M_{15} \\ 4 & \text{for } M_{16} \dots M_{20} \end{cases} \quad (4.20)$$

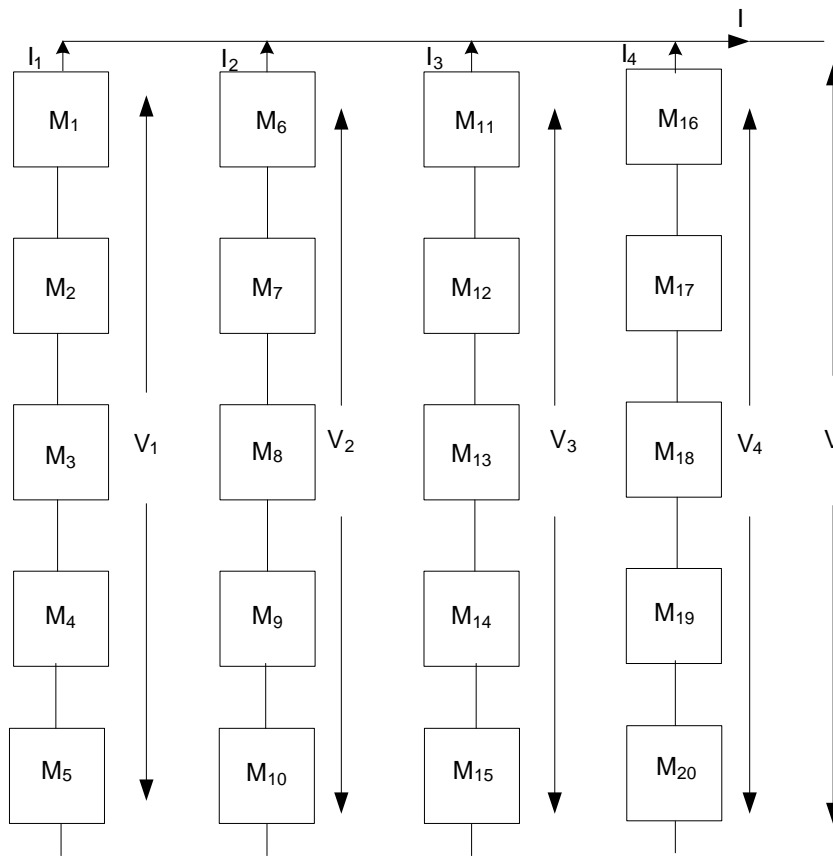


Figure 4.7: SP configuration

Using KCL, the total module current (I) is equal to the sum of four string currents

$$I = I_1 + I_2 + I_3 + I_4 \quad (4.21)$$

The voltage of each parallel string is equal to the equivalent voltage V .

$$\sum_{j=1}^5 V_j = \sum_{j=6}^{10} V_j = \sum_{j=11}^{15} V_j = \sum_{j=16}^{20} V_j = V_p \quad (4.22)$$

From equations (4.21) and (4.22) it is observed that there are 24 unknowns, such as 20 module voltages ($V_1 \dots V_{20}$) and 4 string currents ($I_1 \dots I_4$).

4.6.2 Total Cross Tied Configuration (TCT configuration)

The TCT configuration consists of series connected segments composed of several modules in parallel.

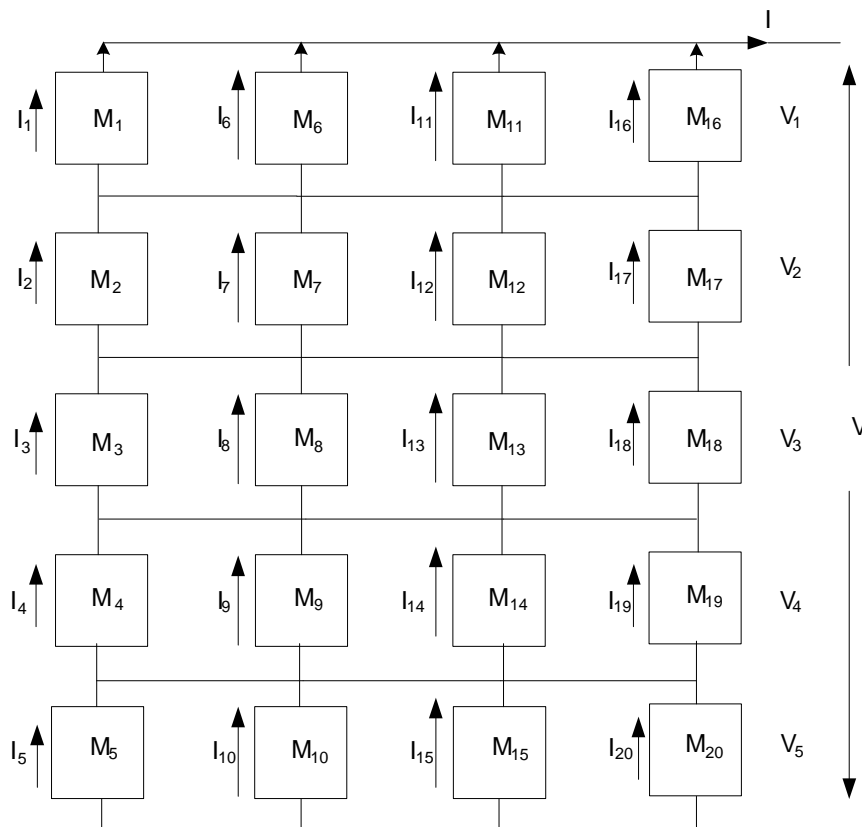


Figure 4.8: TCT configuration

The I-V relation of the 20 modules can be written as

$$f(I_k, V_n, \lambda_k) = 0, \quad k = 1, 2, \dots, 20 \quad (4.23)$$

where k denotes the cell number and voltage subscript n related to k can be written as

$$n = \begin{cases} k & \text{for } 1 \leq k \leq 5 \\ k - 5 & \text{for } 6 \leq k \leq 10 \\ k - 10 & \text{for } 11 \leq k \leq 15 \\ k - 15 & \text{for } 16 \leq k \leq 20 \end{cases} \quad (4.24)$$

The total voltage (V) is the summation of the voltages across all segments i.e.

$$V_{tot-CT} = V_1 + V_2 + V_3 + V_4 + V_5 = \sum_{n=1}^5 V_n \quad (4.25)$$

The total current flowing in the module can be written as

$$I = \sum_{k=1}^{20} I_k \quad (4.26)$$

Here, there are 25 unknowns, containing 20 module currents ($I_1 \dots I_{20}$) and 5 module voltages ($V_1 \dots V_5$).

4.6.3 Bridge Linked Configuration (BL-Configuration)

Fig.4.9 shows the circuit of BL configuration which is quite complicated as compared to previous two configurations namely SP and TCT configurations. The I-V relation of the 20 PV cells can be written as

$$f(I_n, V_j, \lambda_k) = 0, \quad k = 1, 2, \dots, 20 \quad (4.27)$$

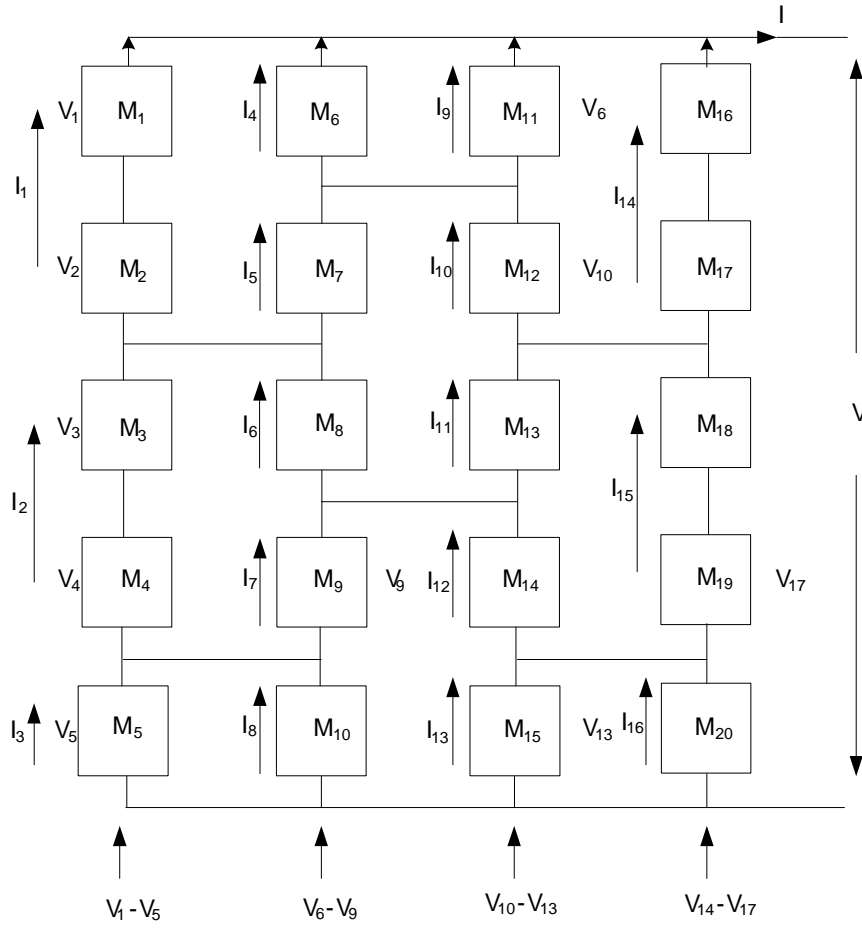


Figure 4.9: BL configuration

The current subscript n and voltage subscript j can be related to module number k as

$$n = \begin{cases} 1, k = M_1, M_2 \\ 2, k = M_3, M_4 \\ 3, k = M_5 \\ 4, k = M_6 \\ 5, k = M_7 \\ 6, k = M_8 \end{cases} \quad n = \begin{cases} 7, k = M_9 \\ 8, k = M_{10} \\ 9, k = M_{11} \\ 10, k = M_{12} \\ 11, k = M_{13} \end{cases} \quad n = \begin{cases} 12, k = M_{14} \\ 13, k = M_{15} \\ 14, k = M_{16}, M_{17} \\ 15, k = M_{18}, M_{19} \\ 16, k = M_{20} \end{cases} \quad (4.28)$$

$$j = \begin{cases} k \text{ for } 1 \leq k \leq 9 \\ k - 5 \text{ for } k = 10, 11 \\ k - 2 \text{ for } 12 \leq k \leq 19 \\ k - 7 \text{ for } k = 20 \end{cases} \quad (4.29)$$

Here, it is found that there are 16 module currents ($I_1 \dots I_{16}$) and 17 module voltages ($V_1 \dots V_{17}$) having a total of 33 unknowns.

4.6.4 Proposed Ring Pattern Configuration (RP-Configuration)

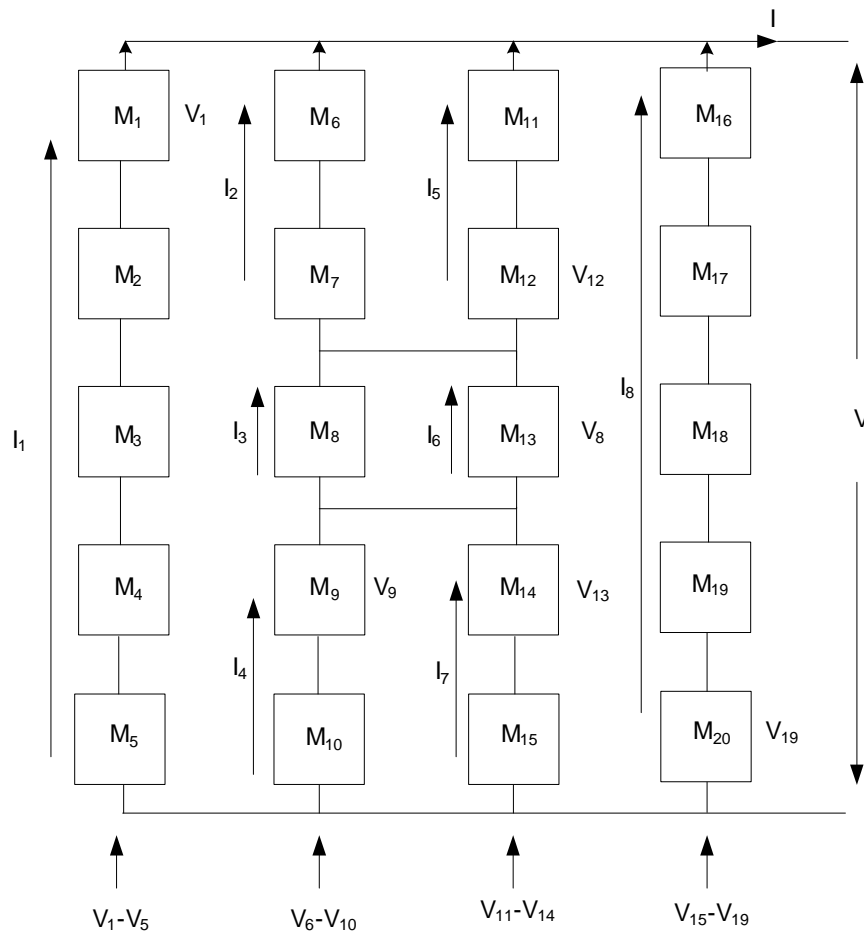


Figure 4.10: RP configuration

The idea behind developing a new configuration is to harvest maximum power which the former configurations are insufficient to deliver. Therefore, a new configuration is developed namely RP configuration and the circuit diagram of the RP configuration is shown in Fig.4.10.

For implementing the proposed structure, the I-V relationship of 20 PV modules is given by

$$f(I_n, V_j, \lambda_k) = 0, \quad k = 1, 2, \dots, 20 \quad (4.30)$$

where current subscript n and voltage subscript j can be related to cell number k as follows

$$n = \begin{cases} 1, k = M_1 \dots M_5 \\ 2, k = M_6, M_7 \\ 3, k = M_8 \\ 4, k = M_9, M_{10} \end{cases} \quad n = \begin{cases} 5, k = M_{11}, M_{12} \\ 6, k = M_{13} \\ 7, k = M_{14}, M_{15} \\ 8, k = M_{16} \dots M_{20} \end{cases} \quad (4.31)$$

$$j = \begin{cases} k, 1 \leq k \leq 12 \\ k - 5, k = 13 \\ k - 1, 14 \leq k \leq 20 \end{cases} \quad (4.32)$$

In this configuration there are 29 unknowns comprising of 8 module currents ($I_1 \dots I_8$) and 19 module voltages ($V_1 \dots V_{19}$).

4.7 Performance Evaluation

The performances of SP, TCT, BL and the proposed RP configurations are evaluated by comparing their global power peaks under a similar shading patterns. Here, 20 PV modules are taken to analyze the configurations analytically in which KCL, KVL and

non-linear implicit equations using I-V relations have been discussed. Fig.4.11 shows the photograph of a solar array simulator(SAS) of Agilent make(E4360A). This has a provision of emulating power at different solar irradiances. The SAS is a current source with 600W dc output source which is equipped to generate I-V and P-V curves of PV arrays under different shading conditions. The SAS is a current source with 600W dc output source which is equipped to generate I-V and P-V curves of PV arrays under different shading conditions. The I-V curve generated is dumped into the Table mode which is fast and accurate for generating different I-V curves for partial shading conditions in SAS. The most efficient configuration is found out by predicting the maximum power using SAS. As illustrated in Fig.4.12, all four configurations exhibit different power peaks at different voltages. Table 4.1 gives a clear comparison among all the four configurations.

From experimental study, the maximum power of an array under a similar shading pattern is investigated for four different configurations. It was observed from Fig.4.12 that TCT and proposed RP configuration exhibit maximum power as compared to SP and BL type configurations. However, in terms of fill factor it was found that the proposed RP configuration has higher value of 0.474 compared to the rest.

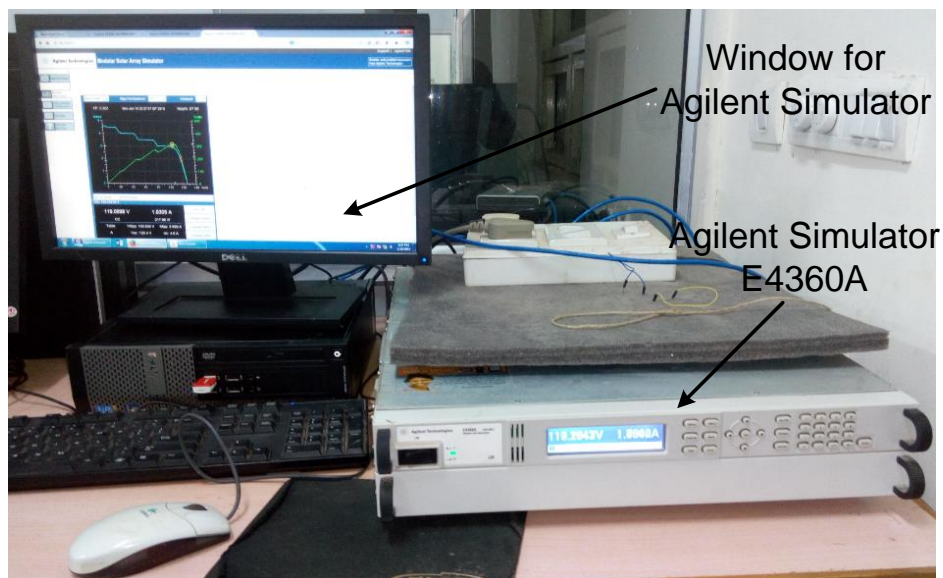
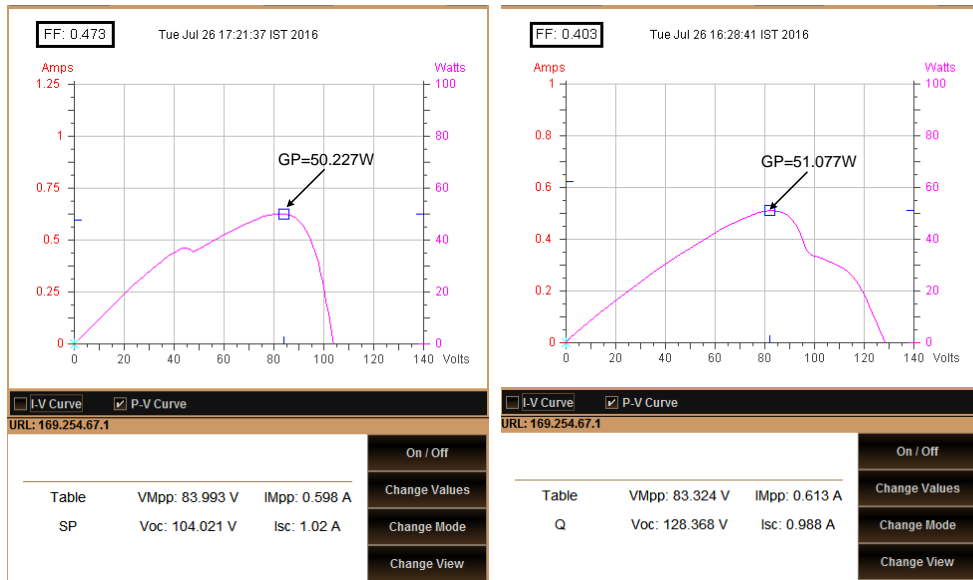
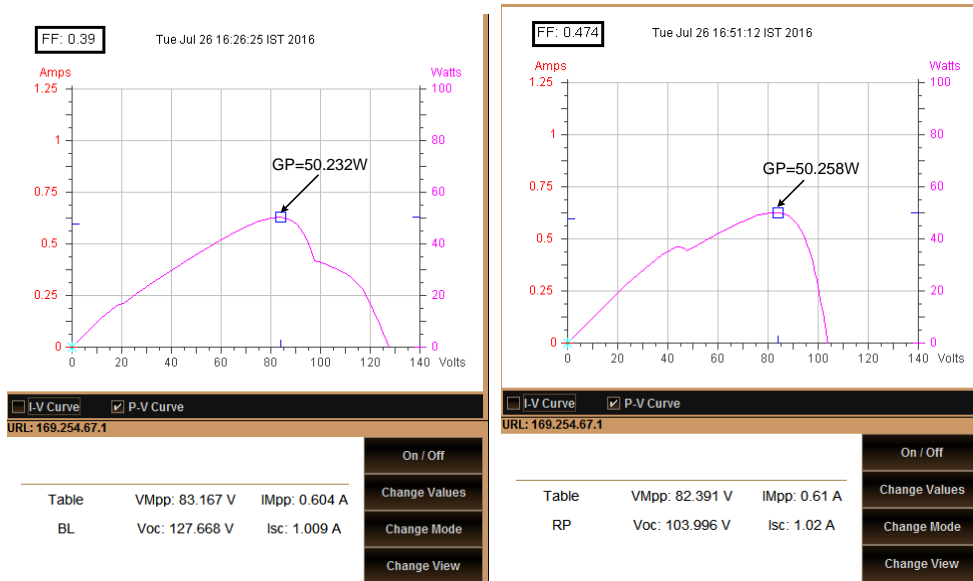


Figure 4.11: Solar Array Simulator



(a)

(b)



(c)

(d)

Figure 4.12: Experimental P-V characteristics curve of a PV array(a) SP, (b) TCT, (c) BL, (d) proposed RP configuration

Table 4.1: Experimental comparison of peak power and fill factor

Configuration	Maximum Power (Watts)	Fill factor (FF)
SP	50.227	0.473
TCT	51.077	0.403
BL	50.232	0.39
Proposed RP	50.258	0.474

4.8 Chapter Summary

Analytical modeling of PV modules under PSCs has been presented for different orientations with and without bypass diode is presented here. The experimental study conclude that the TCT and the proposed RP configuration exhibits maximum power of 51.077W and 50.258W as well as the RP configuration has higher value of fill factor of 0.474 as compared to SP, TCT and BL configurations. Here,all the configurations are examined under same shading pattern on the basis of maximum power and fill factor. Hence, there is a need to implement randomly changing irradiance patterns with different possible configurations simultaneously with the development of global MPPT algorithms which could handle PSCs and can track the global peak.

Chapter 5

A New MPPT Design Using Grey Wolf Optimization Technique for Photovoltaic System Under Partial Shading Conditions

5.1 Abstract

This work presents a maximum power point tracking (MPPT) design for a photovoltaic (PV) system using a grey wolf optimization (GWO) technique. The GWO is a new optimization method which overcomes the limitations such as lower tracking efficiency, steady-state oscillations, and transients as encountered in perturb and observe (P&O) and improved PSO (IPSO) techniques. The problem of tracking the global peak (GP) of a PV array under partial shading conditions (PSCs) is attempted employing the GWO-based MPPT technique. The proposed scheme is studied for a PV array under PSCs which exhibits multiple peaks and its tracking performance is compared with that of two MPPT algorithms, namely P&O-MPPT and IPSO-MPPT. The proposed

GWO-MPPT algorithm is implemented on a PV system using MATLAB/SIMULINK. Furthermore, an experimental setup is developed to verify the efficacy of the proposed system. From the obtained simulation and experimental results, it is observed that the proposed MPPT algorithm outperforms both P&O and IPSO MPPTs.

5.2 Introduction

In Chapter 4, analytical modeling of PV modules has been discussed under the influence of partial shading. Here, the reverse voltage effect occurring in a module is taken into account and has also been modeled and discussed. The evaluation of the four connection configurations on the basis of maximum power and fill factor has been carried out by applying to the 20 modules with a randomly assigned irradiance of 0.02kW/m^2 and 0.04kW/m^2 . Therefore, a need to implement randomly changing insolation patterns with different possible configurations simultaneously with the development of global MPPT is necessary. Hence, two new different configurations namely 4S and 3S2P configuration with rapidly changing insolation patterns is considered in this work which can deal with mismatch problems in a PV system. In view of this, it is observed that there is an opportunity to explore new global optimization techniques for determining the global MPP that arise during PSCs. In view of this in Chapter 5, a new MPPT design using an efficient global optimization called Grey wolf optimization (GWO) is proposed.

Various MPPT algorithms were discussed in literature [88] [89] [90] [45] [46] [47] [43] [44] [7] [50] [91] [92] about the occurrence of mismatched non-uniform insolation resulting in decrease of PV output power and hot-spot generated damages those PV cells. Such situations can be avoided by using bypass and blocking diodes. Since the dynamics of the PV system under partial shading is time-varying, MPPT design for PV power system should be equipped with the following features such as tracking global maximum power point (GMPP) at different conditions e.g. shading, degradation of PV

cell, etc., adaptability to P-V characteristics change of PV array, smooth and steady tracking behavior. Current vs Voltage(I-V) and Power vs Voltage(P-V) characteristics of a PV array under non- uniform insolation due to partial shading conditions(PSCs) with multiple peaks have been discussed in [7] [50] [60] [93] [94] [95] .

A number of MPPT techniques such as fractional open-circuit voltage [96], fractional short-circuit current [97], Hill climbing (HC) [42] [98], Perturb and Observe (P&O) [27] [99] [28] [100], Incremental Conductance (IC) [30] [101] have been proposed for improving the efficiency of a PV system. Among these, the fractional open-circuit voltage or fractional short-circuit current algorithm requires a supplementary circuit, i.e. a series switch or a shunt switch for on-line measurement of the open-circuit voltage and short-circuit current repeatedly [102], which results in power loss and also makes the PV system more complex. The HC method uses a perturbation in the duty ratio of the power converter and the P&O method uses a perturbation in the operating voltage of the PV system [27] [99] [28]. Both these methods yield steady state oscillations after reaching the MPP owing to the fact that the perturbation continuously changes in both directions to maintain the maximum power point (MPP) resulting in power loss. The two influencing parameters in P&O algorithm namely perturbation rate and perturbation size are discussed in [28]. To reduce these oscillations and improve the module efficiency, the IC method was proposed [30]. The IC method has originated with the idea that the slope of P-V curve is zero at the MPP, positive on the left side of MPP and negative on right side of MPP. Hence, the oscillations cannot be reduced completely by the IC method. Both P&O and IC methods are effective under uniform insolation but they fail during those time intervals characterized by changing atmospheric conditions [103] [18].

The focus of the research pursued in this chapter is to determine the global peak during PSCs, in order to alleviate some of the issues like lower tracking efficiency and oscillations generated in the PV output power, an alternative approach is to employ evolutionary algorithm (EA) techniques which has the capability to handle nonlinear

objective functions. Metaheuristic optimization methodologies such as Particle Swarm Optimization (PSO) [71] [70], Fuzzy logic controller [39], firefly [73] etc., have been extensively used for various engineering applications. Recently Mirjalili et al. have developed a metaheuristic algorithm known as grey wolf optimizer (GWO) [104]. This algorithm is inspired by grey wolves to attack preys for hunting purpose.

Further, several works are reported in literature on grey wolf optimization which has attracted considerable interests from the research community compared to other optimization techniques because it is more robust and exhibits faster convergence. Furthermore, it requires fewer parameters for adjustment and less operators compared to other evolutionary approaches, which is an advantage when rapid design process is considered [104]. After a thorough literature survey, it is observed that GWO has not been exploited for designing a MPPT. Hence, this work attempts to exploit the GWO for designing a MPPT to obtain efficient tracking performance of a PV system under PSCs.

5.3 Chapter Objectives

- To develop an efficient tracking algorithm which could be employed in a practical PV system which can harvest maximum power under changing insolation patterns.
- To develop a MPPT algorithm which will overcome the limitations like lower tracking efficiency, steady state oscillations and transients as encountered in conventional techniques.
- To implement the above MPPT control algorithm in a practical photovoltaic system.

5.4 Characteristics of a PV System under Partial Shading Conditions

5.4.1 Basic Characteristics of a PV cell

A PV cell can be represented by an equivalent single diode model as shown in Fig. 5.1.

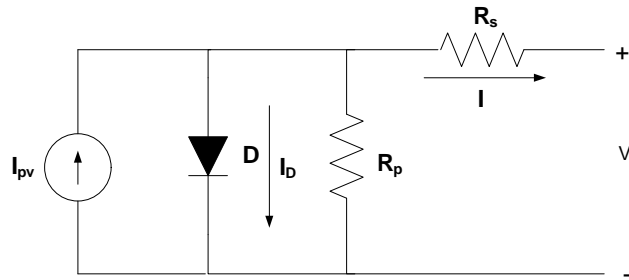


Figure 5.1: Equivalent circuit of a PV cell [6]

The symbols used in this model are defined as follows:

I_{pv} : photovoltaic current source

D : a diode connected in parallel to the current source

R_s : the sum of resistances due to all the components that come in path of current which is desirable to be as low as possible

R_p : which is due to the leakage across the P-N junction and is desirable to be as high as possible

I : difference between the photocurrent I_{pv} and the diode current I_d which is given by

$$I = I_{pv} - I_0 \left[\exp \left(\frac{qV + qR_s I}{N_s k T a} - 1 \right) \right] - \frac{V + R_s I}{R_p} \quad (5.1)$$

where I_0 is the saturation current, a is diode ideality factor, k is Boltzmanns constant, q is charge, T is temperature in kelvin, N_s is no. of cells in series, respectively.

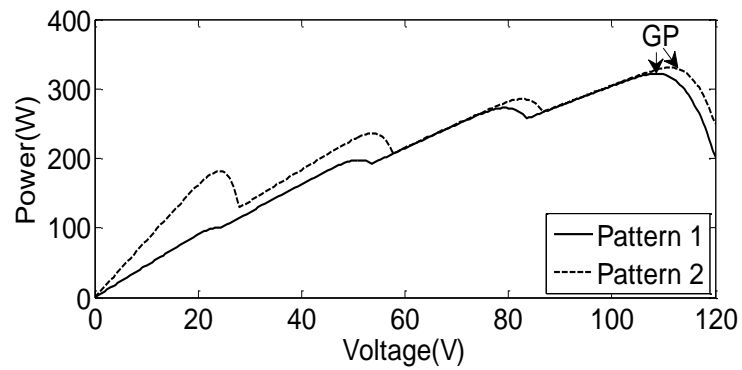
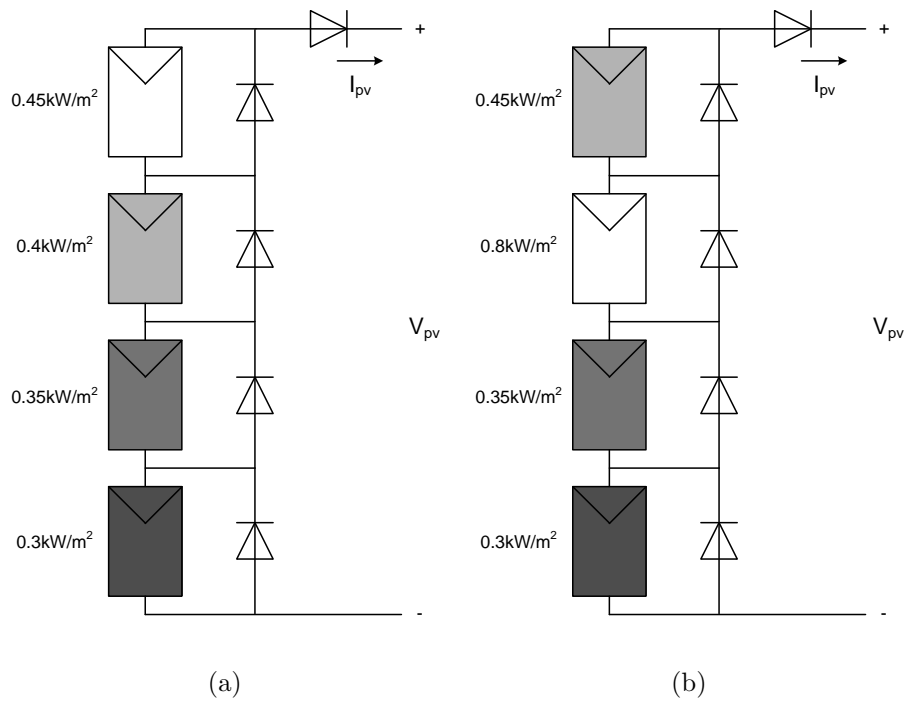
5.4.2 System Description

A PV array consists of several PV modules connected in series to produce a higher voltage and in parallel to increase the current. During PSCs, multiple peaks, i.e., local and global maxima points are observed in the P-V characteristics curve due to the presence of BDs. The presence of bypass diode connected in parallel to each PV module during PSCs reduces the probability of hot-spot during which the shaded module behaves as a load instead of generating power. Two different PV arrays are considered in this work and are shown in Fig.5.2 and Fig.5.3. A configuration consisting of four modules in series (4S configuration) having two different shading patterns with their P-V curves comprising of three LPs and one GP is shown in Fig.5.2. The second PV configuration has two series modules connected in parallel with another two series modules (2S2P configuration) having two different shading patterns with their respective P-V curves comprising of one LP and one GP is shown in Fig.5.3.

5.5 GWO and its Application in MPPT Design

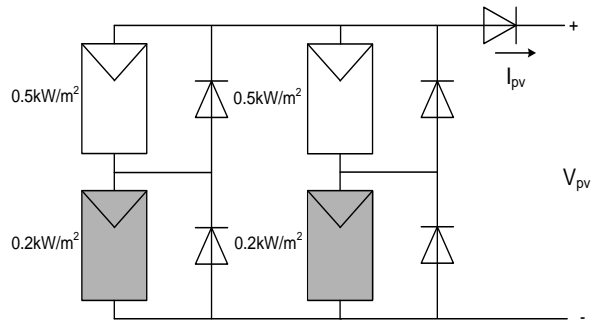
5.5.1 Grey Wolf Optimization

The GWO algorithm imitates the leadership hierarchy and hunting mechanism of grey wolves in nature proposed by Mirjalili et al. [104]. Grey wolves are considered to be at the top of food chain and they prefer to live in a pack. Four types of grey wolves such as alpha (α), beta (β), delta (δ) and omega (ω) are employed for simulating the leadership hierarchy. In order to mathematically model the social hierarchy of wolves while designing GWO, the alpha (α) grey wolves are considered as the fittest

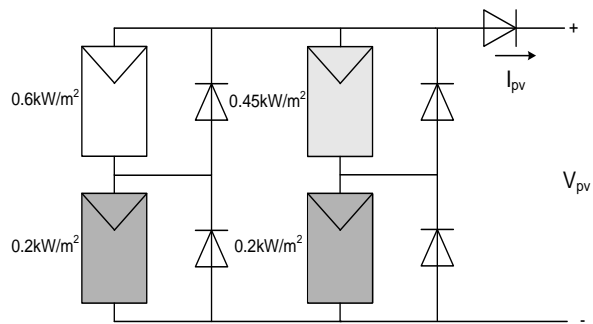


(c)

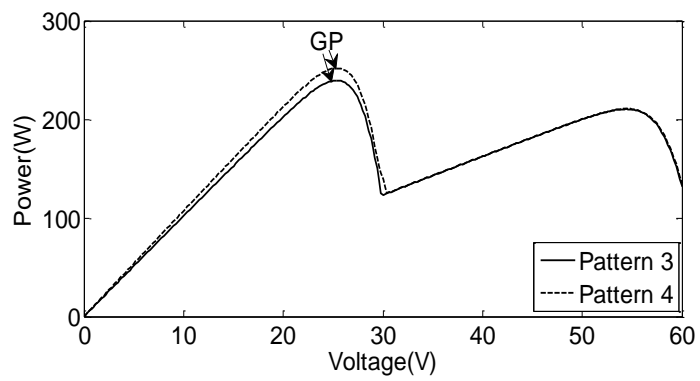
Figure 5.2: 4S configuration under different shading patterns (a) Pattern 1, (b) Pattern 2, (c) P-V curves under PSCs



(a)



(b)



(c)

Figure 5.3: 2S2P configuration under different shading patterns (a) Pattern 3, (b) Pattern 4, (c) P-V curves under PSCs



Figure 5.4: Hunting behavior of grey wolves:(A-C) chasing and tracking prey (D) encircling prey (E) attacking prey

solution. Consequently, the second and third best solutions are named as beta (β) and delta (δ) respectively. The rest of the candidate solutions are assumed to be omega (ω). Fig.5.4 shows three main steps of GWO algorithm namely hunting, chasing and tracking for prey, encircling prey and attacking prey which are implemented to design GWO for performing optimization. Grey wolves encircle a prey during the hunt and the encircling behavior can be modeled by the following equations:

$$\vec{D} = |\vec{C} \cdot \vec{X}_p(t) - \vec{X}_p(t)| \quad (5.2)$$

$$\vec{X}(t+1) = \vec{X}_p(t) - \vec{A} \cdot \vec{D} \quad (5.3)$$

where t denotes the current iteration, \vec{D} , \vec{A} and \vec{C} represent coefficient vectors, \vec{X}_p is the position vector of the prey and \vec{X} indicates the position vector of grey wolf. The vectors \vec{A} and \vec{C} are calculated as follows:

$$\vec{A} = 2\vec{a} \cdot \vec{r}_1 - \vec{a} \quad (5.4)$$

$$\vec{C} = 2 \cdot \vec{r}_2 \quad (5.5)$$

where components of \vec{a} are linearly decreased from 2 to 0 over the course of iterations and \vec{r}_1, \vec{r}_2 are random vectors in $[0, 1]$. Grey wolves have the ability to recognize the location of prey and encircle them. The hunt is usually guided by alpha(α) called leaders followed by beta(β) and delta(δ) which might also participate in hunting occasionally. Lastly, comes delta(δ) and omega(ω) who take care of the wounded wolves in the pack. Therefore, we refer alpha as the candidate solution having better knowledge about the location of prey. The grey wolves finish the hunt by attacking the prey when it stops moving.

5.5.2 Application of GWO for MPP Tracking

Fig.5.5 shows the block diagram of the proposed MPPT scheme for a PV system.

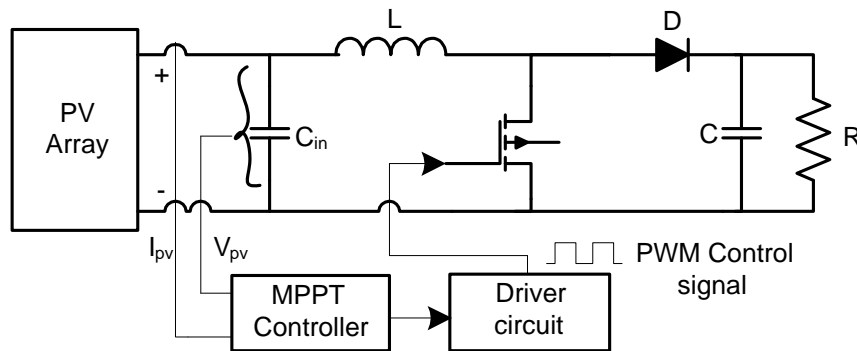


Figure 5.5: Block diagram of the proposed MPPT method

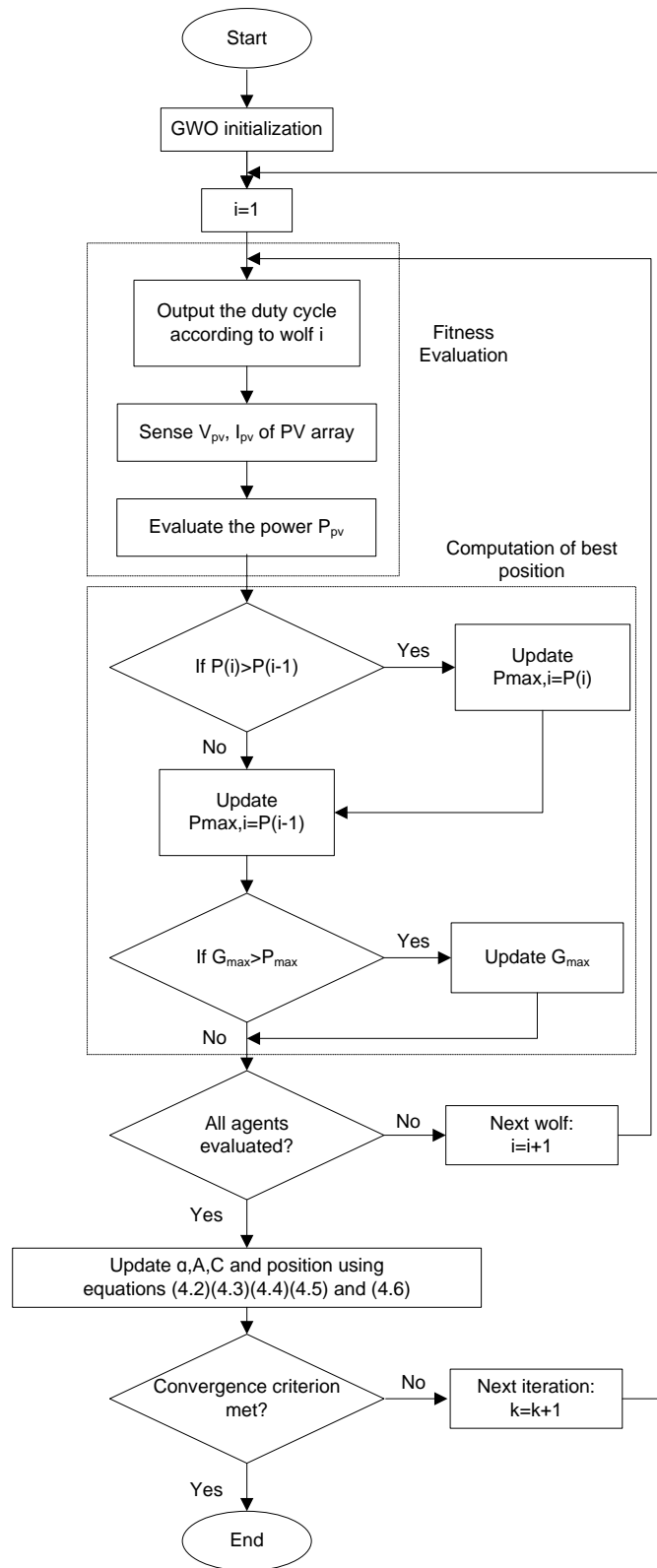


Figure 5.6: Flowchart of the proposed algorithm

For number of grey wolves, i.e., duty ratios, the controller measures PV voltage V_{pv} and PV current I_{pv} through sensors and computes the output power of the PV system. The flowchart of the proposed GWO based MPPT algorithm is shown in Fig.5.6. During partial shading, the P-V curve is categorized by multiple peaks having various local peaks (LP) and one global peak (GP). When the wolves find the MPP, their correlated coefficient vectors become nearly equal to zero. In the proposed method an attempt has been made to combine GWO with direct duty cycle control i.e., at the MPP, duty cycle is sustained at a constant value which in turn reduces the steady state oscillations that exist in conventional MPPT techniques and lastly the power loss due to oscillation is reduced resulting in higher system efficiency. To implement the GWO based MPPT, duty cycle d is defined as a grey wolf. Therefore, equation (5.3) can be modified as follows:

$$d_i(k+1) = d_i(k) - A.D \quad (5.6)$$

Thus, the objective function of the GWO algorithm is formulated as:

$$P(d_i^k) > P(d_i^{k-1}) \quad (5.7)$$

Here, $P = V * I$ for any instant is the operating power of PV array for the tracking problem, where P represents power, d is duty cycle, i is the number of current grey wolves and k is number of iterations.

5.6 Results and Discussion

5.6.1 Simulation Results

To evaluate the performance of the proposed GWO based metaheuristic MPPT algorithm, its performances were compared with that of two popular MPPT techniques

namely P&O and Improved PSO (IPSO) [70] MPPT algorithms. All the above three algorithms were implemented under PSCs and rapidly changing insolation level for both 4S and 2S2P configuration. For simulation studies, the parameters taken for modeling single diode model of a PV module at nominal conditions is given in Table 5.1. The parameters of IPSO and GWO algorithms are given in Table 5.2.

Table 5.1: Parameters of KC200GT PV module at $25^{\circ}C$ and $1000W/m^2$

Maximum Power (P_{max})	200W
Open circuit voltage (V_{oc})	32.8V
Short circuit current (I_{sc})	8.21A
Maximum voltage (V_{mp})	26.3V
Maximum current (I_{mp})	7.61A

Table 5.2: Parameters of IPSO and GWO Algorithms

IPSO Algorithm		GWO Algorithm	
w_{max}	1	a	Linearly decreases from 2 to 0
w_{min}	0.1		
$c_{1,max}$	2		
$c_{1,min}$	1		
$c_{2,max}$	2		
$c_{2,min}$	1		

The power, voltage and current for the 4S configuration with PSCs employing GWO, IPSO and P&O are shown in Fig.5.7. In the simulation study, pattern 1 is made to exist for first 0.1sec and the second pattern appears for next 0.1sec. In pattern 1, GWO based MPPT converges to the GP of 319.4W, IPSO tracks the GP of 319.2W and the P&O algorithm converges to local peak of 100.2W as it is unable to

differentiate between local and global peaks resulting in steady state oscillations i.e. the operating point oscillates around the MPP giving rise to power loss and also results in slowing down the speed of response of the algorithm and reduces the efficiency of the PV system. When shading pattern is changed to pattern 2 at 0.1sec, the MPPT techniques gets restarted and GWO based MPPT is able to locate the GP of 329.6W, IPSO tracks GP of 329.5W and P&O fails to reach GP and gets settled at LP of 180W.

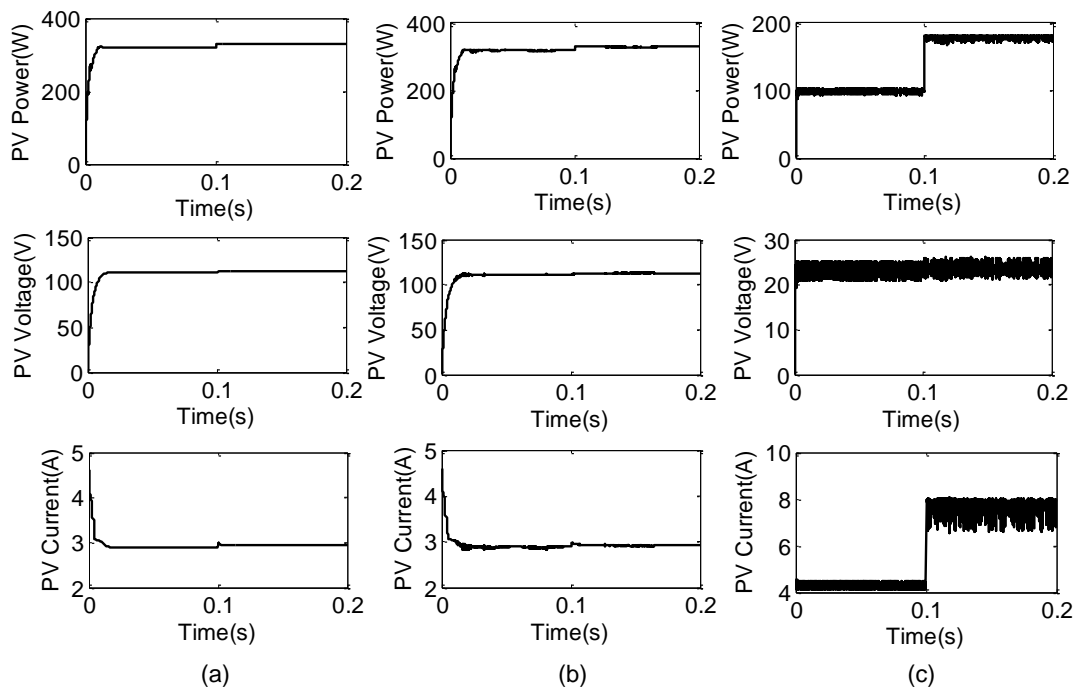


Figure 5.7: Tracking curves for 4S Configuration (a) GWO based MPPT (b) IPSO based MPPT (c) P&O based MPPT

The simulation is now repeated for 2S2P configuration having two different patterns namely pattern 3 and 4. The GWO based MPPT reaches GP of 239.1W, IPSO tracks GP of 239.05W and P&O algorithm reaches GP of 234W anonymously as it tracks the peak which comes in contact first i.e. it may be a GP or LP resulting in oscillations around MPP. All the above findings are implemented for existence of pattern 3 which appears for 0.1sec and pattern 4 appears for next 0.1sec. For pattern 4, the GWO

based MPPT locates the GP of 251.6W, IPSO locates GP at 251.5W and P&O gets settled to the GP of 247W as before in pattern 3 resulting in oscillations around the MPP. The tracking curves are shown in Fig.5.8.

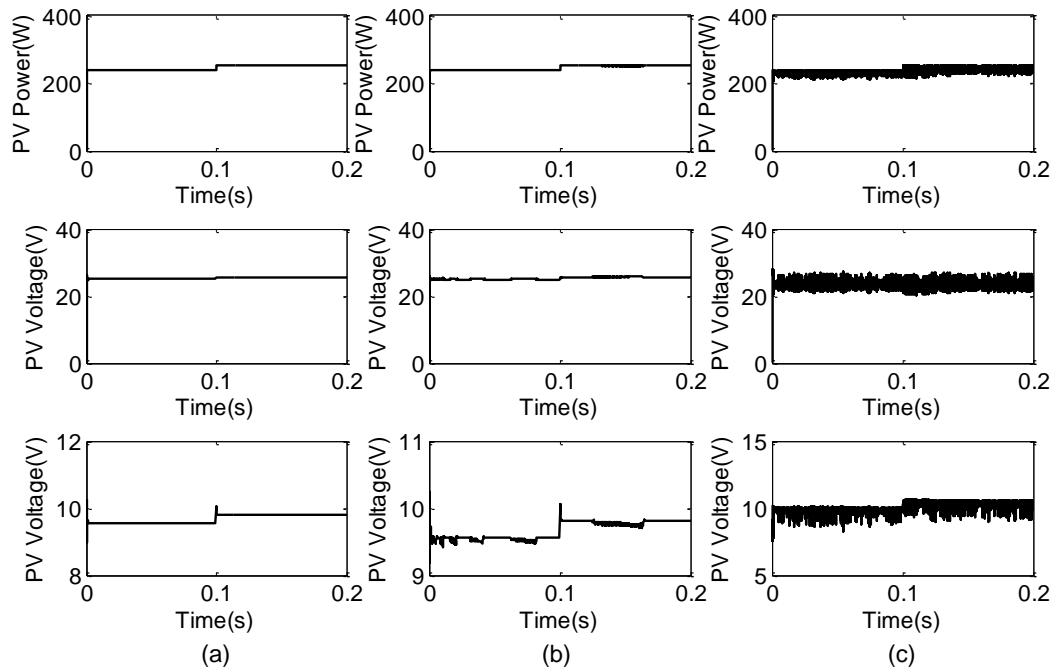


Figure 5.8: Tracking curves for 2S2P Configuration (a) GWO based MPPT (b) IPSO based MPPT (c) P&O based MPPT

The simulation results presented in Fig.5.7 and 5.8 envisage that the GWO based MPPT can handle partial shading efficiently and it outperforms both P&O and IPSO in terms of faster convergence towards GP, zero oscillations and higher tracking efficiency. The simulation results presented in Fig.5.7 and 5.8 are briefly summarized in Table 5.3 and 5.4. The MPPT tracking efficiency is calculated as the ratio between average output power obtained at steady state and maximum available power of the PV array under certain shading pattern [39].

Table 5.3: Performance Comparison of the Proposed MPPT with P&O and IPSO MPPTs for 4S Configuration

Shading Pattern	Maximum power from P-V curve (watts)	Tracking Methods	Power (W)	Voltage (V)	Current (A)	%Tracking Efficiency
1	320	P&O	100.2	24.2	4.14	31.30
		IPSO	319.2	110.52	2.888	99.75
		GWO	319.4	110.55	2.889	99.81
2	330	P&O	180	23.07	7.80	54.54
		IPSO	329.5	112.3	2.934	99.84
		GWO	329.6	112.3	2.934	99.87

Table 5.4: Performance Comparison of the Proposed MPPT with P&O and IPSO MPPTs for 2S2P Configuration

Shading Pattern	Maximum power from P-V curve (watts)	Tracking Methods	Power (W)	Voltage (V)	Current (A)	%Tracking Efficiency
3	239.3	P&O	234	24	9.75	97.78
		IPSO	239.05	25	9.562	99.89
		GWO	239.1	25.01	9.56	99.91
4	251.8	P&O	247	23.9	10.3	98.09
		IPSO	251.5	25.64	9.808	99.88
		GWO	251.6	25.64	9.812	99.92

Table 5.5: Qualitative Comparison of the Proposed with P&O and IPSO MPPT Techniques

Type	P&O	IPSO	Proposed GWO
Tracking Speed	0.005 sec (tracks LP) (Pattern 1)	0.03 sec Medium (Pattern 1)	0.021 sec Very Fast (Pattern 1)
Tracking Accuracy	Low	Accurate	Highly Accurate
Convergence to GP	Tracks which comes in contact first	Yes	Yes
No.of Tuning Parameters	1	6	1
Power Efficiency	High(Uniform Insolation) Low(PSCs)	High	High
Dynamic Response	Poor	Good	Good
Implementation Complexity	Low	Medium	Medium

Further, a qualitative comparison among various fast converging MPPT methods is presented in Table 5.5. To ensure the effectiveness of the proposed MPPT algorithm, different loads such as R-L load ($R=50\Omega, L=15\text{mH}$) is connected in place of resistive load and is studied for pattern 1. Fig.5.9 compares the response of two different type of loads (R and R-L load) from which it is seen in both the cases, the proposed MPPT

is efficient enough to converge to the GP successfully. Usually, for R load fast response is observed compared to any other loads. However, it is seen from Fig.5.9 that GWO is successful in providing similar tracking response but with a higher settling time in case of R-L load.

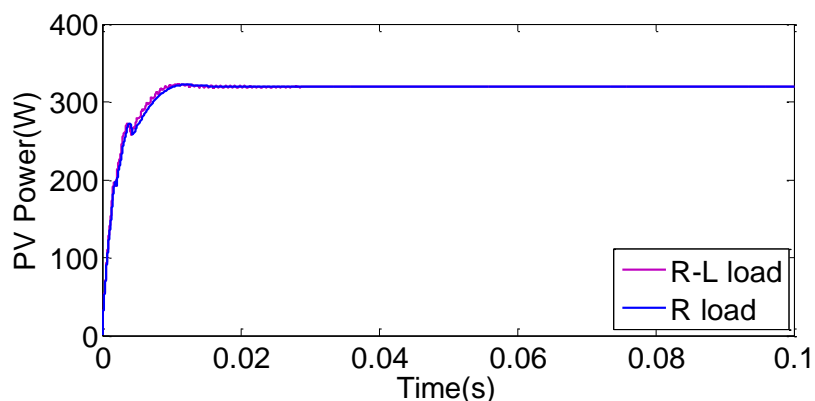
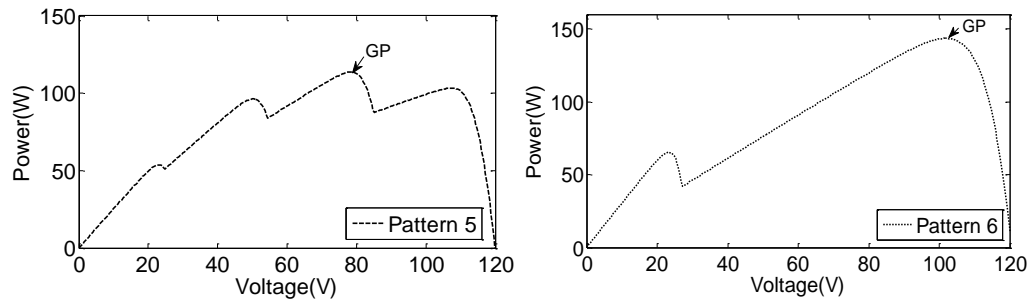


Figure 5.9: Tracking curves for pattern 1 showing response of proposed MPPT having R and R-L load under PSCs

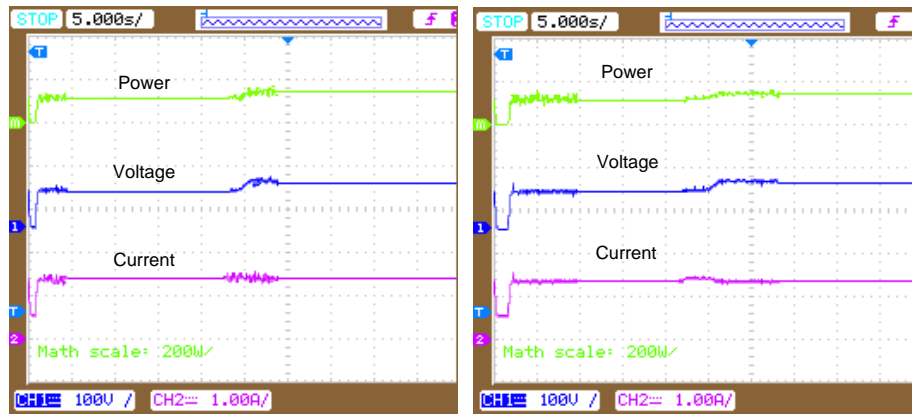
5.6.2 Experimental Results

To validate the effectiveness of the proposed GWO based MPPT, experiments were carried out on real PV array for both 4S and 2S2P configurations. Fig.3.1 shows the experimental setup of the proposed system.

The two distinct patterns are shown in Fig. 5.10(a) marked as pattern 5 having GP of 113.8W with three local peaks(53.64W,96.21W,102.8W) and pattern 6 possess GP of 143.5W with one local peak(65.32W). The experimentally determined tracking curves are shown in Fig. 5.10(b)5.10(c)5.10(d). The tracking curves show that GWO and IPSO based MPPT converge to the GP of 113.8W whereas P&O gets trapped to local peak of 53.44W. The tracking speed of GWO is faster than IPSO since it takes 3.18sec to reach GP compared to IPSO which takes 7.9sec for global convergence. When the shading pattern 5 changes to pattern 6, the current MPPT restarts the

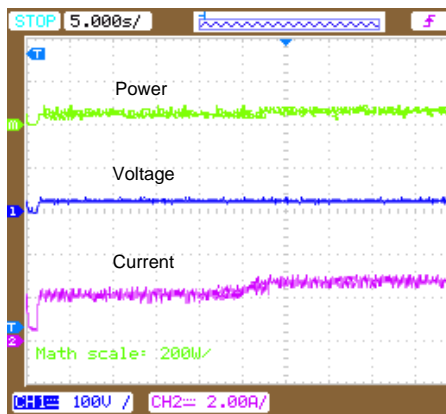


(a)



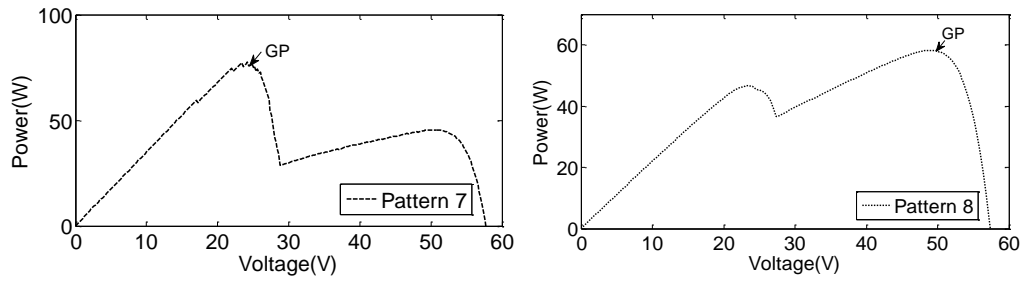
(b)

(c)

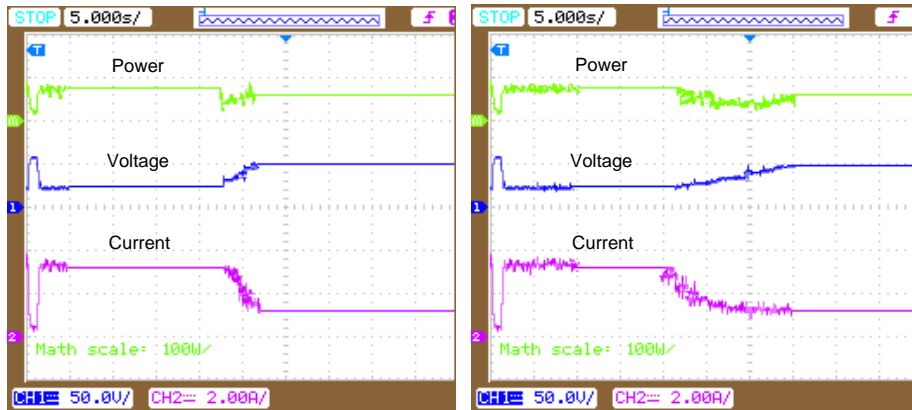


(d)

Figure 5.10: Experimental results for 4S configuration (a) P-V curves, Tracking curves using (b) GWO (c) IPSO (d) P&O

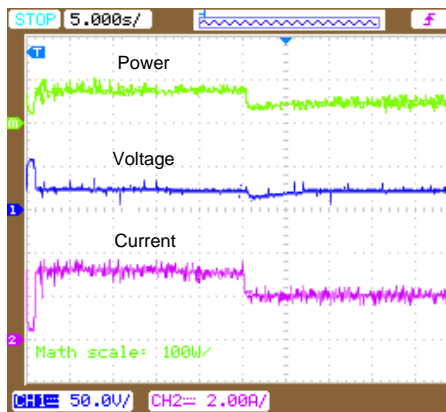


(a)



(b)

(c)



(d)

Figure 5.11: Experimental results for 2S2P configuration (a) P-V curves, Tracking curves using (b) GWO (c) IPSO (d) P&O

search process for the new MPP from the new P-V curve. The tracking curves of GWO and IPSO based MPPT reaches GP of 143.5W whereas P&O gets trapped to local peak of 65.32W. From the above results it is concluded that the proposed GWO based MPPT yields higher tracking speed and the oscillations disappear quickly as compared to other two methods namely IPSO and P&O.

In order to validate the effectiveness of the proposed MPPT for a different random pattern, experiments were carried out for 2S2P configuration having two types of shading as shown in Fig.5.11(a) as pattern 7 having GP of 77.98W and LP of 47W and pattern 8 have GP of 58.25W and LP of 46.64W respectively. The experimentally determined MPPT curves employing the proposed and existing methods are shown in Fig.5.11(b)5.11(c)5.11(d). The tracking curves of proposed and IPSO MPPT is able to converge to GP of 77.98W and P&O by chance settles to the GP resulting in oscillations. After sometime when the shading pattern changes to a new P-V curve marked as pattern 8, once again the three algorithms search the P-V curve for a new MPP. The curves of the proposed MPPT and IPSO based MPPT converges to the GP of 58.25W and P&O gets trapped at a local optimum value of 46.64W.

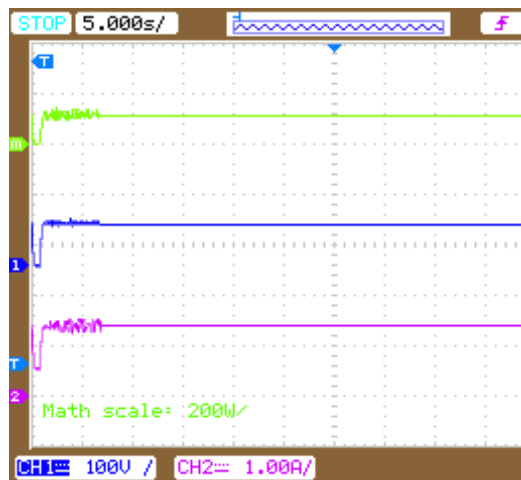


Figure 5.12: Experimental results for pattern 5 showing response of proposed MPPT under R-L load

To verify the effectiveness of the proposed MPPT algorithm is working accurately under R-L load, experiments were carried out for pattern 5. Fig.5.12 shows that the settling time increases but the performance of the proposed MPPT remains the same for convergence towards the GP. Fig.5.10 and 5.11 show that the proposed method can successfully detect the shading pattern variations and reinitialize the MPPT process exhibiting superior performance in terms of faster convergence to GP, reduced steady state oscillations and faster tracking in PV system under PSCs.

5.7 Chapter Summary

In this chapter, a new evolutionary computing approach called Grey wolf optimization to design a maximum power extraction algorithm for PV systems to work under partial shading conditions. The developed MPPT algorithm was first simulated using MATLAB/Simulink and subsequently it has been implemented in an experimental set up. In view of assessing the effectiveness of this new MPPT (Grey wolf based MPPT) its performance were compared with two existing MPPTs namely P&O and IPSO based MPPT methods and from the obtained results it was found that the GWO based MPPT exhibits superior MPPT performance compared to both P&O and IPSO MPPTs. Further, a technique is to be developed which would work both in uniform and non-uniform irradiance levels and would be able to harvest maximum possible power with least time.

Chapter 6

A Grey Wolf Assisted Perturb & Observe Maximum Power Point Tracking Algorithm for a PV System

6.1 Abstract

This chapter proposes a new Hybrid MPPT algorithm combining Grey Wolf Optimization (GWO) and Perturb & Observe (P&O) technique for efficient extraction of maximum power from a Photovoltaic (PV) system subjected to rapid variation of solar irradiance and partial shading conditions (PSCs). GWO handles the initial stages of maximum power point (MPP) tracking followed by application of the P&O algorithm at the final stage in view of achieving faster convergence to the global peak (GP). This MPPT thus overcomes the computational overhead as encountered in the case of a GWO based MPPT algorithm reported earlier [105]. The idea behind using the hybrid technique is to scale down the search space of GWO which helps to

speed up for achieving convergence towards the GP. The proposed MPPT algorithm is first implemented using MATLAB/SIMULINK and subsequently an experimental setup is prepared for its practical implementation. From the obtained results, it is confirmed that the proposed MPPT provides superior tracking performance in any weather conditions compared to both GWO and PSO+PO based MPPT algorithms.

6.2 Introduction

In Chapter 5, a new MPPT is developed using Grey wolf optimization technique which provides determination of global peak under PSCs. GWO handles the initial stages of maximum power point(MPP) tracking followed by application of the P&O algorithm at the final stage in view of achieving faster convergence to the global peak(GP). The idea behind using the hybrid technique is to scale down the search space of GWO which helps to speed up for achieving convergence towards the GP. In contrast to this, in Chapter 6, a new Hybrid-MPPT is developed which can track MPP with higher tracking efficiency in both uniform and non-uniform insolation levels.

The power extracted from PV modules is influenced by variation in solar insolation. It also becomes relatively difficult to maximize power extraction from a PV panel under partial shading conditions (PSCs). Therefore, maximum power point tracking (MPPT) algorithms are to be developed which can extract maximum possible power despite of any deviation in insolation and load [88] [106] [107] [108]. Numerous MPPT techniques have been proposed to improve the efficiency of the PV system as reported in literature, such as fractional open circuit voltage (FOCV) [27] and fractional short circuit current (FSCC) [27], Perturb and Observe (P&O) [103] [28] [29] and Incremental Conductance (IC) [30] [31]. In a PV power system, partial shading is an unavoidable complication that significantly reduces the efficiency of the overall system resulting in multiple peaks with several local and one global peak (GP). Thus, determining this peak leads to a great challenge for designing an appropriate MPP tracker [71] [45] [109] [7] for a PV

system.

In [79], a swarm intelligent technique with P&O algorithm is proposed for achieving faster convergence towards the GP under partial shading. A new sensorless Hybrid MPPT is proposed in [110] which exhibits low power oscillation around the MPP. Relationship between the load line and I-V curve with trigonometric rule [67], has been proposed to obtain a fast MPPT tracking response. An ant colony based MPPT has been proposed in [78], which is found to track the GP with minimum time and low computational overhead.

After having pursued the detailed convergence analysis i.e. the time taken to reach the GP by the GWO and P&O MPPTs, in this current chapter we have attempted to combine these two MPPTs. The above combination is aimed at achieving faster tracking of the GP through the proposed hybrid GWO-P&O MPPT technique to handle rapidly varying insolation patterns. In the proposed combination of GWO-MPPT and P&O-MPPT, the former method is used in off-line to bring the operating point of the PV array near the true MPP and then the later method is used in on-line to track the MPP with higher accuracy. Such fusion of off-line and on-line MPPT techniques makes fast tracking and guarantees global convergence for handling rapidly varying solar insolation patterns. To show the efficacy of the proposed Hybrid MPPT, it has been compared with two popular techniques like Hybrid PSO-PO [79] and GWO [105] based MPPT techniques.

6.3 Chapter Objectives

- To employ a dynamic global MPPT technique by combining a GWO optimizer with P&O MPPT which can handle PSCs resulting in faster convergence towards global peak with least time.
- To implement the above MPPT control algorithm in a practical Photovoltaic system.

6.4 PV System under Partial Shading Conditions

6.4.1 PV System Modeling

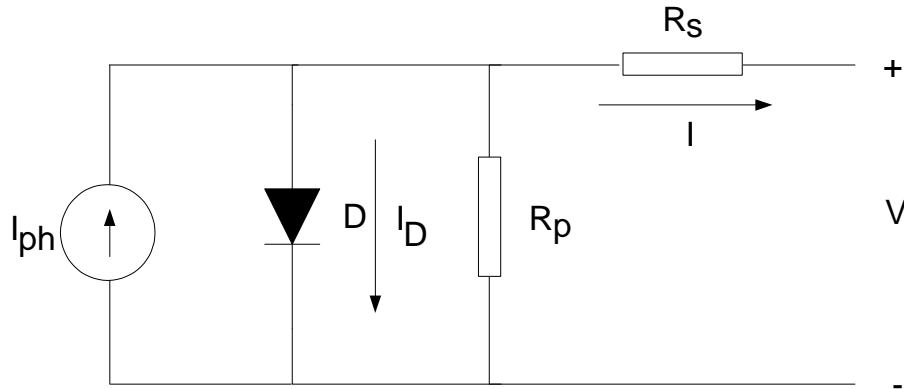


Figure 6.1: Equivalent circuit of a PV cell [7]

The single diode model of a PV cell is shown in Fig.6.1. By neglecting the shunt resistance R_{sh} , the output current can be written as

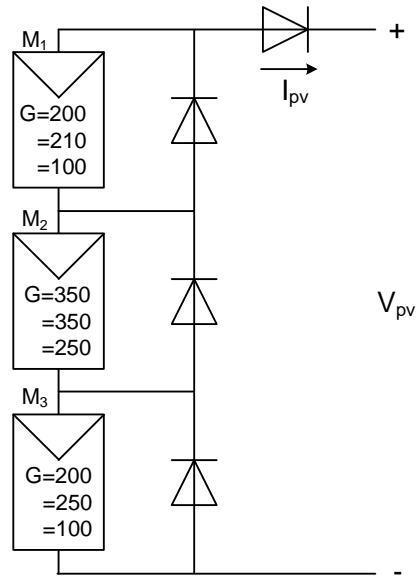
$$I = I_{ph} - I_0 \left[\exp \left(\frac{q(V + R_s I)}{N_s k T a} \right) - 1 \right] \quad (6.1)$$

The light generated current I_{pv} is proportional to irradiance G , and can be written as

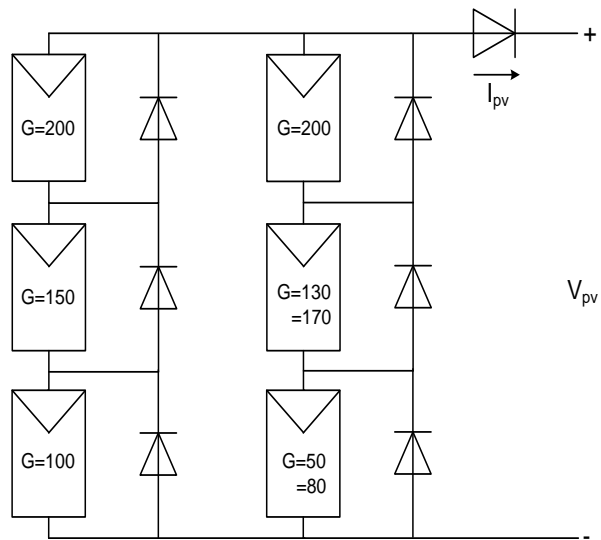
$$I_{ph} = \left(\frac{G}{G_0} \right) I_{g0} + J_0 (T_c - T_{ref}) \quad (6.2)$$

The diode saturation current is dependent upon temperature can be expressed as

$$I_0 = I_{d0} \left(\frac{T}{T_{ref}} \right)^3 \exp \left[\frac{q E_g}{nk} \left(\frac{1}{T_{ref}} - \frac{1}{T} \right) \right] \quad (6.3)$$

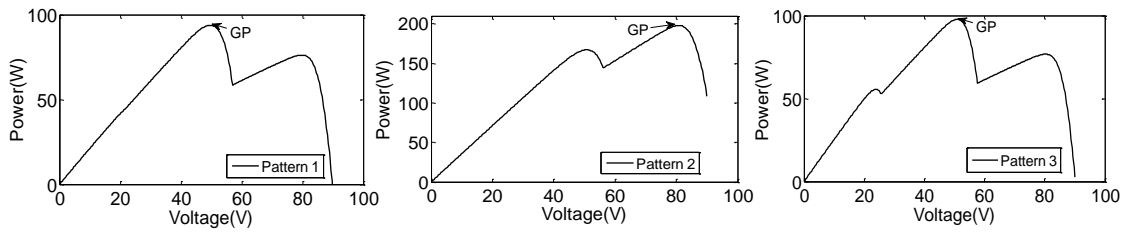


(a)

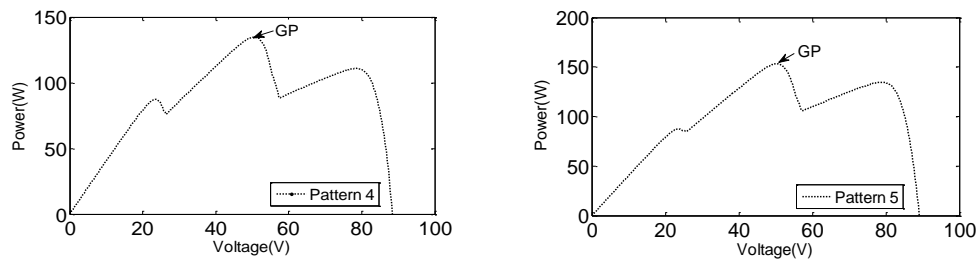


(b)

Figure 6.2: (a) 3S Configuration, (b) 3S2P Configuration



(a)



(b)

Figure 6.3: P-V curves exhibiting multiple peaks for (a) 3S Configuration, (b) 3S2P Configuration

6.4.2 System Description

A 3S configuration is shown in Fig.6.2(a) in which three modules are connected in series. Fig.6.2(b) shows the 3S2P configuration consisting of six PV modules connected in two parallel paths, each path consisting of three series connected modules. The P-V curve of three different shading patterns with clearly distinct GP locations for the 3S configuration is shown in Fig.6.3(a). The P-V curves of two different shading for 3S2P configuration is shown in Fig.6.3(b).

6.5 Problem Formulation

The proposed maximum power extraction can be formulated as an optimization problem as follows:

$$\text{Maximize } P(d) \quad (6.4)$$

$$\text{subjected to } d_{\min} \leq d \leq d_{\max} \quad (6.5)$$

Here, $P(d)$ denotes PV output power, d is duty ratio of the dc-dc converter and d_{\min} and d_{\max} are the lower and upper bounds of the duty ratio taken as 10% and 90% respectively.

6.6 Overview of the Proposed MPPT Method

6.6.1 Grey Wolf Optimization (GWO) application to MPPT Design

GWO is a metaheuristic algorithm inspired by grey wolves, which prefer to live in a pack and can be used to optimize a function that is difficult to express analytically [105]. Fig.6.4 shows a simple idea of the action of the wolf in the search space, where i represents the wolf number, P_i^t and G^t denote the personal and global best values which are to be updated at every iteration during the optimization process. α is the leader and decision maker, β and δ assist α in decision making and ω are the followers employed for replicating the leadership pyramid. The attacking behavior can be exhibited by the following equations [105]:

$$\vec{e} = |\vec{c} \cdot \vec{x}_p(t) - \vec{x}_p(t)| \quad (6.6)$$

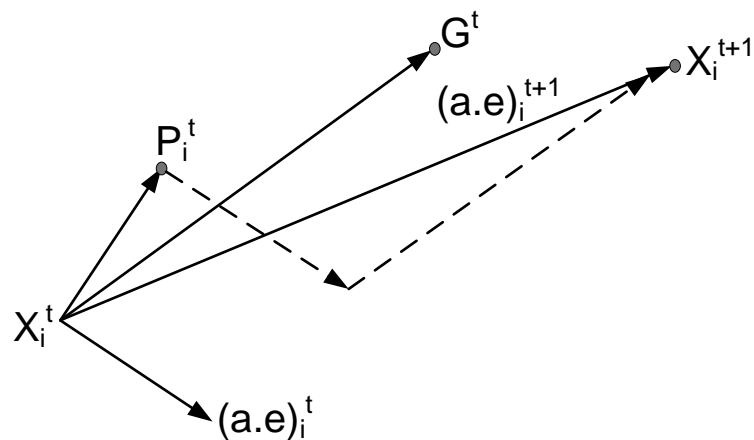


Figure 6.4: Movement of a wolf during search process

$$\vec{x}(t+1) = \vec{x}_p(t) - \vec{a} \cdot \vec{e} \quad (6.7)$$

where t is the current iteration, \vec{a} , \vec{c} and \vec{e} represent coefficient vectors, \vec{x}_p is the position vector of the prey and \vec{x} specifies the position vector of grey wolf.

The vectors \vec{a} and \vec{c} are estimated as follows:

$$\vec{a} = 2\vec{b} \cdot \vec{r}_1 - \vec{b} \quad (6.8)$$

$$\vec{c} = 2 \cdot \vec{r}_2 \quad (6.9)$$

where components of \vec{b} linearly decrease from 2 to 0 and \vec{r}_1 , \vec{r}_2 are random vectors in $[0, 1]$.

6.6.2 Perturb and Observe (P&O) MPPT

P&O MPPT tracks the MPP by perturbing the operating point and then observing the change in power before and after perturbations. This P&O is considered as the reference for any new MPPT to compare, as it is one of the best MPPTs popularly

used. The P&O based MPPT algorithm first calculates the power (P) of the PV array by measuring its voltage and current. Then, it provides a perturbation in the duty cycle based on the variation of power by following the rule [103]:

$$\begin{aligned} d_{new} &= d_{old} + \phi \\ d_{new} &= d_{old} - \phi \end{aligned} \tag{6.10}$$

In (6.10), ϕ denotes perturbed duty cycle. If ϕ is large, convergence is faster and steady state oscillation is high and vice versa.

6.6.3 Proposed Hybrid-MPPT

The fusion of GWO and P&O based MPPT technique which we call as GWO-PO hybrid MPPT is an intelligent computational algorithm which avoids the confusion that may appear during transformation of homogenous to non-homogenous and vice-versa i.e. during uniform insolation, P&O MPPT comes into act to track the MPP but during non-uniform insolation, Hybrid MPPT tracks the GP with initialization of the GWO first followed by the action of P&O, when the grey wolves reach closer to each other, the P&O MPPT gets started at the location of the best wolf in GWO process.

The proposed GWO-PO hybrid-MPPT is applied to the PV system operating under PSCs. In the proposed MPPT algorithm, the position of a wolf refers to duty ratio of the dc-dc converter used for implementation of MPPT which eliminates the PI control loop. This makes the controller more simplified and reduces the computational burden in tuning the controller gain. More number of wolves results in higher MPP accuracy but also increases the computational burden. Therefore, number of grey wolves may be considered as 3 to reduce the computational time. Fig.6.5 shows the flowchart of the proposed Hybrid-MPPT technique.

The following steps are adopted to implement the proposed MPPT algorithm:

Step 1 :Initialize the position of the wolves on fixed positions with equal space to lie between 10% and 90% of the duty ratio.

Step 2 :To maximize the PV array output power P at each wolf position, activate the converter and evaluate output power:

$$P_{pv} = V_{pv} * I_{pv} \quad (6.11)$$

Step 3 :Adjust the position of grey wolf as follows:

$$D_i(k+1) = D_i(k) - a.e \quad (6.12)$$

where D is current grey wolf, k is number of iterations, i is number of current grey wolves and a, e are coefficient vectors.

Step 4 :Repeat steps 3 and 4 until all the wolves converge towards the MPP.

Step 5 :After locating the MPP begin the P&O loop for tracking the maximum power (GP). Choose a small step size to obtain reduced oscillations in PV output power and higher tracking efficiency.

6.7 Simulation Case Studies

To verify the efficacy of the proposed MPPT, simulations were performed for both 3S and 3S2P configurations under both partial shading conditions and rapidly changing insolation levels. Fig.6.6 shows the structural outlay of a PV system consisting of PV array, dc-dc boost converter, MPPT controller and a load. For simulation studies, the parameters of the PV module taken for modelling are as follows: $P_{max}= 200\text{W}$, $V_{oc}=32.8\text{V}$, $I_{sc}=8.21\text{A}$, $V_{mp}=26.3\text{V}$ and $I_{mp}=7.61\text{A}$.

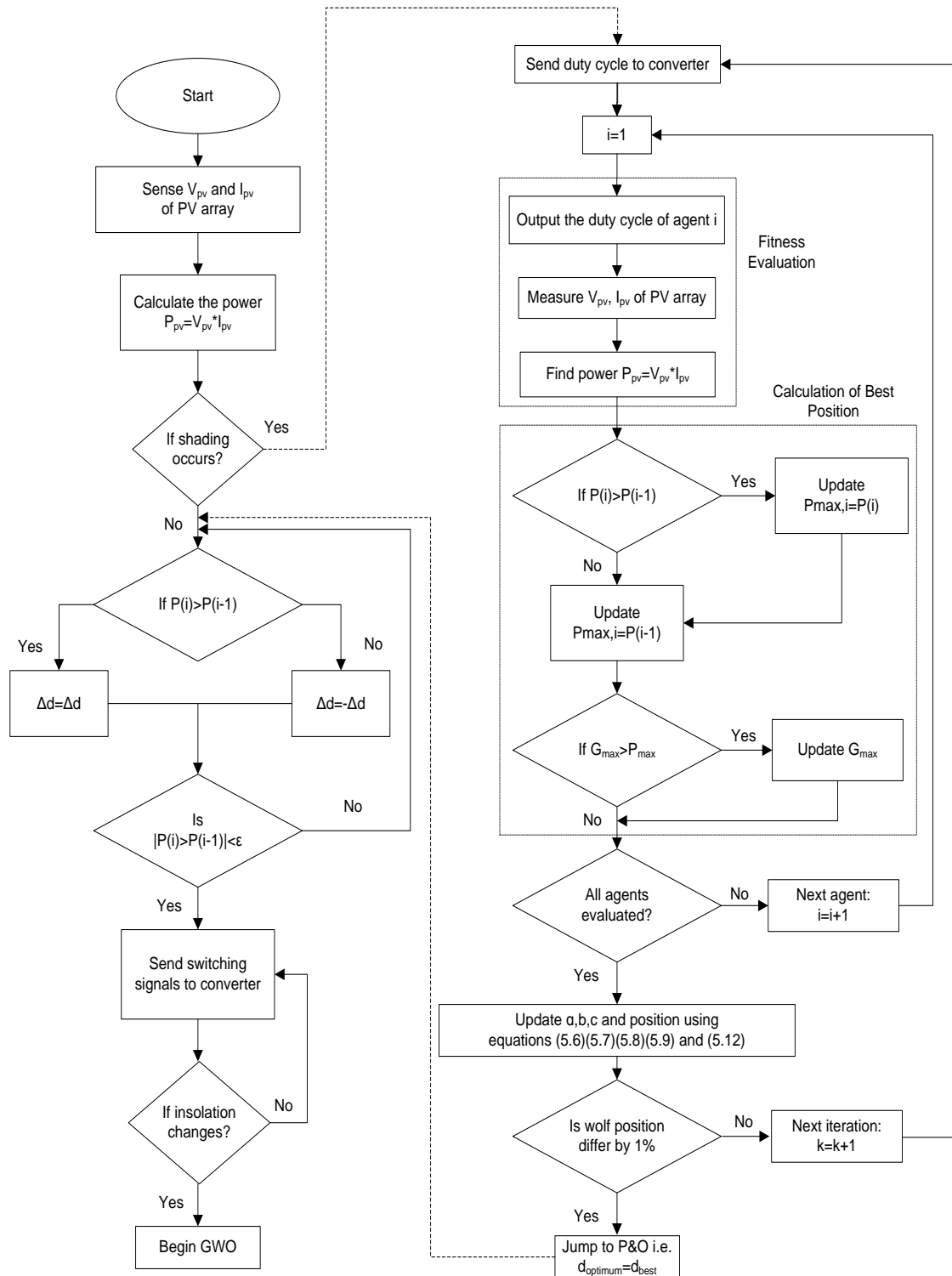


Figure 6.5: Flowchart of the Hybrid-MPPT Algorithm

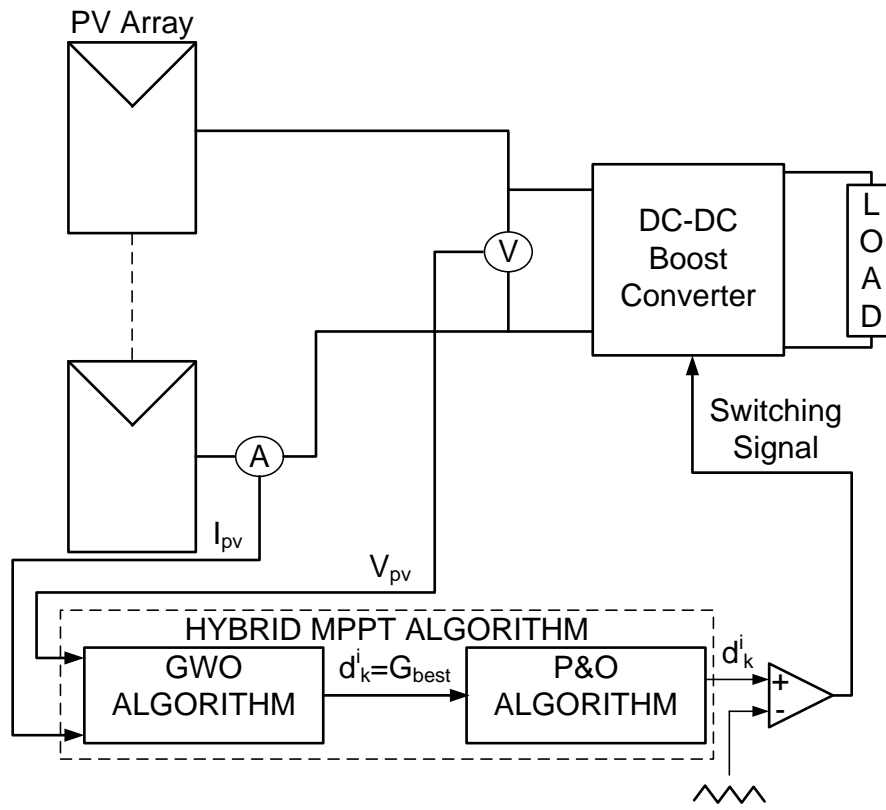


Figure 6.6: Block diagram of the proposed Hybrid-MPPT Algorithm

6.7.1 Partial Shading Conditions

The proposed GWO-PO hybrid MPPT algorithm is applied to the 3S configuration for pattern 1 under PSCs to track the global peak (GP) and it is compared with fast converging techniques such as GWO and PSO-PO based MPPT techniques as shown in Fig.6.7. Similarly, the simulation was repeated for 3S2P configuration for pattern 4 shown in Fig.6.8. Both Fig.6.7 and Fig.6.8 clearly show that the proposed MPPT clearly tracks the GP with faster convergence as compared to GWO and PSO-PO MPPT techniques. From, the results shown below it is concluded that the proposed GWO-PO hybrid MPPT exhibits faster convergence amongst GWO and PSO-PO MPPTs.

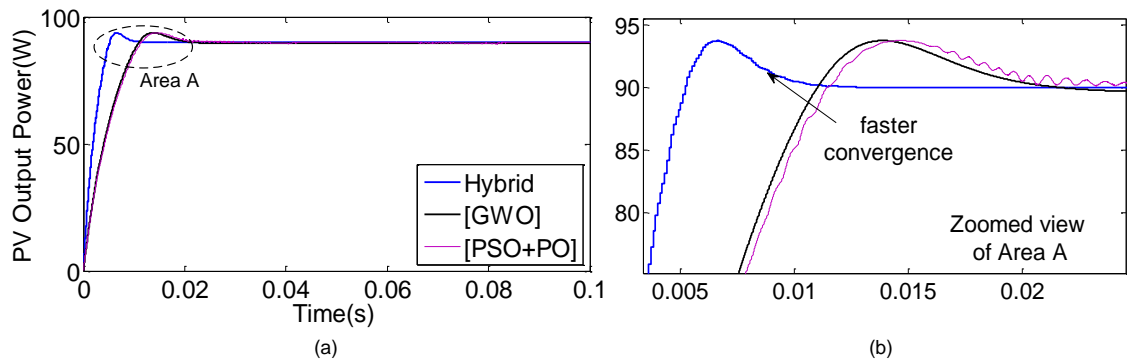


Figure 6.7: Tracking curves for 3S configuration (a) PV power of proposed Hybrid MPPT compared with other techniques like GWO, PSO+PO based MPPT, (b) zoomed view of Area A

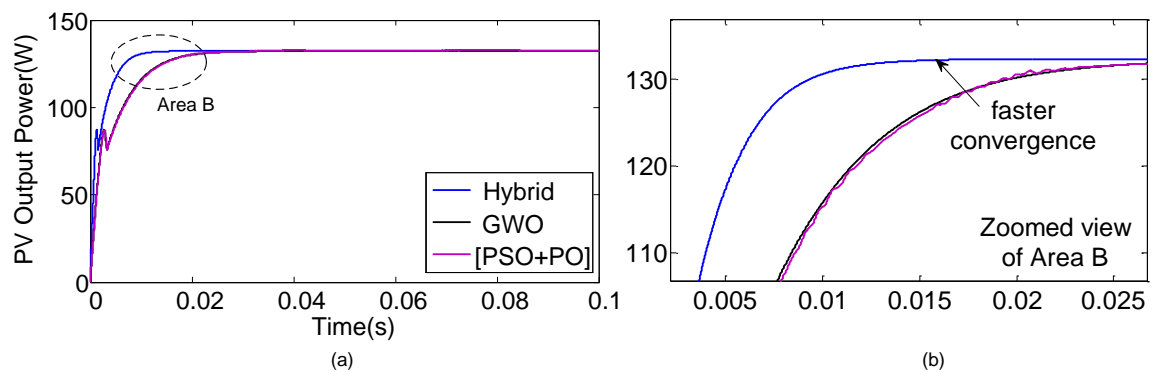


Figure 6.8: Tracking curves for 3S2P configuration (a) PV power of proposed Hybrid MPPT compared with other techniques like GWO, PSO+PO based MPPT, (b) zoomed view of Area B

6.7.2 Rapidly Changing Insolation levels

For 3S configuration, the solar intensities of the PV modules are arbitrarily varied i.e. pattern 1 shifts to pattern 2 as shown in Fig. 6.3(a). Each pattern prevails for 0.1sec. The simulation is now repeated for the 3S2P configuration where insolation is varied for two different patterns namely pattern 4 and pattern 5 (Fig.6.3(b)) which exists for

0.1sec each.

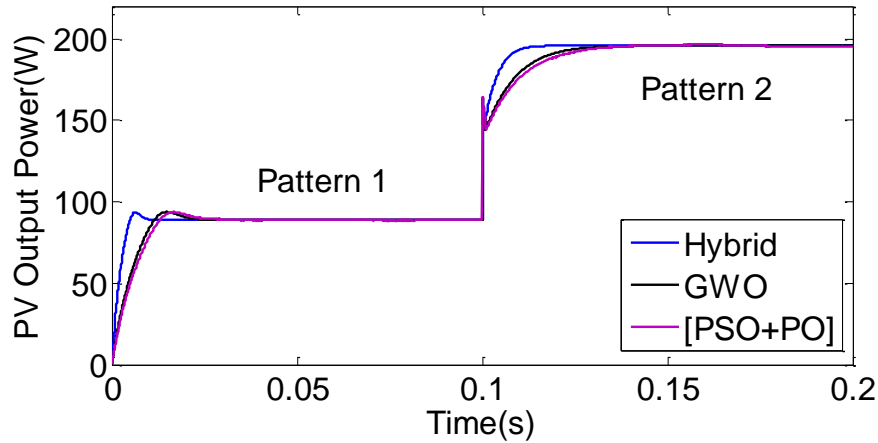


Figure 6.9: Tracking curves for 3S configuration for rapid changes in insolation

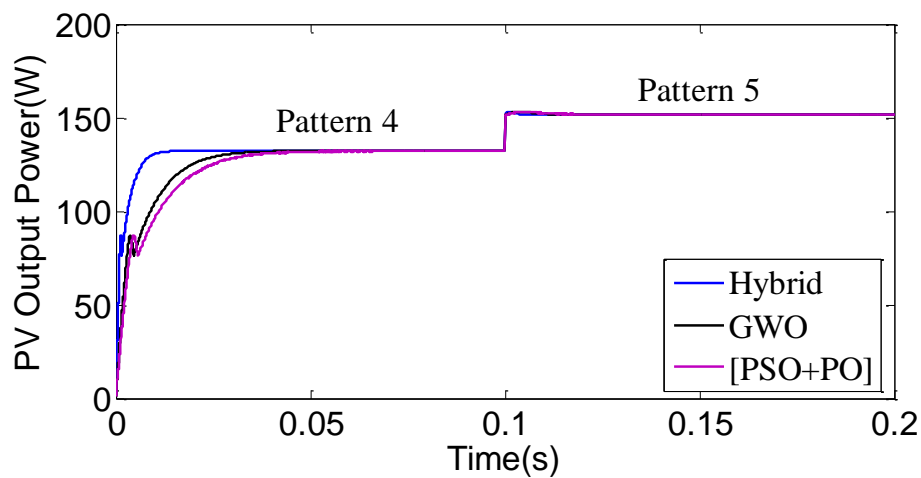


Figure 6.10: Tracking curves for 3S2P configuration for rapid changes in insolation

The above cases show that the proposed and GWO-MPPT are able to track GP with no oscillations. Fig.6.9 and Fig.6.10 clearly show that the proposed GWO-PO hybrid-MPPT converges to the GP faster as compared to the GWO-MPPT and PSO-PO-MPPTs. Both GWO-PO hybrid-MPPT and GWO-MPPT track the GP with no

oscillations whereas PSO-PO-MPPT exhibit oscillations.

6.7.3 Extreme Rapidly Changing Insolation levels

To analyse the robustness of the proposed GWO-PO hybrid-MPPT, the PV array (3S configuration) was exposed to extreme rapidly changing insolation levels such as: pattern 1-pattern 2-pattern 3. Each pattern was changed at 0.1s interval each. Fig.6.11 clearly shows that both GWO-PO and GWO-MPPT track the GP with no oscillation but the GWO-PO hybrid-MPPT reaches the GP at minimal time as compared to the GWO-MPPT. The PSO-PO MPPT is able to track the GP but with oscillations.

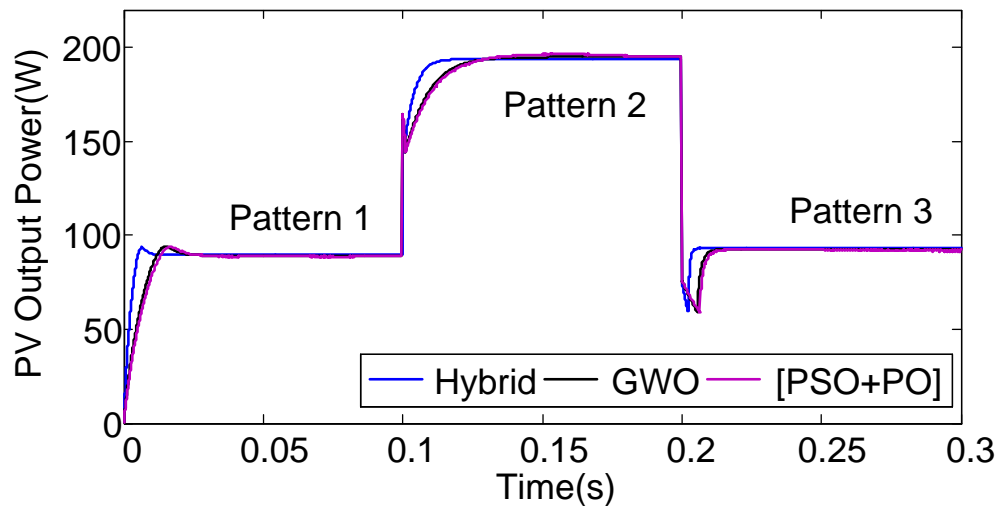


Figure 6.11: Tracking curves for 3S configuration for extreme rapid changes in insolation

From the simulation results presented above, it is observed that the GWO-PO hybrid-MPPT can handle fast changing insolation patterns and it outperforms both PSO-PO and GWO-MPPTs in terms of faster convergence to the GP, tracking speed, reduced oscillations, and higher efficiency. The simulation results shown in Figs.6.7, 6.8,6.9,6.10 and 6.11 are summarized in Table 6.1, where the performance of the proposed GWO-PO hybrid MPPT is found to be superior over PSO-PO and GWO-MPPT

techniques. Further, a characteristics comparison between different fast converging MPPTs are presented in Table 6.2. The tracking efficiency (η) is calculated as the ratio among average output power acquired under steady state condition and maximum obtainable power of the PV array under certain pattern [30].

Table 6.1: Performance Evaluation of the proposed MPPT method for 3S and 3S2P Configuration

Shading Pattern and Maximum power from P-V curve	Tracking Methods	Power (Watts)	Convergence time (sec)	% Tracking Efficiency
Pattern 1 (3S) (90W)	Hybrid	90	0.015	100
	GWO	89.8	0.030	99.77
	[[79]]	89.6	0.045	99.55
Pattern 2 (3S) (196W)	Hybrid	195.9	0.014	99.84
	GWO	195.7	0.040	99.77
	[[79]]	195.7	0.050	99.77
Pattern 3 (3S) (93.2W)	Hybrid	93.16	0.007	99.95
	GWO	92.80	0.025	99.57
	[[79]]	92.41	0.025	99.15
Pattern 4 (3S2P) (132.3W)	Hybrid	132.3	0.015	100
	GWO	132.2	0.040	99.92
	[[79]]	132.2	0.040	99.92
Pattern 5 (3S2P) (151.6W)	Hybrid	151.6	0.010	100
	GWO	151.6	0.025	100
	[[79]]	151.5	0.025	99.93

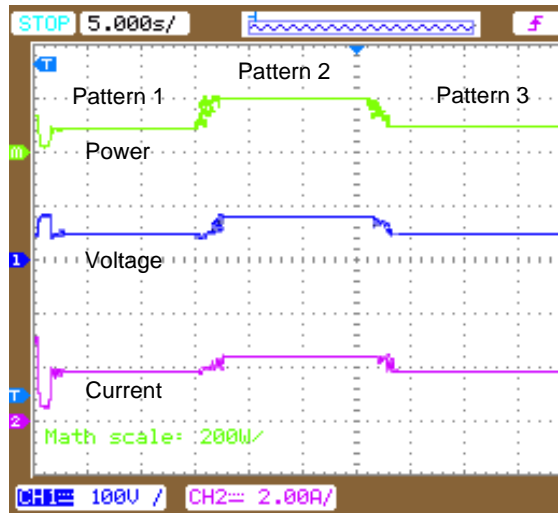
Table 6.2: Characteristics Comparison of the proposed Hybrid MPPT method with other MPPT Methods

MPPT Methods	Periodic tuning	Dynamic Response	Power oscillations	Convergence to GP	Complexity
Proposed	No	Accurate & fast	Very less	Always guaranteed	Medium
GWO	No	Good	Very less	Always guaranteed	Medium
Hybrid [110]	Yes	Accurate & fast	Less	Always guaranteed	Medium
Hybrid PSO [79]	No	Accurate & fast	Less	Always guaranteed	Medium
Hybrid Ant [78]	No	Accurate & fast	Less	Always guaranteed	Medium

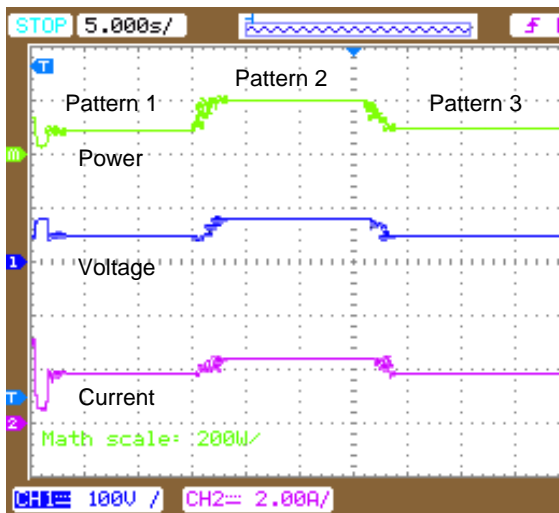
6.8 Experimental Results

In order to verify the efficacy of the proposed Hybrid MPPT, experiments have been carried out for both 3S and 3S2P configurations and the experimental set up is shown in Fig.3.1. In order to verify the effectiveness of the proposed Hybrid-MPPT for the 3S configuration under extreme rapidly changing insolation level, experiments were conducted for 3S configuration (pattern 1, pattern 2 and pattern 3) as shown in Fig.6.12. The proposed Hybrid-MPPT is able to converge to the GP within 2.7sec, GWO-MPPT converges to the GP at 3.1sec, PSO-PO-MPPT converges at 3.2sec resulting in small oscillations around the MPP. Thus, from the aforesaid results it is observed that the proposed method exhibits superior MPPT tracking performance over the other MPPT

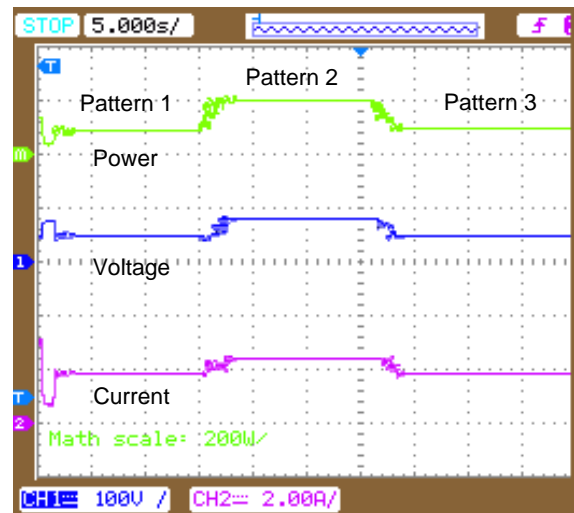
techniques under dissimilar changing insolation patterns in terms of faster convergence towards reaching the GP and yielding higher energy output.



(a)

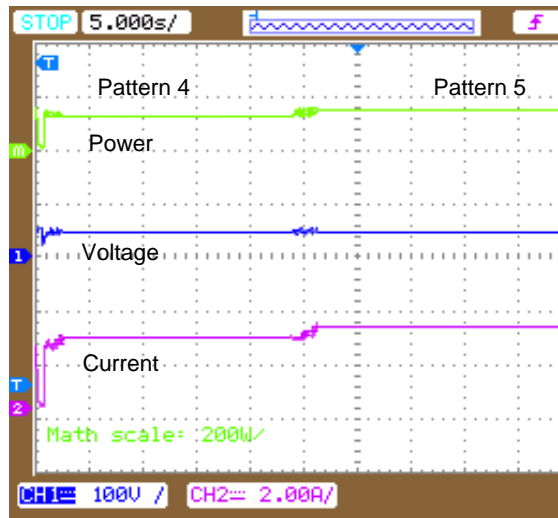


(b)

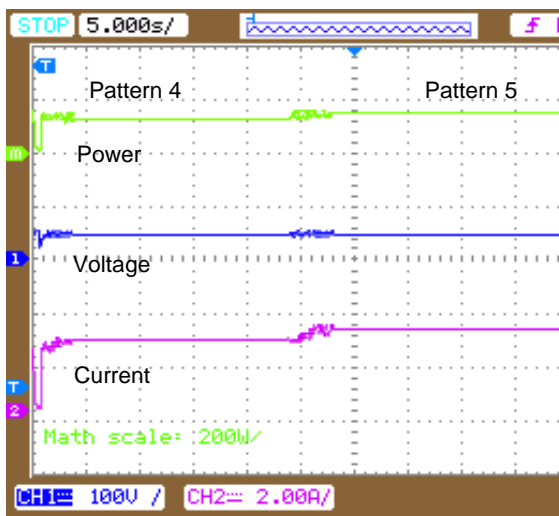


(c)

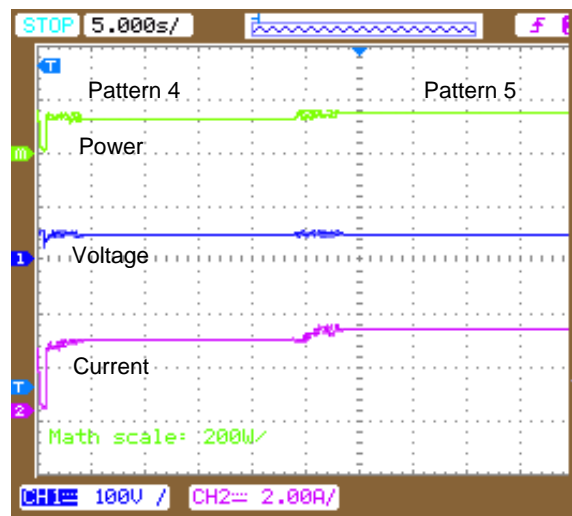
Figure 6.12: Experimental Results for 3S Configuration for extreme rapidly changing insolation patterns (a) Hybrid-MPPT (b) GWO-MPPT (c) PSO-PO MPPT



(a)



(b)



(c)

Figure 6.13: Experimental Results for 3S2P Configuration for rapidly changing insolation patterns (a) Hybrid-MPPT (b) GWO-MPPT (c) PSO-PO MPPT

Next we present the experimentally obtained tracking curves for the 3S2P configuration under rapidly changing insolation patterns (pattern 4 and pattern 5) as shown

in Fig.6.13. From Fig.6.13 it is clearly observed that both Hybrid and GWO MPPT converge to the GP but the convergence time of Hybrid-MPPT is 2.4sec whereas the GWO-MPPT converges at 3.8sec. The proposed technique is also compared with PSO-PO-MPPT which is able to track the GP at 4sec but yields small oscillations. Thus, the proposed GWO-PO Hybrid-MPPT converges faster as compared to the other fast converging MPPTs resulting in higher energy output.

The combination of GWO and P&O algorithm results in faster convergence to the GP with least time enabling highest possible maximum power from the solar PV system. Thus, it is concluded that the Hybrid-MPPT is capable to adapt itself towards sudden variation in insolation and any partial shading while improving the system efficiency.

6.9 Chapter Summary

In this chapter, a new GWO-PO Hybrid-MPPT for maximum power from a PV system with different possible patterns has been developed. The effectiveness of the proposed GWO-PO Hybrid MPPT algorithm was evaluated through both simulation studies followed by experimental studies on a 600W prototype PV system. Comparative studies of the Hybrid-MPPT with other fast converging techniques envisage that the proposed GWO-PO Hybrid-MPPT exhibits superior performance such as higher tracking speed and faster convergence towards the GP.

Chapter 7

Conclusion and Suggestions for Future Work

7.1 Overall Summary of the Thesis

This thesis has presented a modeling of a PV array and extraction of maximum power under partial shading conditions for a Photovoltaic System. Different topologies for PV power generation, maximum power extraction algorithms and partial shading conditions have been described in Chapter 1.

As discussed in the objectives, new MPPT schemes have been developed which is able to extract maximum power output from the PV system with changing insolation levels, temperature variations and other environmental conditions. An extensive review on MPPT algorithms for both uniform and non-uniform insolation levels have been pursued and presented in Chapter 2. Subsequently, an analysis with respect to their merits, demerits and applications has been provided in order to design new MPPTs to achieve higher MPPT efficiency.

Chapter 3 discusses about the experimental setup used for validating the proposed techniques under partial shading conditions in a PV system using MATLAB/SIMULINK software. Here, two different types of PV sources are used i.e. Agilent simulator (E4360A)

and Sukam make panels for experimentation purpose.

Chapter 4 analytically investigates the effects of partial shading on a PV system with and without bypass diode and development of a new configuration which will produce maximum power under changing insolation patterns on the basis of maximum power and fill factor. Also, the proposed RP configuration has been compared with different module configurations like SP, TCT and BL under PSCs with a randomly assigned irradiance of $0.02\text{kW}/\text{m}^2$ and $0.04\text{kW}/\text{m}^2$. Also, the experimental study conclude that the TCT and the proposed RP configuration exhibits maximum power of 51.077W and 50.258W as well as the RP configuration has higher value of fill factor of 0.474 as compared to the rest.

Metaheuristic optimization methodologies such as Particle Swarm Optimization (PSO) [71] [70], firefly [73] etc., have been extensively used for different applications. After a thorough literature survey, it was found that GWO [104] has never been exploited for designing a MPPT. Therefore, a new evolutionary computing approach called Grey wolf optimization is employed to design a maximum power extraction algorithm for PV systems to work under partial shading conditions which is discussed in Chapter 5. In view of assessing the effectiveness of this new MPPT (Grey wolf based MPPT), its performance was compared with that of two existing MPPTs namely P&O and Improved-PSO based MPPT algorithms. From the obtained results, it was found that the GWO based MPPT exhibits superior MPPT performance compared to both P&O and IPSO MPPT on the basis of dynamic response, faster convergence to GP and higher tracking efficiency.

In Chapter 6, a new Hybrid-MPPT for maximum power from a PV system with different possible patterns has been developed. The idea behind using the hybrid technique is to scale down the search space of GWO which helps to speed up for achieving convergence towards the GP. This MPPT thus overcomes the computational overhead as encountered in the case of a GWO based MPPT algorithm reported earlier in [105]. The effectiveness of the proposed GWO-PO Hybrid MPPT algorithm was

evaluated through both simulation studies followed by experimental studies on a 600W prototype PV system. Comparative studies of the Hybrid-MPPT with other fast converging techniques envisage that the proposed GWO-PO Hybrid-MPPT exhibits superior performance such as higher tracking speed and faster convergence towards the GP.

7.1.1 Contributions of the Thesis

- A new analytical modeling of PV panels for producing maximum power and fill factor is pursued. From the analysis, it is observed that the proposed new Ring pattern configuration is suitable for achieving maximum power and fill factor.
- In view of achieving maximum power from PV panels subjected to non-uniform solar irradiances, such as PSCs a new evolutionary computing technique i.e. Grey wolf optimization is employed to design a global MPPT.
- This new Grey wolf based MPPT has been employed both in simulation and experiment and it is found that this new GWO-MPPT is very efficient in providing maximum power yield from PV panels under non-uniform solar irradiances.
 - S. Mohanty, B. Subudhi and P. K Ray, A New MPPT Design using Grey wolf optimization technique for Photovoltaic system under partial shading conditions, *IEEE Trans on Sustainable Energy*, vol. 7, no. 1, pp. 181-188, Jan 2016.
- In order to reduce the computational burden of GWO based MPPT algorithm and achieve faster convergence towards the GP, a dynamic global MPPT technique is designed by combining a GWO optimizer with P&O MPPT is developed. Here, GWO handles the initial stages of maximum power point(MPP) tracking followed by application of the P&O algorithm at the final stage in view of achieving faster convergence to the global peak (GP). So, the resulting GWO-PO

exhibits superior performance in terms of faster convergence to GP and reduced computational burden.

- S. Mohanty, B. Subudhi and P. K Ray, A Grey Wolf Assisted Perturb & Observe MPPT Algorithm for a PV System, *IEEE Trans on Energy Conversion*, DOI:10.1109/TEC.2016.2633722.

7.2 Suggestions for the future work

- In this thesis, an analytical modeling of PV modules for handling non-uniform solar irradiances is pursued first and subsequently a new Ring pattern configuration for PV modules is developed to achieve maximum power and fill factor. Further, the thesis proposed two new MPPT techniques namely GWO and Hybrid based MPPT for tracking global peak under PSCs for standalone PV systems. An immediate extension of the above work is to apply these algorithms to a Grid connected PV system. An utility grid may have different conventional and nonconventional sources. If the PV system is not properly controlled, then grid may become unstable. As the dynamics of PV system is dependent greatly on fluctuation of solar irradiance and temperature, there is a strong research need of studying dynamic stability of the PV system.
- Other evolutionary computing techniques can also be explored for determining maximum power for a PV system subjected to PSCs. The obtained MPPT can be applied to Solar-Wind Hybrid system to achieve higher efficiency of energy conversion.

References

- [1] (24-Jan-17) Growth of photovoltaics. [Online]. Available: https://en.wikipedia.org/wiki/Growth_of_photovoltaics
- [2] (2-Jan-17) How solar power works. [Online]. Available: <https://www.pinterest.com/lasolarpower/how-solar-power-works/>
- [3] V. Kolluru, "Design and development of fpga based controllers for photovoltaic power system," Ph.D. dissertation, 2016.
- [4] (24-Jan-17) Shading. [Online]. Available: <http://www.homepower.com/articles/solar-electricity/design-installation/energy-basics-shading-and-solar-electric-systems>
- [5] (24-Jan-17) Renewableenergy. [Online]. Available: http://giridaran-solar.blogspot.in/2012_12_01_archive.html
- [6] M. G. Villalva, J. R. Gazoli, and E. Ruppert Filho, "Comprehensive approach to modeling and simulation of photovoltaic arrays," *IEEE Transactions on Power Electronics*, vol. 24, no. 5, pp. 1198–1208, 2009.
- [7] H. Patel and V. Agarwal, "Matlab-based modeling to study the effects of partial shading on pv array characteristics," *IEEE Transactions on Energy Conversion*, vol. 23, no. 1, pp. 302–310, 2008.
- [8] K. Peng, Y. Xu, Y. Wu, Y. Yan, S.-T. Lee, and J. Zhu, "Aligned single-crystalline si nanowire arrays for photovoltaic applications," *small*, vol. 1, no. 11, pp. 1062–1067, 2005.
- [9] R. Karki and R. Billinton, "Reliability/cost implications of pv and wind energy utilization in small isolated power systems," *IEEE Transactions on Energy Conversion*, vol. 16, no. 4, pp. 368–373, 2001.
- [10] H. Ravaee, S. Farahat, and F. Sarhaddi, "Artificial neural network based model of photovoltaic thermal (pv/t) collector," *The Journal of Mathematics and Computer Science*, vol. 4, no. 3, pp. 411–417, 2012.

-
- [11] G. K. Singh, "Solar power generation by pv (photovoltaic) technology: a review," *Energy*, vol. 53, pp. 1–13, 2013.
- [12] R. Chenni, M. Makhoulf, T. Kerbache, and A. Bouzid, "A detailed modeling method for photovoltaic cells," *Energy*, vol. 32, no. 9, pp. 1724–1730, 2007.
- [13] A. C. Kyritsis, E. Tatakis, and N. Papanikolaou, "Optimum design of the current-source flyback inverter for decentralized grid-connected photovoltaic systems," *IEEE Transactions on Energy Conversion*, vol. 23, no. 1, pp. 281–293, 2008.
- [14] J. Gow and C. Manning, "Development of a photovoltaic array model for use in power-electronics simulation studies," *IEE Proceedings-Electric Power Applications*, vol. 146, no. 2, pp. 193–200, 1999.
- [15] B. Parida, S. Iniyar, and R. Goic, "A review of solar photovoltaic technologies," *Renewable and sustainable energy reviews*, vol. 15, no. 3, pp. 1625–1636, 2011.
- [16] S.-K. Kim, J.-H. Jeon, C.-H. Cho, J.-B. Ahn, and S.-H. Kwon, "Dynamic modeling and control of a grid-connected hybrid generation system with versatile power transfer," *IEEE Transactions on Industrial Electronics*, vol. 55, no. 4, pp. 1677–1688, 2008.
- [17] M. T. Ameli, S. Moslehpour, and M. Shamlo, "Economical load distribution in power networks that include hybrid solar power plants," *Electric Power Systems Research*, vol. 78, no. 7, pp. 1147–1152, 2008.
- [18] N. Femia, G. Petrone, G. Spagnuolo, and M. Vitelli, "Optimization of perturb and observe maximum power point tracking method," *IEEE Transactions on Power Electronics*, vol. 20, no. 4, pp. 963–973, 2005.
- [19] H. N. Zainudin and S. Mekhilef, "Comparison study of maximum power point tracker techniques for pv systems," in *Proceedings of the 14th international middle east power systems conference (MEPCON10)*, Cairo University, Egypt, 2010, pp. 750–755.
- [20] O. López-Lapeña, M. T. Penella, and M. Gasulla, "A new mppt method for low-power solar energy harvesting," *IEEE Transactions on Industrial Electronics*, vol. 57, no. 9, pp. 3129–3138, 2010.
- [21] F. Blaabjerg, Z. Chen, and S. B. Kjaer, "Power electronics as efficient interface in dispersed power generation systems," *IEEE Transactions on Power Electronics*, vol. 19, no. 5, pp. 1184–1194, 2004.

- [22] T. T. Khatib, A. Mohamed, N. Amin, and K. Sopian, "An efficient maximum power point tracking controller for photovoltaic systems using new boost converter design and improved control algorithm," *WSEAS Transactions on power systems*, vol. 5, no. 4, pp. 53–63, 2010.
- [23] V. Salas, E. Olias, A. Lazaro, and A. Barrado, "Evaluation of a new maximum power point tracker (mppt) applied to the photovoltaic stand-alone systems," *Solar Energy Materials and Solar Cells*, vol. 87, no. 1, pp. 807–815, 2005.
- [24] S. R. Chowdhury and H. Saha, "Maximum power point tracking of partially shaded solar photovoltaic arrays," *Solar Energy Materials and Solar Cells*, vol. 94, no. 9, pp. 1441–1447, 2010.
- [25] R. Ramaprabha, M. Balaji, and B. Mathur, "Maximum power point tracking of partially shaded solar pv system using modified fibonacci search method with fuzzy controller," *International Journal of Electrical Power & Energy Systems*, vol. 43, no. 1, pp. 754–765, 2012.
- [26] J. Phang, D. Chan, and J. Phillips, "Accurate analytical method for the extraction of solar cell model parameters," *Electronics Letters*, vol. 20, no. 10, pp. 406–408, 1984.
- [27] B. Subudhi and R. Pradhan, "A comparative study on maximum power point tracking techniques for photovoltaic power systems," *IEEE Transactions on Sustainable Energy*, vol. 4, no. 1, pp. 89–98, 2013.
- [28] M. A. Elgendy, B. Zahawi, and D. J. Atkinson, "Operating characteristics of the p&o algorithm at high perturbation frequencies for standalone pv systems," *IEEE Transactions on Energy Conversion*, vol. 30, no. 1, pp. 189–198, 2015.
- [29] T. Radjai, J. P. Gaubert, L. Rahmani, and S. Mekhilef, "Experimental verification of p&o mppt algorithm with direct control based on fuzzy logic control using cuk converter," *International Transactions on Electrical Energy Systems*, vol. 25, no. 12, pp. 3492–3508, 2015.
- [30] M. A. Elgendy, B. Zahawi, and D. J. Atkinson, "Assessment of the incremental conductance maximum power point tracking algorithm," *IEEE Transactions on Sustainable Energy*, vol. 4, no. 1, pp. 108–117, 2013.
- [31] M. A. Elgendy, D. J. Atkinson, and B. Zahawi, "Experimental investigation of the incremental conductance maximum power point tracking algorithm at high perturbation rates," *IET Renewable Power Generation*, vol. 10, no. 2, pp. 133–139, 2016.

- [32] T. Esum, J. W. Kimball, P. T. Krein, P. L. Chapman, and P. Midya, "Dynamic maximum power point tracking of photovoltaic arrays using ripple correlation control," *IEEE Transactions on Power Electronics*, vol. 21, no. 5, pp. 1282–1291, 2006.
- [33] V. Salas, E. Olias, A. Barrado, and A. Lazaro, "Review of the maximum power point tracking algorithms for stand-alone photovoltaic systems," *Solar energy materials and solar cells*, vol. 90, no. 11, pp. 1555–1578, 2006.
- [34] W. Xiao, W. G. Dunford, P. R. Palmer, and A. Capel, "Application of centered differentiation and steepest descent to maximum power point tracking," *IEEE Transactions on Industrial Electronics*, vol. 54, no. 5, pp. 2539–2549, 2007.
- [35] W. L. Yu, T.-P. Lee, G.-H. Wu, Q. S. Chen, H.-J. Chiu, Y.-K. Lo, and F. Shih, "A dsp-based single-stage maximum power point tracking pv inverter," in *Applied Power Electronics Conference and Exposition (APEC), 2010 Twenty-Fifth Annual IEEE*. IEEE, 2010, pp. 948–952.
- [36] N. Femia, D. Granozio, G. Petrone, G. Spagnuolo, and M. Vitelli, "Optimized one-cycle control in photovoltaic grid connected applications," *IEEE Transactions on Aerospace and Electronic Systems*, vol. 42, no. 3, pp. 954–972, 2006.
- [37] K. Tse, M. Ho, H.-H. Chung, and S. Hui, "A novel maximum power point tracker for pv panels using switching frequency modulation," *IEEE Transactions on Power Electronics*, vol. 17, no. 6, pp. 980–989, 2002.
- [38] N. Pongratananukul, "Analysis and simulation tools for solar array power systems," Ph.D. dissertation, University of Central Florida Orlando, Florida, 2005.
- [39] T. L. Kottas, Y. S. Boutalis, and A. D. Karlis, "New maximum power point tracker for pv arrays using fuzzy controller in close cooperation with fuzzy cognitive networks," *IEEE Transactions on Energy Conversion*, vol. 21, no. 3, pp. 793–803, 2006.
- [40] T. Hiyama and K. Kitabayashi, "Neural network based estimation of maximum power generation from pv module using environmental information," *IEEE Transactions on Energy Conversion*, vol. 12, no. 3, pp. 241–247, 1997.
- [41] C.-C. Chu and C.-L. Chen, "Robust maximum power point tracking method for photovoltaic cells: A sliding mode control approach," *Solar Energy*, vol. 83, no. 8, pp. 1370–1378, 2009.
- [42] T. Esum, P. L. Chapman *et al.*, "Comparison of photovoltaic array maximum power point tracking techniques," *IEEE Transactions on Energy Conversion EC*, vol. 22, no. 2, p. 439, 2007.

- [43] A. Woyte, V. Van Thong, R. Belmans, and J. Nijs, "Voltage fluctuations on distribution level introduced by photovoltaic systems," *IEEE Transactions on Energy Conversion*, vol. 21, no. 1, pp. 202–209, 2006.
- [44] R. Kadri, J.-P. Gaubert, and G. Champenois, "An improved maximum power point tracking for photovoltaic grid-connected inverter based on voltage-oriented control," *IEEE Transactions on Industrial Electronics*, vol. 58, no. 1, pp. 66–75, 2011.
- [45] J. M. Carrasco, L. G. Franquelo, J. T. Bialasiewicz, E. Galván, R. C. PortilloGuisado, M. M. Prats, J. I. León, and N. Moreno-Alfonso, "Power-electronic systems for the grid integration of renewable energy sources: A survey," *IEEE Transactions on Industrial Electronics*, vol. 53, no. 4, pp. 1002–1016, 2006.
- [46] M. E. Ropp and S. Gonzalez, "Development of a matlab/simulink model of a single-phase grid-connected photovoltaic system," *IEEE Transactions on Energy Conversion*, vol. 24, no. 1, pp. 195–202, 2009.
- [47] T. Andrejasic, M. Jankovec, and M. Topic, "Comparison of direct maximum power point tracking algorithms using en 50530 dynamic test procedure," *IET Renewable Power Generation*, vol. 5, no. 4, pp. 281–286, 2011.
- [48] M. Lei, S. Yaojie, L. Yandan, B. Zhifeng, T. Liqin, and S. Jieqiong, "A high performance mppt control method," in *Materials for Renewable Energy & Environment (ICMREE), 2011 International Conference on*, vol. 1. IEEE, 2011, pp. 195–199.
- [49] S. M. R. Kazmi, H. Goto, O. Ichinokura, and H.-J. Guo, "An improved and very efficient mppt controller for pv systems subjected to rapidly varying atmospheric conditions and partial shading," in *Power Engineering Conference, 2009. AUPEC 2009. Australasian Universities*. IEEE, 2009, pp. 1–6.
- [50] H. Patel and V. Agarwal, "Maximum power point tracking scheme for pv systems operating under partially shaded conditions," *IEEE Transactions on Industrial Electronics*, vol. 55, no. 4, pp. 1689–1698, 2008.
- [51] A. Zbeeb, V. Devabhaktuni, and A. Sebak, "Improved photovoltaic mppt algorithm adapted for unstable atmospheric conditions and partial shading," in *Clean Electrical Power, 2009 International Conference on*. IEEE, 2009, pp. 320–323.
- [52] M. Sokolov and D. Shmilovitz, "Load line emulation based maximum power point tracking," in *2008 IEEE Power Electronics Specialists Conference*. IEEE, 2008, pp. 4098–4101.

- [53] S. Patel and W. Shireen, "Fast converging digital mppt control for photovoltaic (pv) applications," in *2011 IEEE Power and Energy Society General Meeting*. IEEE, 2011, pp. 1–6.
- [54] K. Kobayashi, I. Takano, and Y. Sawada, "A study of a two stage maximum power point tracking control of a photovoltaic system under partially shaded insolation conditions," *Solar energy materials and solar cells*, vol. 90, no. 18, pp. 2975–2988, 2006.
- [55] N. Femia, G. Lisi, G. Petrone, G. Spagnuolo, and M. Vitelli, "Distributed maximum power point tracking of photovoltaic arrays: Novel approach and system analysis," *IEEE Transactions on Industrial Electronics*, vol. 55, no. 7, pp. 2610–2621, 2008.
- [56] B. N. Alajmi, K. H. Ahmed, S. J. Finney, and B. W. Williams, "Fuzzy-logic-control approach of a modified hill-climbing method for maximum power point in microgrid standalone photovoltaic system," *IEEE Transactions on Power Electronics*, vol. 26, no. 4, pp. 1022–1030, 2011.
- [57] G. Petrone, G. Spagnuolo, R. Teodorescu, M. Veerachary, and M. Vitelli, "Reliability issues in photovoltaic power processing systems," *IEEE Transactions on Industrial Electronics*, vol. 55, no. 7, pp. 2569–2580, 2008.
- [58] K. Ding, X. Bian, H. Liu, and T. Peng, "A matlab-simulink-based pv module model and its application under conditions of nonuniform irradiance," *IEEE Transactions on Energy Conversion*, vol. 27, no. 4, pp. 864–872, 2012.
- [59] Y.-H. Liu, S.-C. Huang, J.-W. Huang, and W.-C. Liang, "A particle swarm optimization-based maximum power point tracking algorithm for pv systems operating under partially shaded conditions," *IEEE Transactions on Energy Conversion*, vol. 27, no. 4, pp. 1027–1035, 2012.
- [60] E. Koutroulis and F. Blaabjerg, "A new technique for tracking the global maximum power point of pv arrays operating under partial-shading conditions," *IEEE Journal of Photovoltaics*, vol. 2, no. 2, pp. 184–190, 2012.
- [61] P. Lei, Y. Li, and J. E. Seem, "Sequential esc-based global mppt control for photovoltaic array with variable shading," *IEEE Transactions on Sustainable Energy*, vol. 2, no. 3, pp. 348–358, 2011.
- [62] S. Moballegh and J. Jiang, "Modeling, prediction, and experimental validations of power peaks of pv arrays under partial shading conditions," *IEEE Transactions on Sustainable Energy*, vol. 5, no. 1, pp. 293–300, 2014.

- [63] Y.-J. Wang and P.-C. Hsu, "Analytical modelling of partial shading and different orientation of photovoltaic modules," *IET Renewable Power Generation*, vol. 4, no. 3, pp. 272–282, 2010.
- [64] M. Alonso-Garcia, J. Ruiz, and F. Chenlo, "Experimental study of mismatch and shading effects in the i–v characteristic of a photovoltaic module," *Solar Energy Materials and Solar Cells*, vol. 90, no. 3, pp. 329–340, 2006.
- [65] M. Alonso-García and J. Ruíz, "Analysis and modelling the reverse characteristic of photovoltaic cells," *Solar Energy Materials and Solar Cells*, vol. 90, no. 7, pp. 1105–1120, 2006.
- [66] K. S. Tey and S. Mekhilef, "Modified incremental conductance algorithm for photovoltaic system under partial shading conditions and load variation," *IEEE Transactions on Industrial Electronics*, vol. 61, no. 10, pp. 5384–5392, 2014.
- [67] T. K. Soon and S. Mekhilef, "A fast-converging mppt technique for photovoltaic system under fast-varying solar irradiation and load resistance," *IEEE Transactions on Industrial Informatics*, vol. 11, no. 1, pp. 176–186, 2015.
- [68] M. Seyedmahmoudian, S. Mekhilef, R. Rahmani, R. Yusof, and E. T. Renani, "Analytical modeling of partially shaded photovoltaic systems," *Energies*, vol. 6, no. 1, pp. 128–144, 2013.
- [69] R. Kotti and W. Shireen, "Efficient mppt control for pv systems adaptive to fast changing irradiation and partial shading conditions," *Solar Energy*, vol. 114, pp. 397–407, 2015.
- [70] K. Ishaque, Z. Salam, M. Amjad, and S. Mekhilef, "An improved particle swarm optimization (pso)-based mppt for pv with reduced steady-state oscillation," *IEEE Transactions on Power Electronics*, vol. 27, no. 8, pp. 3627–3638, 2012.
- [71] K. Ishaque, Z. Salam, A. Shamsudin, and M. Amjad, "A direct control based maximum power point tracking method for photovoltaic system under partial shading conditions using particle swarm optimization algorithm," *Applied Energy*, vol. 99, pp. 414–422, 2012.
- [72] A. Khare and S. Rangnekar, "A review of particle swarm optimization and its applications in solar photovoltaic system," *Applied Soft Computing*, vol. 13, no. 5, pp. 2997–3006, 2013.
- [73] K. Sundareswaran, S. Peddapati, and S. Palani, "Mppt of pv systems under partial shaded conditions through a colony of flashing fireflies," *IEEE Transactions on Energy Conversion*, vol. 29, no. 2, pp. 463–472, 2014.

- [74] L. L. Jiang, D. L. Maskell, and J. C. Patra, "A novel ant colony optimization-based maximum power point tracking for photovoltaic systems under partially shaded conditions," *Energy and Buildings*, vol. 58, pp. 227–236, 2013.
- [75] J. Ahmed and Z. Salam, "A maximum power point tracking (mppt) for pv system using cuckoo search with partial shading capability," *Applied Energy*, vol. 119, pp. 118–130, 2014.
- [76] M. Balato and M. Vitelli, "A hybrid mppt technique based on the fast estimate of the maximum power voltages in pv applications," in *Ecological Vehicles and Renewable Energies (EVER), 2013 8th International Conference and Exhibition on*. IEEE, 2013, pp. 1–7.
- [77] A. F. Murtaza, H. A. Sher, M. Chiaberge, D. Boero, M. De Giuseppe, and K. E. Addoweesh, "A novel hybrid mppt technique for solar pv applications using perturb & observe and fractional open circuit voltage techniques," in *MECHATRONIKA, 2012 15th International Symposium*. IEEE, 2012, pp. 1–8.
- [78] K. Sundareswaran, V. Vigneshkumar, P. Sankar, S. P. Simon, P. S. R. Nayak, and S. Palani, "Development of an improved p&o algorithm assisted through a colony of foraging ants for mppt in pv system," *IEEE Transactions on Industrial Informatics*, vol. 12, no. 1, pp. 187–200, 2016.
- [79] K. Sundareswaran, S. Palani *et al.*, "Application of a combined particle swarm optimization and perturb and observe method for mppt in pv systems under partial shading conditions," *Renewable Energy*, vol. 75, pp. 308–317, 2015.
- [80] N. Kaushika and A. K. Rai, "An investigation of mismatch losses in solar photovoltaic cell networks," *Energy*, vol. 32, no. 5, pp. 755–759, 2007.
- [81] Y.-J. Wang and P.-C. Hsu, "An investigation on partial shading of pv modules with different connection configurations of pv cells," *Energy*, vol. 36, no. 5, pp. 3069–3078, 2011.
- [82] R. Ramabadran and B. Mathur, "Effect of shading on series and parallel connected solar pv modules," *Modern Applied Science*, vol. 3, no. 10, p. 32, 2009.
- [83] A. Woyte, J. Nijs, and R. Belmans, "Partial shadowing of photovoltaic arrays with different system configurations: literature review and field test results," *Solar energy*, vol. 74, no. 3, pp. 217–233, 2003.
- [84] S. Silvestre, A. Boronat, and A. Chouder, "Study of bypass diodes configuration on pv modules," *Applied Energy*, vol. 86, no. 9, pp. 1632–1640, 2009.

- [85] D. Picault, B. Raison, S. Bacha, J. De La Casa, and J. Aguilera, "Forecasting photovoltaic array power production subject to mismatch losses," *Solar Energy*, vol. 84, no. 7, pp. 1301–1309, 2010.
- [86] L. Gao, R. A. Dougal, S. Liu, and A. P. Iotova, "Parallel-connected solar pv system to address partial and rapidly fluctuating shadow conditions," *IEEE Transactions on Industrial Electronics*, vol. 56, no. 5, pp. 1548–1556, 2009.
- [87] A. Dolara, G. C. Lazaroiu, S. Leva, and G. Manzolini, "Experimental investigation of partial shading scenarios on pv (photovoltaic) modules," *Energy*, vol. 55, pp. 466–475, 2013.
- [88] S. Mekhilef, R. Saidur, and A. Safari, "A review on solar energy use in industries," *Renewable and Sustainable Energy Reviews*, vol. 15, no. 4, pp. 1777–1790, 2011.
- [89] R. Pradhan and B. Subudhi, "Design and real-time implementation of a new auto-tuned adaptive mppt control for a photovoltaic system," *International Journal of Electrical Power & Energy Systems*, vol. 64, pp. 792–803, 2015.
- [90] S. Mishra and P. RAY, "Power quality improvement using photovoltaic fed dstatcom based on jaya optimization," *IEEE Transactions on Sustainable Energy*, vol. 7, no. 4, pp. 1672–1680, 2016.
- [91] K. Ishaque, Z. Salam, H. Taheri *et al.*, "Modeling and simulation of photovoltaic (pv) system during partial shading based on a two-diode model," *Simulation Modelling Practice and Theory*, vol. 19, no. 7, pp. 1613–1626, 2011.
- [92] N. Mutoh, M. Ohno, and T. Inoue, "A method for mppt control while searching for parameters corresponding to weather conditions for pv generation systems," *IEEE Transactions on Industrial Electronics*, vol. 53, no. 4, pp. 1055–1065, 2006.
- [93] A. Bidram, A. Davoudi, and R. S. Balog, "Control and circuit techniques to mitigate partial shading effects in photovoltaic arrays," *IEEE Journal of Photovoltaics*, vol. 2, no. 4, pp. 532–546, 2012.
- [94] P. S. Rao, G. S. Ilango, and C. Nagamani, "Maximum power from pv arrays using a fixed configuration under different shading conditions," *IEEE Journal of Photovoltaics*, vol. 4, no. 2, pp. 679–686, 2014.
- [95] P. Sharma and V. Agarwal, "Maximum power extraction from a partially shaded pv array using shunt-series compensation," *IEEE Journal of Photovoltaics*, vol. 4, no. 4, pp. 1128–1137, 2014.

- [96] J. Ahmad, "A fractional open circuit voltage based maximum power point tracker for photovoltaic arrays," in *Software Technology and Engineering (ICSTE), 2010 2nd International Conference on*, vol. 1. IEEE, 2010, pp. V1–247.
- [97] T. Noguchi, S. Togashi, and R. Nakamoto, "Short-current pulse-based maximum-power-point tracking method for multiple photovoltaic-and-converter module system," *IEEE Transactions on Industrial Electronics*, vol. 49, no. 1, pp. 217–223, 2002.
- [98] S. B. Kjær, "Evaluation of the hill climbing and the incremental conductance maximum power point trackers for photovoltaic power systems," *IEEE Transactions on Energy Conversion*, vol. 27, no. 4, pp. 922–929, 2012.
- [99] M. A. Elgendy, B. Zahawi, and D. J. Atkinson, "Assessment of perturb and observe mppt algorithm implementation techniques for pv pumping applications," *IEEE Transactions on Sustainable Energy*, vol. 3, no. 1, pp. 21–33, 2012.
- [100] M. Killi and S. Samanta, "Modified perturb and observe mppt algorithm for drift avoidance in photovoltaic systems," *IEEE Transactions On Industrial Electronics*, vol. 62, no. 9, pp. 5549–5559, 2015.
- [101] P.-C. Chen, P.-Y. Chen, Y.-H. Liu, J.-H. Chen, and Y.-F. Luo, "A comparative study on maximum power point tracking techniques for photovoltaic generation systems operating under fast changing environments," *Solar Energy*, vol. 119, pp. 261–276, 2015.
- [102] M. A. Masoum, H. Dehbonei, and E. F. Fuchs, "Theoretical and experimental analyses of photovoltaic systems with voltageand current-based maximum power-point tracking," *IEEE Transactions on Energy Conversion*, vol. 17, no. 4, pp. 514–522, 2002.
- [103] M. A. G. De Brito, L. Galotto, L. P. Sampaio, G. d. A. e Melo, and C. A. Canesin, "Evaluation of the main mppt techniques for photovoltaic applications," *IEEE Transactions on Industrial Electronics*, vol. 60, no. 3, pp. 1156–1167, 2013.
- [104] S. Mirjalili, S. M. Mirjalili, and A. Lewis, "Grey wolf optimizer," *Advances in Engineering Software*, vol. 69, pp. 46–61, 2014.
- [105] S. Mohanty, B. Subudhi, and P. K. Ray, "A new mppt design using grey wolf optimization technique for photovoltaic system under partial shading conditions," *IEEE Transactions on Sustainable Energy*, vol. 7, no. 1, pp. 181–188, 2016.
- [106] A. Chouder, S. Silvestre, N. Sadaoui, and L. Rahmani, "Modeling and simulation of a grid connected pv system based on the evaluation of main pv module parameters," *Simulation Modelling Practice and Theory*, vol. 20, no. 1, pp. 46–58, 2012.

-
- [107] A. Yazdani and P. P. Dash, "A control methodology and characterization of dynamics for a photovoltaic (pv) system interfaced with a distribution network," *IEEE Transactions on Power Delivery*, vol. 24, no. 3, pp. 1538–1551, 2009.
- [108] M. Killi and S. Samanta, "An adaptive voltage-sensor-based mppt for photovoltaic systems with sepic converter including steady-state and drift analysis," *IEEE Transactions on Industrial Electronics*, vol. 62, no. 12, pp. 7609–7619, 2015.
- [109] K. Chen, S. Tian, Y. Cheng, and L. Bai, "An improved mppt controller for photovoltaic system under partial shading condition," *IEEE Transactions on Sustainable Energy*, vol. 5, no. 3, pp. 978–985, 2014.
- [110] H. A. Sher, A. F. Murtaza, A. Noman, K. E. Addoweesh, K. Al-Haddad, and M. Chiaberge, "A new sensorless hybrid mppt algorithm based on fractional short-circuit current measurement and p&o mppt," *IEEE Transactions on Sustainable Energy*, vol. 6, no. 4, pp. 1426–1434, 2015.

Thesis Dissemination

Journals

1. S. Mohanty, B. Subudhi and P. K Ray, A New MPPT Design using Grey wolf optimization technique for Photovoltaic system under partial shading conditions, *IEEE Transactions on Sustainable Energy*, vol. 7, no. 1, pp. 181-188, Jan 2016.
2. S. Mohanty, B. Subudhi and P. K Ray, A Grey Wolf Assisted Perturb & Observe MPPT Algorithm for a PV System, *IEEE Transactions on Energy Conversion*, DOI:10.1109/TEC.2016.2633722.

Conferences

1. S. Mohanty, B. Subudhi and P. K Ray, An Experimental Study on Effect of Shading Conditions in PV Power Generation, *Recent Advances in Power, Energy and Control*, National Conference, Rourkela, India, 23-24 Nov 2013.
2. S. Mohanty, B. Subudhi and P. K Ray, A Grey Wolf Optimization Based MPPT for PV System under Changing Insolation level, *IEEE Students Technology Symposium*, Kharagpur, India, 30 Sep - 2 Oct 2016.

Article Under Preparation

1. S. Mohanty, B. Subudhi and P. K Ray, Analytical Modeling and Experimental Prediction of Global Peak under Partial Shading of PV modules for a Photo-

voltaic System, *IEEE Transactions on Energy Conversion*.

Author's biography

Satyajit Mohanty was born to Sri. Sarat Kumar Mohanty and Smt. Namita Patnaik on 13th June, 1988 at Cuttack, Odisha, India. He obtained a Bachelor's degree in Electrical Engineering from B.P.U.T, Rourkela, Odisha in 2009 and Master's degree in Power Electronics and Drives from Siksha O Anusandhan University, India in 2012. He joined as a Institute Ph.D Scholar in the Department of Electrical Engineering, National Institute of Technology Rourkela in Jan 2013. His areas of academic pursuit include modeling and control of photovoltaic systems.

Communications:

Address: Department of Electrical Engineering, National Institute of Technology Rourkela, Orissa, PIN: 769008.

e-mail: kmsatyajit@gmail.com